

Letter to the Editor

ACP Discussions doi: 10.5194/acp-2018-724

(Editor - Peter Haynes)

‘Lagrangian simulations of the transport of young air masses to the top of the Asian monsoon anticyclone and into the tropical pipe’

Dear Peter Haynes,

many thanks for handling our manuscript. We prepared and submitted a revised version of our manuscript and are confident that we have satisfactorily addressed all comments of referee s#1 to #3. A detailed point-by-point response to all referee comments (#1 to #3) is attached. Further, a document specifying all changes in the revised manuscript compared to the ACPD version is added.

Best wishes

Bärbel Vogel

Author Comment to Referee #1: page 2-34

Author Comment to Referee #2: page 35-60

Author Comment to Referee #3: page 61-76

All Changes: page 77-121

Author Comment to Referee #1

ACP Discussions doi: 10.5194/acp-2018-724

(Editor - Peter Haynes)

‘Lagrangian simulations of the transport of young air masses to the top of the Asian monsoon anticyclone and into the tropical pipe’

We thank Referee #1 for further guidance on how to to revise our paper. Following the reviewers advice we revised some parts of the paper for the purpose of clarification. In particular, we want to thank the reviewer for the elaborate language corrections. This was a very great support. Our reply to the reviewer comments is listed in detail below. Questions and comments of the referee are shown in italics. Passages from the revised version of the manuscript are shown in blue.

This manuscript uses back trajectories and full 3D CLaMS simulations in conjunction with MIPAS HCFC-22 measurements to elucidate the transport pathway of air masses emitted in defined boundary layer regions through the Asian summer monsoon anticyclone and into the tropical pipe. The modeling tools and measurements are well suited to the investigation, the analysis is generally well thought out and well executed, and the findings will certainly be of interest to the journal readership. I do, however, have a number of substantive comments that I would like to see addressed before the paper is accepted for publication in ACP.

Specific substantive comments and questions:

Sections 2.2 and 3.2.1: 40 days seems like a very long period for trajectory calculations. I realize that CLaMS 40-day trajectories have been published previously, but nevertheless I think that a sentence or two on how much error has accumulated over the course of such long trajectory calculations would be appropriate, either in Section 2.2 or in Section 3.2.1.

We agree and have thus added a few sentences in Section 3.2.1. to discuss the errors of the trajectory length as follows.

In general, trajectory calculations have limitations due to trajectory dispersion by errors through interpolation of the wind data to the position of the air parcel at a specific time. Over the timescales in question, mixing can also be relevant (e.g., McKenna et al., 2002). These errors can accumulate depending on the trajectory length over the course of the simulation. However, the frequently employed trajectory length to study transport processes in the Asian monsoon region is ranging from a couple of weeks to a few months (e.g., Chen et al., 2012; Bergman et al., 2013; Vogel et al., 2014; Garny and Randel, 2016; Müller et al., 2016; Li et al., 2017). In our trajectory analysis, the focus is to demonstrate the large-scale transport pathways of the air parcels at the top of the anticyclone, small changes of the trajectory position will therefore not affect our findings.

Section 2.4: I miss in the description of the MIPAS HCFC-22 any information about the accuracy, precision, or horizontal or vertical resolution of the measurements. Some discussion of the data quality is warranted to help evaluate the comparisons with CLaMS results later in the manuscript. This information may be contained in the paper by Chirkov et al., but some basic data quality information needs to be included here as well for the convenience of the reader. See related comment below.

As suggested we provide some additional information about the MIPAS HCFC-22 data quality in Section 2.4 as follows.

The limited vertical resolution of the MIPAS HCFC-22 data needs to be taken into account in comparisons to model results. The precision of an individual data point in the altitude region of the Asian monsoon tropopause is 7 to 8 pptv in terms of measurement noise. Parameter errors contribute to a total uncertainty of about 15 pptv in this region for each data point. Thus, the scatter of the HCFC-22 data points (e.g. as shown in Fig. 3) is consistent to the total error. According to Chirkov et al. (2016), the vertical resolution (in terms of the full width at half maximum of the vertical averaging kernel) increases from about 3.3 km at 12 km to 5.5 km at 20 km altitude (see Fig. 2 in Chirkov et al., 2016). The horizontal resolution (in terms of the full width at half maximum of the horizontal averaging kernel) increases from 300 km

at 15 km altitude to 600 km at 20 km altitude. Given the rather smooth profiles expected in this study, the limited altitude resolution has a minor effect only; in contrast, it turns out to be crucial when highly structured profiles, such as typically occur at the edge of the polar vortex, are analysed. Further it has to be noted that tropical HCFC-22 profiles from MIPAS seem to have a high bias below 30 km, that, however, is broadly constant with altitude (Chirkov et al., 2016); thus, it does not affect the comparisons made here.

P7, L29 - P8, L11: These paragraphs are confusing, because the first sentence (P7, L29), as well as the subsection title, refer to transport of emission tracers to ‘the top of the Asian monsoon anticyclone’, yet Figure 2 (top row) and the related discussion focus on 360 K, which is obviously not at the top of the anticyclone. It may be that the discussion begins with 360 K because that level is where regions ‘inside’ and ‘outside’ the anticyclone are defined, which seems to be what is implied by the sentence in P8, L9-10, but if so then that motivation needs to come earlier in the paragraph to set the stage. Moreover, if that is the case, then I am confused by that as well - why define inside/outside the anticyclone at a single level, rather than at each considered level, since the shape of the anticyclone changes considerably with height? And Fig. 3 defines the anticyclone by the 20% contour of the India/China tracer at 380 K (not 360 K). So this entire discussion needs to be clarified.

We agree that here we have to provide a better motivation to explain our analysis. We introduced a motivation/introduction to Sect. 3.1.1 as follows.

It is known that the Asian monsoon anticyclone has a strong horizontal transport barrier at about 380 K (e.g., Ploeger et al., 2015), however this transport barrier is not well defined at higher levels of potential temperature. The less strong transport barrier at higher levels has consequences on the vertical transport at the top of the anticyclone. Before the transport at the top is discussed we show the horizontal distribution of different emission tracers at 360 K and then their subsequent transport to the top of the anticyclone up to 460 K. Vogel et al. (2015) showed that the emission tracer for India/China is a good proxy for the location and shape of the Asian monsoon anticyclone using pattern correlations with potential vorticity (PV), and MLS O₃ and CO satellite measurements between 360 K and 400 K. Therefore here we use the India/China tracer as proxy for the location of the anticyclone.

P8, L15: To my eye, it looks as though fractions as high as 40% extend lower than 350 K, down to at least 340 K, if not lower.

Yes, we agree the fractions as high as 40% extend lower down to ≈ 340 K. We revised the paragraph as follows.

We would like to emphasise the horizontal transport of air masses with high contributions from India/China (40%–90%) from the eastern part of the anticyclone to both the western part and into the eddy over the western Pacific between ≈ 340 K and ≈ 380 K.

P8, L20-21: It is not clear exactly which regions are being referred to for these values; in particular, in some areas (≈ 310 - 330 K, 10° N) fractions from the tropical adjacent regions much higher than 10%-40% are seen.

We revised this paragraph to be more precise as follows.

In the western mode there is still a high contribution from the India/China tracer between 20% and 60% and lower fractions about 10%–40% from the tropical adjacent regions (Fig. 2g/h inside the thick white line). Below the western mode, in the tropics below ≈ 330 K at around 10° N fractions from the tropical adjacent regions (in that case from Northern Africa) are up to 90% caused by local upward transport.

P8, L28-29: First, the region ‘inside the anticyclone’ is referred to here, but it is not possible for the reader to identify where the anticyclone boundary falls at different altitudes in the cross sections of Fig. 2. The authors should think about how to convey information about the approximate location of the anticyclone in these panels. Second, it is stated that near the tropopause the fraction from the tropical adjacent regions reaches as high as 35%, but I am not sure exactly where is being referred to, as most TAR fractions in the vicinity of the monsoon in Fig. 2d are no larger than 25-30%.

A clear definition of the edge anticyclone over a large range of different altitudes is not possible such as a PV-based criterion (e.g., Ploeger et al., 2015). We use here as a proxy the distribution of the India/China tracer. Further, we agree the TAR fractions are to about 30%. We revised the respective

sentence as follows.

Below 360 K in the region with high values of the India/China tracer, the fractions from the tropical adjacent regions are below 10%, however above 360 K around the tropopause the fractions are much higher, up to about 30%, and up to about 15% around 420 K (see Fig. 2d/f).

P9, L11-25: I agree that the HCFC-22 data show good agreement with the India/China emission tracer and that they are a very useful element of the analysis. However, Fig. 3 reveals quite a few stray data points well outside the anticyclone that also have elevated HCFC-22 abundances. As mentioned earlier, the precision of an individual data point should be given so that the agreement in Fig. 3 can be fully evaluated. It seems to me that the enhancement in the thin filament (L15) does not particularly stand out in the measurements; indeed, in the absence of the CLaMS results to guide the eye, it likely would be overlooked altogether. Likewise, the measured enhancements at the top of the anticyclone above the tropopause (L20) are also fairly modest; in fact, they are not much different from other high MIPAS points well away from where CLaMS indicates a signal (e.g., at the EQ at 370 K, at 5N at 420 K, and at 30N at 430 K). It might help to also overlay on these plots (both the map and the cross sections) a solid contour highlighting a selected HCFC-22 mixing ratio. Although the ‘dot plots’ are very valuable for representing the sampling of the MIPAS measurements, they do make it more difficult to get an impression of the overall morphology. Overlaying one specific contour from a gridded HCFC-22 field might strengthen the case for good agreement with the modeled tracer. Finally, although I do see a steep vertical gradient in the HCFC-22 data from ≈ 350 to 360 K in the ≈ 25 -40N region, I do not see a corresponding signature in the India/China tracer in that region (L25); there is a steep gradient in that tracer in Fig. 2g, but at altitudes below 350 K, so the patterns in the 350-360 K region are not really that similar.

We thank the reviewer for the advice to modify Fig. 3 by overlaying a solid contour highlighting a selected HCFC-22 mixing ratio. We tested different plotting types as shown in Fig. 1 of this author comment. Because of the coarse vertical resolution of the MIPAS measurements a solid contour depends strongly on the grid used for interpolation. Therefore, we prefer to show the plots without a solid contour line for a selected HCFC-22 mixing ratio.

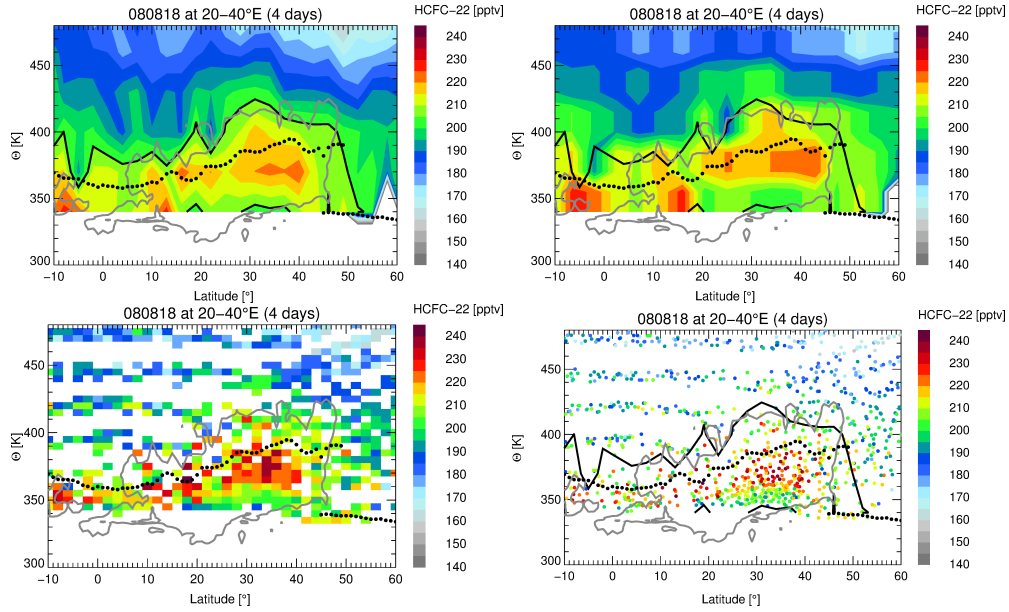


Figure 1: Latitude–theta cross sections at 30°E (western part of the anticyclone) on 18 August 2008: contour plot, contour plot with a resampled finer grid (congrid), plotcell, and xy-plot. The contour line of 200 pptv HCFC-22 is shown in black. The contour line of 20% of the India/China tracer is shown by thick grey lines.

P10, L6-11: Again, this discussion refers to ‘within’ and ‘in the core of’ the anticyclone, so some means of delineating exactly where that region is at each level is needed. In Fig. 3, the 20% contour for the India/China tracer is used to approximate the boundary of the anticyclone at 380 K, but what about at the higher levels shown in Fig. 4? How is the reader to gauge that the largest contributions of both emission tracers are found within the anticyclone at 400 K but around its edge at 420-460 K, as stated here? In fact, I am not convinced that either statement is true: the eastern lobe of the anticyclone ($\approx 100E$) shows the largest fractions of the TAR tracer along what looks to me more like the edge of the anticyclone at 400 K, whereas the largest values of both tracers seem to be concentrated in the core region at that longitude at 420 K.

We agree that this discussion is a bit confusing. We revised this paragraph as follows.

Young air masses (age < 6 months) from both India/China and tropical adjacent regions are found up to ≈ 460 K. It was shown earlier that the horizontal distribution of the India/China tracer is a good proxy for the location of the anticyclone (Vogel et al., 2015). The horizontal distribution of the tropical adjacent regions compared to the horizontal distribution of the India/China tracer strongly differs depending on the level of potential temperature from a nearly disjoint distribution at 360 K (see Fig. 2) to a more coincident distribution from 400 K to 460 K (see Fig. 5).

At 380 K, the highest fractions from tropical adjacent regions are found at the edge of the anticyclone and at 400 K within the anticyclone. Above 400 K both tracers India/China and tropical adjacent regions show a similar horizontal distribution. We emphasise that at these levels of potential temperature the tracer distributions have the shape of rotating filaments in contrast to the more compact distribution at lower levels. The variation of the distribution of the tracer for the tropical adjacent regions with altitude is an indication that the upward transport of young air masses at the top of the anticyclone occurred more towards the edge and less inside the anticyclone itself.

P10, L16-19: How were the percentages of young air masses for the selected air parcels chosen? In the absence of any explanation these values seem arbitrary. Are these trajectories initiated from the entire region within the defined lat/lon boxes? I'm wondering if these percentages can be related to the values shown for the India/China tracer in Fig. 4.

We agree that the description of the initialisation procedure of the trajectories is a bit short. We revised this paragraph as follows.

To analyse the transport pathways to the top of the anticyclone in more detail, 40-day backward trajectories are calculated starting in the western (20–50°N, 0–70°E) and eastern (20–50°N, 70–140°E) modes of the anticyclone. The trajectories are started at the position of the air parcels from the 3-dimensional CLaMS simulation at different levels of potential temperature ($\Theta = 380, 400, 420, 440$ K ± 0.25 K) on 18 August 2018. Note that the air

parcels in the 3-dimensional CLaMS simulation are distributed on an irregular grid. To take into account the distribution of the boundary emission tracer at the top of the Asian monsoon anticyclone, only air parcels are selected with contributions of young air masses (age < 6 months, Summer 08) larger than 70% (380 K), 50% (400 K), 20% (420 K), and 5% (440 K) (not all levels of potential temperature are presented here). The percentages are chosen in a way to obtain a number of trajectories (less than 30) that can be reasonably visualised. The results of the 40-day backward trajectories are similar at different levels of potential temperature; therefore we show a selection of trajectories to demonstrate the main transport pathway to the top of the Asian monsoon. A larger set of 20-day backward trajectories analysed statistically will be discussed below in Section 3.2.2.

P10, L22-23: How consistent are the trajectory results, which indicate that the Tibetan Plateau and the western Pacific are preferred regions for fast uplift, with prior studies (in other words, some citations would be appropriate here).

We revised this paragraph in Sect. 3.2.1 as follows and added a small discussion within Sect. 4 about convective source regions contributing to the composition of the Asian monsoon anticyclone following the advice by reviewer #2.

Fig. 5 shows trajectories started in the eastern and western part of the Asian monsoon anticyclone around the thermal tropopause at 380 K on 18 August 2018. Air masses are uplifted to approximately 360 K very rapidly by various convective events occurring at different times and locations. Our 40-day backward trajectories show that preferred regions for fast uplift are continental Asia (mainly the region of the south slope of the Himalayas and the Tibetan Plateau) and the western Pacific (not shown here). A lower fraction of trajectories originates in the free troposphere. The trajectories in Fig. 2 demonstrating convection below 380 K are only a snapshot for 18 August 2018. There are several previous studies (e.g., Randel and Park, 2006; Park et al., 2007, 2009; Wright et al., 2011; Chen et al., 2012; Bergman et al., 2013; Fadnavis et al., 2014; Tissier and Legras, 2016) quantifying the contribution of different source regions to the composition of the Asian monsoon anticyclone during the course of the monsoon season (see discussion in Sect. 4).

We added in the Discussion Section (Sect. 4) the following discussion.

It is well known that the composition of the Asian monsoon anticyclone is strongly affected by convection over continental Asia (e.g. the south slope of the Himalayas and the Tibetan Plateau), Bay of Bengal, and the western Pacific, (e.g., Randel and Park, 2006; Park et al., 2007, 2009; Wright et al., 2011; Chen et al., 2012; Bergman et al., 2013; Fadnavis et al., 2014; Tissier and Legras, 2016). However there is a debate about the contribution of different source regions to the composition of the Asian monsoon anticyclone. Further, there are differences in the conclusions in the literature about the contribution of different source regions depending on the used reanalysis data (e.g., Wright et al., 2011; Bergman et al., 2013). Findings by Vogel et al. (2015) show that there is a strong intraseasonal variability of boundary source regions to the composition of the Asian monsoon anticyclone during a particular monsoon season. We would like to emphasise that the trajectories presented in Fig. 6 demonstrating convection below 380 K are only a snapshot for 18 August 2018 with convection over the western Pacific and continental Asia mainly in the region of the south slope of the Himalayas and the Tibetan Plateau.

P10, L24-26: Is there a reason that the corresponding plots for the eastern lobe of the anticyclone were not shown in Fig. 5, as they were in Fig. 6? I would have thought that they would be relevant to the discussion here.

We didn't show the eastern mode of the anticyclone because the trajectories show similar results as for the western mode. We did not want to extend the paper to much. However, we decided to show also the plots for the eastern mode as shown in Fig. 2 (of this author comment) and Fig. 5 in the revised version of the manuscript to avoid the reader is confused why we didn't show the plots for the eastern mode.

P11, L14-26: What exactly is meant by 'substantial' upward transport (L14)? Does 'substantial' mean 0.5 K/day, 1 K/day, or?? It would be better to be more quantitative. In addition, here the discussion is cast in terms of heating rate (K per day), whereas Fig. 7 and Fig. A1 show the change in potential temperature (in K) along 20-day trajectories, making the reader do the (admittedly easy) math. Once the meaning of 'substantial' is established, it would be better to qualify the transport experienced by air parcels grouped in

filaments as being ‘substantial’ or ‘strong’ (L16) - filamentary structure is not present everywhere that air parcels have experienced some uplift. I also think it would be better to say ‘largely’, rather than ‘only’, in L26 because there are red dots outside the monsoon region, especially in July and August.

As proposed we revised this paragraph as following including also comments by reviewer #2.

Above 360 K, air parcels that experienced strong upward transport larger than 20–30 K within 20 day (corresponding to a mean value of 1–1.5 K per day) are largely found in the region of the anticyclone. This rate of upwelling is much slower compared to convective upwelling shown at 360 K. Air parcels that experienced strong upward transport are mainly grouped in curved elongated filaments, reflecting a rotating movement of the air parcels at the top of the anticyclone. Often air parcels with strong $\Delta\Theta$ above 360 K are located more at the edge of the eastern and western modes of the anticyclone and at the edge of the eastward-migrating eddy at the eastern flank of the anticyclone. Thus the upward transport in the region of the anticyclone is inhomogeneous and not homogeneously distributed over the entire anticyclone as suggested from climatological studies (e.g., Randel et al., 2010; Ploeger et al., 2017). This is consistent with results presented above in Sect. 3.2.1 demonstrating that for single selected trajectories the transport at the top of the Asian monsoon anticyclone is a slow upward transport of about 1–1.5 K per day in a large-scale spiral above the anticyclone caused by diabatic heating. In the backward trajectory calculations mixing processes are not included, however the results of the trajectory calculations are consistent with patterns found in the 3-dimensional CLaMS simulation including mixing as discussed in Sect. 3.1.3, demonstrating that young air masses above 400 K are found at the edge of the anticyclone. Above 400 K, air masses in the tropics also experienced upward transport, but the vertical uplift is in general lower than 20 K within 20 day, (i.e. lower than 1 K per day).

P12, L11: It might be good to explain why the emphasis has shifted from the tropical adjacent regions examined in previous figures to Southeast Asia specifically in Fig. 9, especially since Fig. 12 shows that the TPO also makes a substantial contribution to the air at 550 K.

Many thanks for this comment. We agree that it would be more stringent

to show the emission tracer for the tropical adjacent regions instead of the emission tracer for Southeast Asia in Figure 9 of the manuscript. You are right also TPO contribute much to the signal within the tropical pipe (see Fig 3 of this author comment). We changed Figure 9 in the revised version of the manuscript as shown in Fig. 4 within this author comment.

P12, L14-17: It is stated that an enhanced signal from Southeast Asia of up to 25% (L14 and L17) is seen around 550 K for the S07 pulse, but as far as I can tell from Fig. 9, the largest S07 enhancement (at $\approx 10S$) is only $\approx 12\%$, not 25%.

Yes, we agree. However, we changed Fig. 9 (of the manuscript) showing TAR instead of SEA. For TAR 25% is correct. We changed this sentence as follows.

For the Summer 07 pulse, an enhanced signal from TAR (up to 25%) is found at around 550 K within the tropics similar as for India/China tracer.

P12, L27-28: I do think it is important to point out the uncertainties in the reanalysis heating rates, as done in these lines. However, the way this paragraph ends leaves the reader hanging a bit. What is the take-away message? Can we trust the results in Fig. 10 or not? What are the possible implications for the ‘upward spiraling range’?

We revised the paragraph following the reviewers advice.

...It is known that the radiative heating rates in the tropical UTLS are different in current reanalysis models (e.g., Wright and Fueglistaler, 2013) and are most likely overestimated in ERA-Interim (e.g., Ploeger et al., 2012; Schoeberl et al., 2012). Therefore, the rates of diabatic heating in the upward spiralling range found in our study are most likely somewhat too high, however slow upward transport in the UTLS in the region of the Asian monsoon anticyclone associated with positive heating has been addressed previously (e.g., Park et al., 2007; Bergman et al., 2012; Garny and Randel, 2016; Ploeger et al., 2017).

P12, L29: It is stated that Fig. 11 shows the same cross sections as Figs. 8 and 9. The latter two figures, however, show results only for the eastern lobe (90E), whereas Fig. 11 also shows the cross section for 30E. Although we

have some information about S08 in that region from Fig. 2, we do not get the full picture from that figure, and thus we have little to compare to the left panel of Fig. 11. I note that, in terms of major features, the HCFC-22 results look quite similar at 30E and 90E. Is that also the case for the CLaMS results, that is, do the corresponding plots at 30E look similar to those in Figs. 8 and 9? If so, then that should be mentioned, and perhaps the left panel of Fig. 11 should also be omitted. If not, discussion of the differences should be included.

Yes, we agree that the eastern mode is not shown in Figs. 8 and 9. Similar features are found in the western and eastern mode, therefore there is no added values to show the eastern mode. Following the reviewers advice the removed the plots for the eastern part.

P16, L3-4: Has evidence for a coherent signature of the existence of the anticyclone and influence of monsoon air up to altitudes as high as 460 K been reported previously? It seems to me that this may be an important finding that has been underemphasized in this manuscript.

There are a few studies looking also in this altitude range (e.g., Garny and Randel, 2016; Ploeger et al., 2017), however with an other focus. We added the following paragraph to the Discussion Sect. 4.

In this study, we focus on transport at the top of the anticyclone in an altitude range higher than 380 K potential temperature (≈ 100 hPa) up to 460 K (≈ 60 hPa). Further, in addition to previous studies (e.g., Garny and Randel, 2016; Ploeger et al., 2017), we relate the transport of air masses from inside the Asian monsoon anticyclone to air masses uplifted outside the anticyclone. Subsequently these air masses are jointly transported upwards to the top of the anticyclone at ≈ 460 K.

P26, Fig. 2: Perhaps it would make the maps in the top row too cluttered, but I think it would be helpful to draw on them a horizontal line at 25N and vertical lines at 30E and 90E to orient the reader for the cross sections in the bottom panels. In addition, I understand that a common color bar is used for all panels in this figure, and I agree that that is probably the best approach, and I further agree that extending the color bar to 100% is appropriate for the cross sections. However, I note that employing such a color bar renders some of the features in the maps less prominent. For example, the filament at 50E

seen so clearly at 380 K in Fig. 3, where the tracer color bar extends only to 50%, is nearly invisible in Fig. 2 but might show up well if the color bar range were reduced. I am not suggesting that the color bar should necessarily be changed, merely pointing out the issue.

We also discussed extensively these issues. To draw three lines in Fig. 2a and 2b would make the plots very cluttered and cover some features. The color bar is a compromise between covering the full date range within the longitude-theta and latitude-theta cross sections and having the same range within the horizontal distribution at 360 K. Therefore, some features within the horizontal distribution at 360 K are less prominent. We added the following paragraph to Sect. 3.1.1.

Note that in Fig. 2 the same data range is used for all colour bars for a better comparability between the horizontal and different vertical cross sections. Therefore some features at the horizontal cross section at 360 K are not too prominent for example the thin filament at around 50°E between 40°N and 60°N in Fig. 2a (see next section Fig. 3).

P27, Fig. 3: I found the figure layout and accompanying discussion hard to follow. Here the latitude-theta cross section at 30E comes first, then the one at 90E, and finally the longitude-theta cross section, which is essentially opposite to the order followed in Fig. 2. It would make it easier to compare the CLaMS and MIPAS results if Fig. 3 were configured as a single-column figure following the same layout as Fig. 2 (with an extra panel at the top for the India/China tracer and the MIPAS panels corresponding to those in Fig. 2 below). In addition, I do not understand why only in Fig. 2 are the panels labelled. Panel labels would be helpful in Fig. 3 and all other multi-panel figures as well. This would simplify referencing the figures in the text, eliminating the need to always point to top, middle, bottom, left, right, etc.

We rearranged Fig. 3 following the reviewer's advise as shown in Figs. 5 and 6 of this author comment.

P31, Fig. 7: Again, I think this figure would work better laid out in a single column. In addition, I find the transition between upwelling and downwelling in these maps awkward - the zero value of delta(theta) lies between two pale blue colors, and thus cannot be readily identified.

As proposed we grouped Fig. 7 in a single column and adjusted the color bar in order that the zero value can be better identified as shown in Fig. 7 of this author comment. Further we also adjusted the color bar in Fig. A1 within the Appendix of the manuscript.

Minor points of clarification, wording suggestions, and grammar / typo corrections:

1. *P1, L9: To avoid any possibility of confusion, I think ‘boundary sources’ should be ‘boundary layer sources’; also in this line ‘transport pathway’ should just be ‘transport’*

done

2. *P2, L1: I think it would be better to add ‘and is’ between ‘summer’ and ‘associated’*

done

3. *P2, L9: a large variability – > large variability; anticyclone reaching – > anticyclone, which reaches*

done

4. *P2, L13: referred – > referred to*

done

5. *P3, L7-8: relation . . . influence – > relationship . . . influences*

done

6. *P3, L11-12: with observations of global . . . measurements of the - > with global . . . measurements from the*

done

7. *P3, L25: the the - > the; between 360 K - > from 360 K*

done

8. *P3, L33: as - > us*

done

9. *P4, L5: at top - > at the top*

done

10. *P5, L27: having ‘Tropical AR’ in quotes and bold font gives the reader the impression that this is an important acronym that will be used again, whereas ‘tropical adjacent regions’ is always written out in full in the text. ‘Tropical AR’ seems to be used only in figure labels; in Table 1 this area is referred to as ‘TAR’. It would be better to be more consistent in the usage.*

We removed the bold font of ‘Tropical AR’. We revised Section 3.3.3 and discussed the TAR tracer instead of SEA. Therefore, TAR tracer is more prominent and consistently used in the revised version of the manuscript.

11. *P6, L5: an added - > added*

done

12. *P6, L22-23: associated to – > associated with; delete ‘anymore’*

done

13. *P6, L26: Asia – > Asian*

done

14. *P7, L6 and also L8: synoptical – > synoptic*

done

15. *P7, L26: the 18 August – > 18 August*

done

16. *P8, L1: and for the – > and that for the*

done

17. *P8, L6-8: the lack of strong tracer gradients on the equatorward side of the anticyclone has been noted several times, so some references to previous work would be appropriate here.*

We introduced the following references (e.g., Ploeger et al., 2015; Santee et al., 2017).

18. *P8, L15: low values of the tropical adjacent regions – > low fractions from the tropical adjacent regions*

done

19. *P8, L24-25: this wording is confusing. It would be clearer to say: ‘At 90E (Fig. 2c), a layer of young air masses with enhanced India/China fractions extends well above the thermal tropopause, with values as high as 20% up to 420 K.’*

done

20. *P9, L4-5: ‘in particular’ is repeated twice in these lines, thus ‘restricted regions, such as’ would be better. In addition, this point was made previously not only in Section 1 as noted, but also in Section 2.4 (P6). It may not be necessary to provide this information three times, so the authors might consider deleting it from Section 2.4.*

We replaced ‘in particular’ and removed the statement in Sect. 2.4.

21. *P9, L9: delete ‘percentages of’; are marked – > is marked on the cross sections*

done

22. *P9, L18: mode – > modes; also, I feel it would be more appropriate to say ‘broadly consistent’*

done

23. *P9, 26: it would be clearer to say ‘smaller’ rather than ‘lower’ mixing ratios (since this sentence also talks about ‘below’ and ‘above’)*

done

24. *P10, L6-8: Restructuring this sentence would make it easier to interpret: ‘At 380 K, the highest fractions of air from India/China and from the tropical adjacent regions are found in the core of the anticyclone and*

at its edge, respectively.'

done

25. *P10, L10: 'vertical upward' is redundant in this context; use one or the other, not both*

done

26. *P10, L15: started - > starting; mode - > modes*

done

27. *P10, L26: upward transport - > vertical transport (to avoid repeating 'upward')*

done

28. *P10, L27: part - > parts*

done

29. *P10, L29: western and eastern part - > western and eastern parts of the anticyclone*

done

30. *P10, L30: 'vertical upward' - same comment as above*

done

31. *P11, L10: mode – > modes*

done

32. *P11, L11: to what does ‘in this region’ refer? The tropics, or 360 K, or ???*

‘in this region’ refer to the anticyclone at 360 K.

The pattern of $\Delta\Theta$ at 360 K within the anticyclone and in the tropics are very patchy, reflecting that the strong upward transport in this region is caused by single convective events.

33. *P11, L18: mode – > modes*

done

34. *P11, L29: the Appendix A – > Appendix A*

done

35. *P12, L7: boundary regions – > boundary layer regions*

done

36. *P12, L9: winter time – > winter*

done

37. *P12, L10: boundary emissions – > boundary layer emissions*

done

38. *P12, L17: larger as – > larger than; also delete '(Winter 07/08 pulse)' after 'tracer'*

done

39. *P12, L18: winter time – > winter*

done

40. *P12, L23: analysis – > reanalysis*

done

41. *12, L26: tropopause which again are – > tropopause, which in turn are*

done

42. *P12, L29: longitude – > latitude*

done

43. *P12, L32: from Summer – > from the Summer*

done

44. *P12, L34: Asia – > Asian*

done

45. *P12, L31: it might be good to add 'just' here: 'a combination of just two signals', to make a stronger contrast*

done

46. *P13, L1: winter time - > winter*

done

47. *P13, L4: velocity - > velocities; summer time - > summer*

done

48. *P13, L6: exists; that - > exist that*

done

49. *P13, L11: This point was already made in Figs. 8 and 9; thus it would be better to refer back to those figures here than to point ahead to Fig. 12, which is not introduced until the following paragraph.*

done

50. *P13, L12: boundary - > boundary layer*

done

51. *P13, L26: highest - > largest*

done

52. P13, L30: *boundary emission – > boundary layer emission*

done

53. P14, L3: *the the – > the*

done

54. P15, L17: *is already – > has already been*

done

55. P16, L20: *1 K per day - 1.5 K per day – > 1-1.5 K per day (as done everywhere else in the paper)*

done

56. P16, L22-30: *these lines are a bit garbled. First, it is odd to have a 1-sentence paragraph (L22-24). Second, L30 starts with ‘Further’ but then repeats verbatim the sentence in L23-24. These sentences need to be merged / rearranged / rewritten. Third, the sentence in L25-26 is hard to read. It would be clearer to say: ‘Thus, within the upward spiralling range above the anticyclone, young air masses from along its edge originating in the tropical adjacent regions are mixed with air masses from inside the anticyclone mainly originating in India/China.’ Finally, L29: *consisted – > consistent**

done

57. P17, L2-5: *It is stated that fresh emissions from the 2008 monsoon season do not contribute to the distribution within the tropical pipe at 550 K. However, emissions from that season would eventually reach 550 K, so this statement needs to be qualified in some way (for example, by*

adding 'before October 2008' or something similar). Similarly, it might be good to add 'in October 2008' after '550 K' in L5.

done

58. *P17, L8: here too I think it would be better to delete 'pathway'*

done

59. *P17, L13-14: region air masses from the tropical adjacent regions (Southeast Asia/tropical Pacific/northern Africa/northwestern Pacific) are transported in a substantial percentage by this pathway into the tropical pipe – > region, a substantial percentage of air masses from the tropical adjacent regions (Southeast Asia/tropical Pacific/northern Africa/northwestern Pacific) is transported by this pathway into the tropical pipe.*

done

60. *P26, Fig. 2 caption: Rather than 'first' and 'second', it may be better to refer to the tropopause as 'primary' and 'secondary'. Also, in the last sentence, 'percentages' should be deleted, and '(cross sections)' should be added after 'white lines'.*

done

61. *P27, Fig. 3 caption: thick black or grey lines – > thick black (maps) or grey (cross sections) lines*

done

62. *P29, Fig. 5 caption: reversed – > back; single – > successive*

done

63. *P30, Fig. 6 caption: reversed – > back*

done

64. *P31, Fig. 7 caption: are shown – > is shown; 1st row – > 1st panel; rows – > panels*

done

65. *P32, Fig. 8 caption: again, ‘primary’ and ‘secondary’ may be better than ‘first’ and ‘second’*

done

66. *P33, Fig. 10 caption: again, ‘primary’ and ‘secondary’ may be better than ‘first’ and ‘second’*

done

67. *P34, Fig. 11 caption: eastern mode (80E-100E) – > eastern (80E-100E) mode*

done

68. *P35, Fig. 12 caption: (1) this would be easier to read if ‘(top)’ were moved to before ‘The contribution’ in L1 and ‘(bottom)’ were moved to before ‘The contribution’ in L5. (2) ‘by October 2008’ should be added at the end of ‘550 K’ in L4. (3) ‘The contribution of the three time pulses’ – > ‘The contributions of the time pulses’ (it is confusing to say three since only two are shown). (4) in the legend of the figure itself,*

‘Residual’ should be ‘Residual surface’ to be consistent with the text.

done

69. *P36, Fig. 13 caption: transport pathway – > transport*

done

70. *P38, Fig. A2: In the legend, Residual – > Residual surface*

done

References

- Bergman, J. W., Jensen, E. J., Pfister, L., and Yang, Q.: Seasonal differences of vertical-transport efficiency in the tropical tropopause layer: On the interplay between tropical deep convection, large-scale vertical ascent, and horizontal circulations, *J. Geophys. Res.*, 117, <https://doi.org/10.1029/2011JD016992>, 2012.
- Bergman, J. W., Fierli, F., Jensen, E. J., Honomichl, S., and Pan, L. L.: Boundary layer sources for the Asian anticyclone: Regional contributions to a vertical conduit, *J. Geophys. Res.*, 118, 2560–2575, <https://doi.org/10.1002/jgrd.50142>, 2013.
- Chen, B., Xu, X. D., Yang, S., and Zhao, T. L.: Climatological perspectives of air transport from atmospheric boundary layer to tropopause layer over Asian monsoon regions during boreal summer inferred from Lagrangian approach, *Atmos. Chem. Phys.*, pp. 5827–5839, <https://doi.org/10.5194/acp-12-5827>, 2012.
- Chirkov, M., Stiller, G. P., Laeng, A., Kellmann, S., von Clarmann, T., Boone, C. D., Elkins, J. W., Engel, A., Glatthor, N., Grabowski, U., Harth, C. M., Kiefer, M., Kolonjari, F., Krummel, P. B., Linden, A., Lunder, C. R., Miller, B. R., Montzka, S. A., Mühle, J.,

- O'Doherty, S., Orphal, J., Prinn, R. G., Toon, G., Vollmer, M. K., Walker, K. A., Weiss, R. F., Wiecele, A., and Young, D.: Global HCFC-22 measurements with MIPAS: retrieval, validation, global distribution and its evolution over 2005-2012, *Atmos. Chem. Phys.*, 16, 3345–3368, <https://doi.org/10.5194/acp-16-3345-2016>, URL www.atmos-chem-phys.net/16/3345/2016/, 2016.
- Fadnavis, S., Schultz, M. G., Semeniuk, K., Mahajan, A. S., Pozzoli, L., Sonbawne, S., Ghude, S. D., Kiefer, M., and Eckert, E.: Trends in peroxyacetyl nitrate (PAN) in the upper troposphere and lower stratosphere over southern Asia during the summer monsoon season: regional impacts, *Atmos. Chem. Phys.*, 14, 12 725–12 743, <https://doi.org/10.5194/acp-14-12725-2014>, 2014.
- Garny, H. and Randel, W. J.: Transport pathways from the Asian monsoon anticyclone to the stratosphere, *Atmos. Chem. Phys.*, 16, 2703–2718, <https://doi.org/10.5194/acp-16-2703-2016>, 2016.
- Li, D., Vogel, B., Bian, J., Müller, R., Pan, L. L., Günther, G., Bai, Z., Li, Q., Zhang, J., Fan, Q., and Vömel, H.: Impact of typhoons on the composition of the upper troposphere within the Asian summer monsoon anticyclone: the SWOP campaign in Lhasa 2013, *Atmos. Chem. Phys.*, 17, 4657–4672, <https://doi.org/10.5194/acp-17-4657-2017>, URL <https://www.atmos-chem-phys.net/17/4657/2017/>, 2017.
- McKenna, D. S., Konopka, P., Groöß, J.-U., Günther, G., Müller, R., Spang, R., Offermann, D., and Orsolini, Y.: A new Chemical Lagrangian Model of the Stratosphere (CLaMS): 1. Formulation of advection and mixing, *J. Geophys. Res.*, 107, 4309, <https://doi.org/10.1029/2000JD000114>, 2002.
- Müller, S., Hoor, P., Bozem, H., Gute, E., Vogel, B., Zahn, A., Bönisch, H., Keber, T., Krämer, M., Rolf, C., Riese, M., Schlager, H., and Engel, A.: Impact of the Asian monsoon on the extratropical lower stratosphere: trace gas observations during TACTS over Europe 2012, *Atmos. Chem. Phys.*, 16, 10 573–10 589, <https://doi.org/10.5194/acp-16-10573-2016>, 2016.
- Park, M., Randel, W. J., Gettleman, A., Massie, S. T., and Jiang, J. H.: Transport above the Asian summer monsoon anticyclone inferred from Aura Microwave Limb Sounder tracers, *J. Geophys. Res.*, 112, D16309, <https://doi.org/10.1029/2006JD008294>, 2007.

- Park, M., Randel, W. J., Emmons, L. K., and Livesey, N. J.: Transport pathways of carbon monoxide in the Asian summer monsoon diagnosed from Model of Ozone and Related Tracers (MOZART), *J. Geophys. Res.*, 114, D08303, <https://doi.org/10.1029/2008JD010621>, 2009.
- Ploeger, F., Konopka, P., Müller, R., Fueglistaler, S., Schmidt, T., Manners, J. C., Groß, J.-U., Günther, G., Forster, P. M., and Riese, M.: Horizontal transport affecting trace gas seasonality in the Tropical Tropopause Layer (TTL), *J. Geophys. Res.*, 117, D09303, <https://doi.org/10.1029/2011JD017267>, 2012.
- Ploeger, F., Gottschling, C., Griebbach, S., Groß, J.-U., Günther, G., Konopka, P., Müller, R., Riese, M., Stroh, F., Tao, M., Ungermann, J., Vogel, B., and von Hobe, M.: A potential vorticity-based determination of the transport barrier in the Asian summer monsoon anticyclone, *Atmos. Chem. Phys.*, 15, 13 145–13 159, <https://doi.org/doi:10.5194/acp-15-13145-2015>, 2015.
- Ploeger, F., Konopka, P., Walker, K., and Riese, M.: Quantifying pollution transport from the Asian monsoon anticyclone into the lower stratosphere, *Atmos. Chem. Phys.*, 17, 7055–7066, <https://doi.org/10.5194/acp-17-7055-2017>, URL <https://www.atmos-chem-phys.net/17/7055/2017/>, 2017.
- Randel, W. J. and Park, M.: Deep convective influence on the Asian summer monsoon anticyclone and associated tracer variability observed with Atmospheric Infrared Sounder (AIRS), *J. Geophys. Res.*, 111, D12314, <https://doi.org/10.1029/2005JD006490>, 2006.
- Randel, W. J., Park, M., Emmons, L., Kinnison, D., Bernath, P., Walker, K. A., Boone, C., and Pumphrey, H.: Asian Monsoon Transport of Pollution to the Stratosphere, *Science*, 328, 611–613, <https://doi.org/10.1126/science.1182274>, 2010.
- Santee, M. L., Manney, G. L., Livesey, N. J., Schwartz, M. J., Neu, J. L., and Read, W. G.: A comprehensive overview of the climatological composition of the Asian summer monsoon anticyclone based on 10 years of Aura Microwave Limb Sounder measurements, *Journal of*

- Geophysical Research: Atmospheres, 122, 5491–5514, <https://doi.org/10.1002/2016JD026408>, URL <https://agupubs.onlinelibrary.wiley.com/doi/abs/10.1002/2016JD026408>, 2017.
- Schoeberl, M. R., Dessler, A. E., and Wang, T.: Simulation of stratospheric water vapor and trends using three reanalyses, *Atmos. Chem. Phys.*, 12, 6475–6487, <https://doi.org/10.5194/acp-12-6475-2012>, 2012.
- Tissier, A.-S. and Legras, B.: Convective sources of trajectories traversing the tropical tropopause layer, *Atmos. Chem. Phys.*, 16, 3383–3398, <https://doi.org/10.5194/acp-16-3383-2016>, 2016.
- Vogel, B., Günther, G., Müller, R., Groß, J.-U., Hoor, P., Krämer, M., Müller, S., Zahn, A., and Riese, M.: Fast transport from Southeast Asia boundary layer sources to northern Europe: rapid uplift in typhoons and eastward eddy shedding of the Asian monsoon anticyclone, *Atmos. Chem. Phys.*, 14, 12745–12762, <https://doi.org/10.5194/acp-14-12745-2014>, URL <http://www.atmos-chem-phys.net/14/12745/2014/>, 2014.
- Vogel, B., Günther, G., Müller, R., Groß, J.-U., and Riese, M.: Impact of different Asian source regions on the composition of the Asian monsoon anticyclone and of the extratropical lowermost stratosphere, *Atmos. Chem. Phys.*, 15, 13699–13716, <https://doi.org/10.5194/acp-15-13699-2015>, URL <http://www.atmos-chem-phys.net/15/13699/2015/>, 2015.
- Wright, J. S. and Fueglistaler, S.: Large differences in reanalyses of diabatic heating in the tropical upper troposphere and lower stratosphere, *Atmos. Chem. Phys.*, 13, 9565–9576, <https://doi.org/10.5194/acp-13-9565-2013>, 2013.
- Wright, J. S., Fu, R., Fueglistaler, S., Liu, Y. S., and Zhang, Y.: The influence of summertime convection over Southeast Asia on water vapor in the tropical stratosphere, *J. Geophys. Res.*, 116, D12302, <https://doi.org/10.1029/2010JD015416>, 2011.

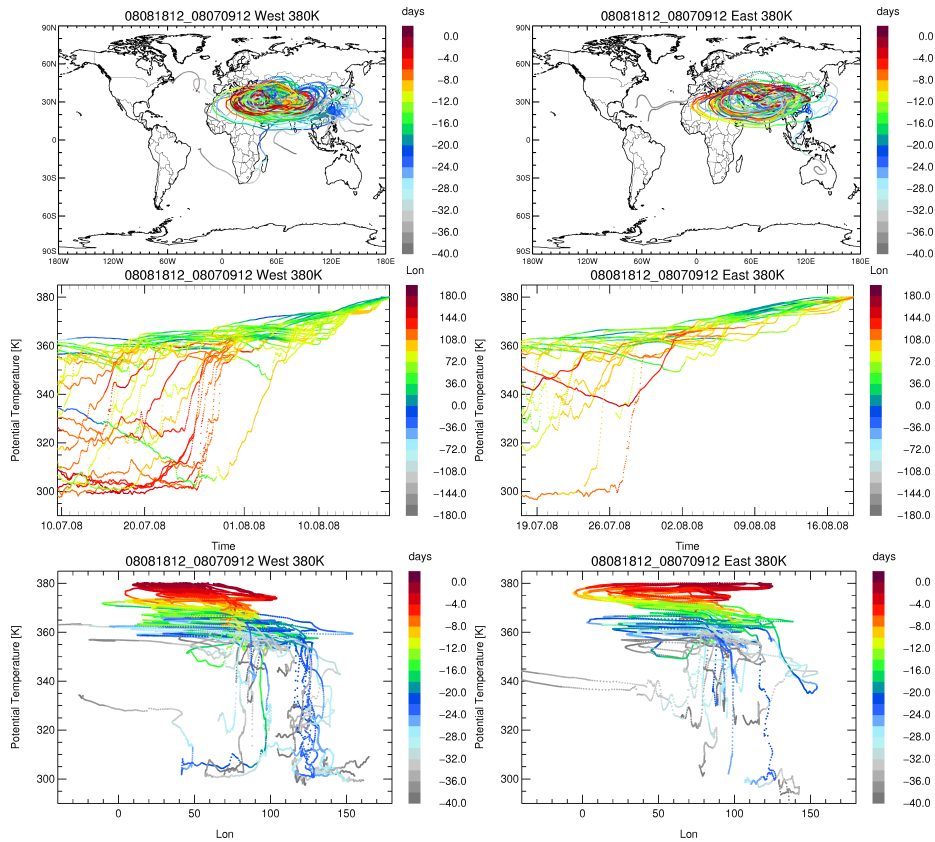


Figure 2: Different 40-day backward trajectories started at 380 K in the western (left) and eastern (right) mode of the Asian monsoon anticyclone are shown colour-coded by days back from 18 August 2008 (top). Further, potential temperature versus time (in UTC) along 40-day backward trajectories colour-coded by longitude (middle) and potential temperature versus longitude colour-coded by days back from 18 August 2008 (bottom) are shown. The trajectory positions are plotted every hour (coloured dots). Large distances between successive positions indicate rapid uplift.

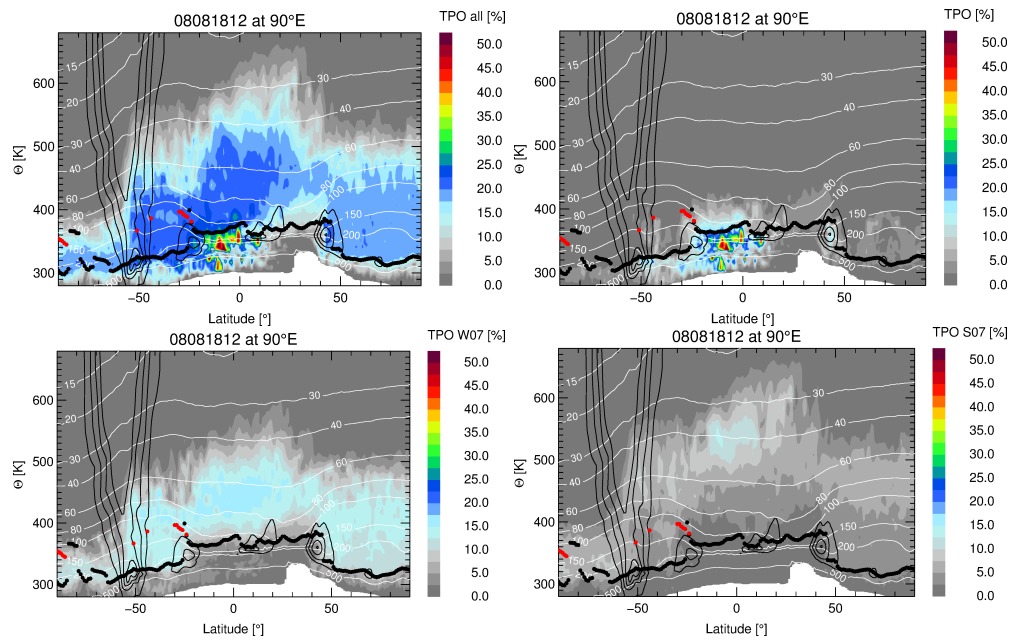


Figure 3: Latitude–theta cross sections at 90°E for the fraction of the TPO tracer for the simulation period (1 May 2007 - 18 August 2008 labeled as 'all'), for the Summer 08 (S08) pulse, for the Winter 07/08 (W07) pulse, and for the Summer 07 (S07) pulse on 18 August 2008. The thermal tropopause (primary in black dots and secondary in red dots) and horizontal winds (black lines) are shown. The corresponding levels of pressure are marked by thin white lines.

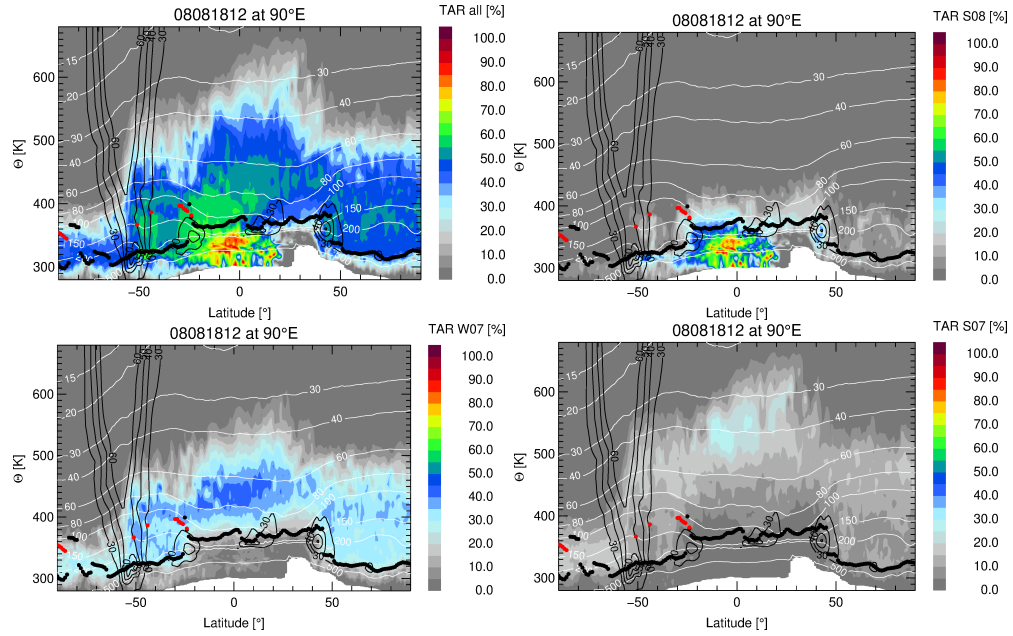


Figure 4: As Fig. 3 but for the fraction of the tracer for tropical adjacent regions (TAR)

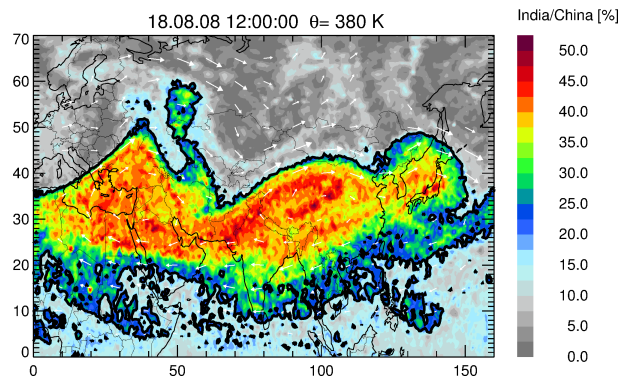


Figure 5: Horizontal distribution of the fraction of air originating in India/China at 380 K potential temperature. The contour line of 20% of the India/China tracer is shown by thick black line.

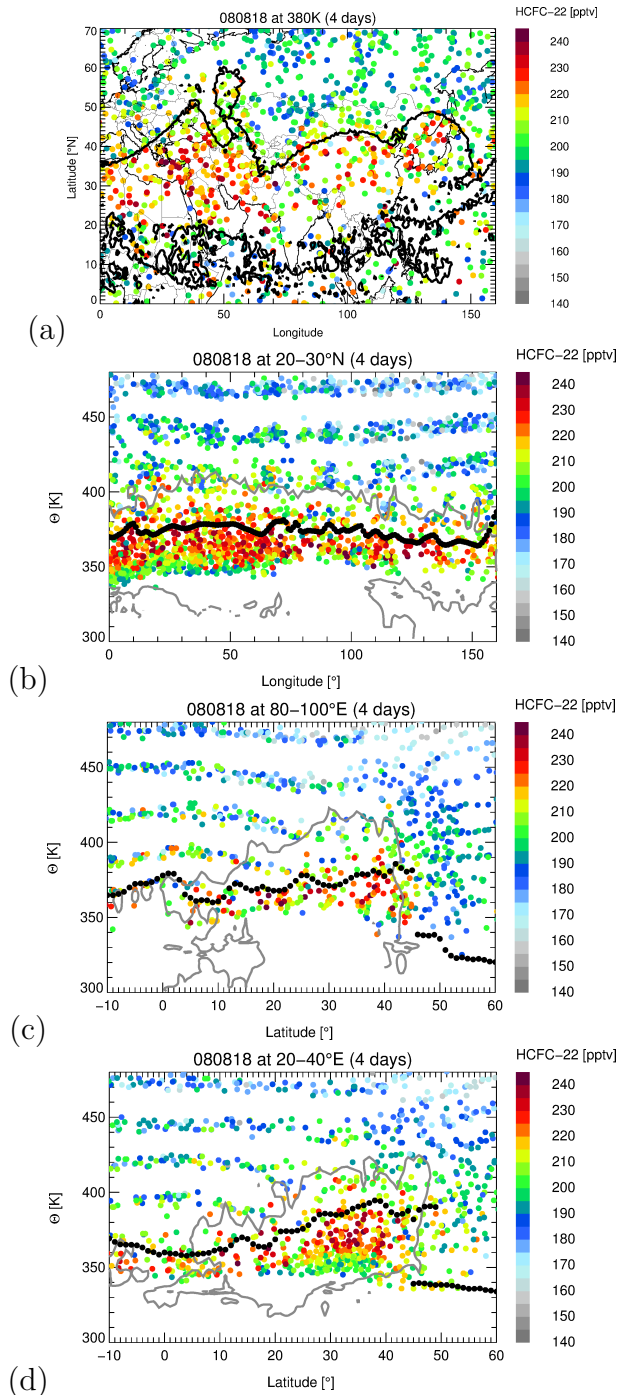


Figure 6: Horizontal distribution of MIPAS HCFC-22 measurements at 380 K potential temperature (a). The MIPAS measurements are synoptically interpolated within 4 days (for details see Sect. 2.4). Longitude–theta cross section at 25°N (b) is shown as well as latitude–theta cross sections at 90°E (eastern part of the anticyclone) (c) and at 30°E (western part of the anticyclone) (d) on 18 August 2008. The contour line of 20% of the India/China tracer is shown by thick black (maps) or grey (cross sections) lines as shown in Figs. 2 and 3. The thermal tropopause is marked by black dots.

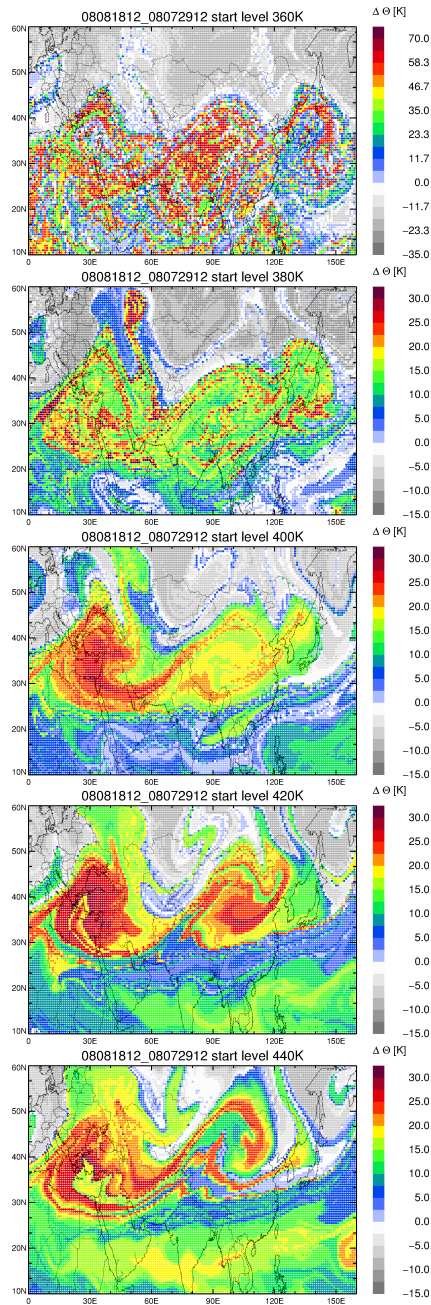


Figure 7: The change in potential temperature ($\Delta\Theta$) along 20-day backward trajectories initialised on 18 August 2008 is shown for different levels of potential temperature (360 K, 380 K, 400 K, 420 K, and 440 K). Note that the range of the colour bar in the 1st panel is much larger than in the other panels. At the lower potential temperature levels (360 K, 380 K), some 20-day backward trajectories exist that reach the model boundary layer within a time period shorter than 20 days (in cases of very strong uplift by convection). For these trajectories $\Delta\Theta$ is shown for the shorter time period.

Author Comment to Referee #2

ACP Discussions doi: 10.5194/acp-2018-724

(Editor - Peter Haynes)

‘Lagrangian simulations of the transport of young air masses to the top of the Asian monsoon anticyclone and into the tropical pipe’

We thank Referee #2 for further guidance on how to revise our paper. Following the reviewers advice we have elaborate the relation of our findings to previously published work and introduced an extended discussion of the presented results with respect to previous publications. Our reply to the reviewer comments is listed in detail below. Questions and comments of the referee are shown in italics. Passages from the revised version of the manuscript are shown in blue.

The study "Lagrangian simulations of the transport of young air masses to the top of the Asian monsoon anticyclone and into the tropical pipe" investigates transport processes from the boundary layer to the monsoon anticyclone and further into the stratosphere by employing 3-D CLaMS simulations with mixing and additional backtrajectory data. Further, comparisons with satellite data (MIPAS) are included, which increase the confidence in the presented results. Overall, the manuscript is well written and the figures and analyses are well composed. Further, the study contains interesting results suitable for publication in ACP. Nevertheless, I think that the following comments need to be addressed before the manuscript can be published. In particular, the manuscript would benefit from (and in my opinion needs) an extended discussion of the presented results with respect to previous publications.

General Comments

In the abstract and in the text, you distille the transport processes from the boundary layer to the tropical stratosphere into 3 separate regimes. In my opinion, this result is in agreement with previous notions on transport of

ASM air masse, i.e. I think it is known that the upper troposphere in the Asian summer monsoon region is strongly affected by convection (e.g. Randel and Park, 2006, show a strong impact from convection at 350- 360K), slow upward movement within the anticyclone is addressed e.g. in Park et al. (2007, 2009; see also the schematic Fig. 14 in the latter publication). Further, Ploeger et al. (2017) show slow upward transport of Asian summer monsoon air masses in the tropical pipe (cf. also Randel et al. 2010) and also presents an overview of transport processes in the ASM region in its introduction. There are also other studies addressing transport in the Asian monsoon and some that also mention slow ascent in the UT in the monsoon region: e.g. Wright et al. (2011), Bergman et al. (2012) and Garny and Randel (2016). Nevertheless, it is indeed interesting to have a single study (and model) that shows all of the transport regimes and your study includes additional information. Please, relate your results to these previous findings or suggestions and carve out how your study differs/agrees with the processes described there. How do your results complement these previous suggestions/findings? Maybe you could comment also on the influence of extremely deep (or even overshooting) convection on air masses within the UTLS in the Asian monsoon region.

Following the reviewer's advice we introduced an extended discussion of the presented results with respect to previous publications within the Discussion Section 4 in the revised version of the manuscript (see below). Further, we introduced in the Conclusion Section 5 additional references to better link to previous published work.

It is well known that the composition of the Asian monsoon anticyclone is strongly affected by convection over continental Asia (e.g. the south slope of the Himalayas and the Tibetan Plateau), Bay of Bengal, and the western Pacific, (e.g., Randel and Park, 2006; Park et al., 2007, 2009; Wright et al., 2011; Chen et al., 2012; Bergman et al., 2013; Fadnavis et al., 2014; Tissier and Legras, 2016). However there is a debate about the contribution of different source regions to the composition of the Asian monsoon anticyclone. Further, there are differences in the conclusions in the literature about the contribution of different source regions depending on the used reanalysis data (e.g., Wright et al., 2011; Bergman et al., 2013). Findings by Vogel et al. (2015) show that there is a strong intraseasonal variability of boundary source regions to the composition of the Asian monsoon anticyclone during

a particular monsoon season. We would like to emphasise that the trajectories presented in Fig. 6 demonstrating convection below 380 K are only a snapshot for 18 August 2018 with convection over the western Pacific and continental Asia mainly in the region of the south slope of the Himalayas and the Tibetan Plateau.

Here, in contrast to earlier studies, we focus on transport at the top of the anticyclone at altitudes greater than 380 K potential temperature (≈ 100 hPa) reaching up to 460 K (≈ 60 hPa). Further, in addition to previous studies (e.g., Garny and Randel, 2016; Ploeger et al., 2017), we relate the transport of air masses from inside the Asian monsoon anticyclone to air masses uplifted outside the anticyclone. Subsequently these air masses are jointly transported upwards to the top of the anticyclone at ≈ 460 K. ... (further see revised version of the manuscript).

We added in Sect. 3.3.1 the following discussion:

It is known that the radiative heating rates in the tropical UTLS are different in current reanalysis models (e.g., Wright and Fueglistaler, 2013) and are most likely overestimated in ERA-Interim (e.g., Ploeger et al., 2012; Schoeberl et al., 2012). Therefore, the rates of diabatic heating in the upward spiralling found in our study are most likely somewhat too high, however slow upward transport in the UTLS in the region of the Asian monsoon anticyclone associated with positive heating has been addressed previously (e.g., Park et al., 2007; Bergman et al., 2012; Garny and Randel, 2016; Ploeger et al., 2017).

Regarding the influence of extremely deep convection, note that in CLaMS convection is driven by ERA-Interim reanalysis data. We introduced the following paragraph within Section 2 to explain convection in CLaMS in more detail. Small-scale overshooting convection is not included in ERA-Interim, however the focus of our paper is to understand the main transport pathways at the top of the anticyclone higher than 380 K up to 460 K (≈ 100 -60 hPa) which is above the main level of tropical deep convection (e.g., Devasthale and Fueglistaler, 2010; Bergman et al., 2012).

The upward transport and convection in CLaMS (in both three-dimensional simulations as well as in trajectory calculations) is driven by ERA-Interim

reanalysis data in which changes are implemented to improve deep and mid-level convection compared to previous reanalysis data (Dee et al., 2011). However, small-scale rapid uplift in convective cores is not included. Therefore convection over Asia is most likely underestimated in ERA-Interim. However, the focus of our paper is to understand the main transport pathways at the top of the anticyclone greater than 380 K and up to 460 K (≈ 100 -60 hPa) which is above the main level of tropical deep convection (e.g., Devasthale and Fueglistaler, 2010; Bergman et al., 2012). Further, previous studies demonstrated that the vertical transport in CLaMS allows the spatio-temporal distribution of CO within the Asian monsoon anticyclone measured by the Aura Microwave Limb Sounder (MLS) to be reproduced (Vogel et al., 2015; Ploeger et al., 2017).

Related to this issue, you state a convective regime and I wonder how convection is treated in your simulations and backward trajectory calculations. Please incorporate some notion on how the setup of your simulations/trajectories will affect your results.

We revised this paragraph in Sect. 2 regarding convection in CLaMS as already stated above (see previous comment).

P.8 L.31-31: "...how can air masses...?": you pose this question, however, to me it is not clear where it is answered. Are you thinking about inmixing from the outside to the inside/edge of the AC and subsequent vertical transport. Please connect to the parts in the text where this question is answered and/or e.g. repeat the question and give the answer to it in the conclusion. Would it be possible to include the transport of air masses from adjacent regions above 380K also in your Fig. 13?

We agree it would be helpful to revisit to these questions posed within the introduction. Therefore, we refer to these two questions within the conclusions as follows.

Further between 420 K and 460 K, highest contributions from young air masses are found around the edge of the anticyclone, indicating a spatially strongly inhomogeneous ascent in the monsoon with strongest ascent at the edge. The higher in the upward spiralling range the more air masses from the stratospheric background are mixed with the young air masses transported

upwards within this upward spiralling range. Thus in this paper, we could answer the question of what are the transport pathways of young air masses at the top of the Asian monsoon into the stratosphere by the concept of the upward spiralling range.

To answer our second question of how boundary layer source regions in Asia affect the composition of the middle stratosphere within the tropical pipe at 550 K, the transport times from the Earth's surface up to this level of potential temperature need to be taken into account. In a two-monsoon-season simulation...

Moreover, following the reviewer advice we added Fig. 1 (= Fig. 15 of the revised version of the manuscript) to our manuscript.

Most of the analysis are focused on one day (18 August 2008), only. For some of the analyses this might not be important, however, other analyses might depend on the specific conditions (e.g. the split of the anticyclone) during that date/period as for example the trajectory analysis in Fig. 5. Please include some additional discussion regarding that issue. Partly, you have already addressed this issue, e.g. to complement Fig. 7 you additionally include Figure A1. I would guess that in particular the backward trajectories results are affected by the choice of the starting date and might vary throughout the monsoon season. This issue also extends to the comparison with MIPAS data and to the inferred transport on the eastern/western side of the anticyclone.

We agree that the most of the analysis is focused on 18 August 2008 as a case study. However, the results of the 3-dimensional CLaMS simulation for 18 August 2008 is a result of the interplay between convection, large-scale upward transport (driven by radiative heating), and the anticyclonic flow in the UTLS during the last weeks of the simulation. The same is true for the 40-day and 20-day backward trajectories as well as for the MIPAS measurements. Thus our results are representative for August 2008. To give a broader view, we already include 20-day backward trajectories showing different days during the monsoon season 2008 within the Appendix.

Fig. 8 in Garny and Randel (2016) shows kinematic and diabatic vertical velocities and Fig. 12 a) in Park et al. (2007) shows pressure tendencies.

These figures show ascent on the eastern side of the anticyclone and descent on the western side at levels close to (but still mostly below) the tropopause. How do your statements and your Fig. 10 relate to that? How does the climatological picture of Fig. 10 look like? Is there always (i.e. on a climatological basis) stronger heating above the western side of the anticyclone above the tropopause but cooling below? How is it on the eastern side?

Fig. 10 (= Fig. 11 of the revised version of this manuscript) shows in agreement with Garny and Randel (2016) and Park et al. (2007) downward transport (negative radiative heating) below ≈ 360 K in the western mode of the anticyclone and upward transport (positive radiative heating) above ≈ 360 K in the eastern mode on 18 August 2008. Fig. 8 in Garny and Randel (2016) shows monthly mean vertical velocity for July 2006 at 360 K using ERA-Interim data. Fig. 12a in (Park et al., 2007) shows July–August average ERA40 vertical velocity for 2000–2002 at 104 hPa. Further, also Fig. 10a in Pan et al. (2016) confirm ascent on the eastern side of the anticyclone and descent on the western side showing June–July–August vertical velocity from WACCM4-SD at 100 hPa for 2014. Thus, ascent in the eastern side of anticyclone and descent on the western side in the upper troposphere is a common feature found in our case study for the 18 August 2008 as well as in a more climatological picture reported in the literature (Park et al., 2007; Garny and Randel, 2016; Pan et al., 2016).

The focus of our study is to demonstrate that in the upward spiralling range (above 360 K) a slow upward transport is found over the region of entire anticyclone (west and east mode) with diabatic heating rates of up to 1–1.5 K inferred from ERA-interim. Our 40-day backward trajectory calculations (see Fig. 6 and 7 of the revised version of this manuscript) demonstrate that a diabatic heating above 360 K is found at both the western and eastern side of the anticyclone during August 2008. A broader climatological analysis about differences in heating rates between the western and eastern side of the anticyclone above the tropopause would be an additional project and is therefore not included in this paper.

Additionally, I think it would be very helpful if you relate the results of your tracer pulses shown in Figs. 8 and 9 to the results in Ploeger et al. (2017). In particular with respect to transport of air masses from the anticyclone to the deep stratosphere.

We extended the discussion regarding the paper by Ploeger et al. (2017) within the Discussion Section 4 as follows below. Our results agree in general with findings by Ploeger et al. (2017), however in our paper in addition the contribution of the tropical adjacent regions to the tropical pipe are quantified. Further, the tracer approach is different between Ploeger et al. (2017) and our paper.

In Ploeger et al. (2017) the anticyclone tracer is initialised with unity inside the PV contour enclosing the anticyclone core in the 370-380 K layer on each day during July-August of the years 2010-2013 and is advected as an inert tracer during the following year. On 1 July of the year thereafter, the tracer is set to zero everywhere and is then reinitialised for the following monsoon season. Thus, the anticyclone tracer is set to zero during the monsoon season in July.

In our paper, the boundary emission tracers are released within the model boundary layer each day during the course of the two-monsoon-season simulation from 1 May 2007 until 1 November 2008. Thus, the transport from the troposphere through the Asian monsoon anticyclone into the tropical pipe is continuously covered over two succeeding years.

It has been proposed that the Asian monsoon constitutes an effective transport pathway from the surface, through the Asian monsoon anticyclone, and deep into the tropical pipe based on satellite observations of hydrogen cyanide (HCN) (Randel et al., 2010). HCN is a tropospheric pollutant produced mainly by biomass burning with a strong sink on ocean surfaces. Therefore tropical ocean regions cannot be the source for HCN found in the tropical pipe. Ploeger et al. (2017) addressed this issue using CLaMS simulations marking air masses within the Asian monsoon anticyclone by a PV-gradient criterion (Ploeger et al., 2015). They find that the air mass fraction from the anticyclone correlates well with satellite measurements of HCN within the tropical pipe.

In our study, we found a similar behaviour for contributions of the India/China tracer within the tropical pipe as Randel et al. (2010) for HCN and Ploeger et al. (2017) for the simulated anticyclone air mass fraction. Ploeger et al. (2017) found a maximum anticyclone air mass fractions around 5% in the tropical pipe using 3-dimensional CLaMS simulations for 2010-2013. This is consistent to our simulations finding about 6% contributions of the India/China tracer within the tropical pipe at 550 K in 2008.

However in addition to Randel et al. (2010) and Ploeger et al. (2017), we

show that the contributions from emissions from Southeast Asia and the tropical Pacific during summer are larger than the contribution from India/China within the tropical pipe. This demonstrates that the Asian monsoon anticyclone is a more effective transport pathway for the tropical adjacent regions than for air masses from inside the anticyclone itself (India/China). From the tropical adjacent regions air masses can be transported to the edge of the Asian monsoon anticyclone and then further into the tropical pipe.

Specific comments

P1 L19-20: Regarding the effectiveness of horizontal mixing and vertical transport, Garny and Randel (2016) seem to come to a different conclusion. Please discuss (e.g. in Sect. 4) how your results agree and differ. In case of the latter please also discuss why they differ.

Many thanks for this comment. This shows that we have to be more precise in our formulations to avoid any misunderstandings. Our statement on P1 L19-20 is related to the vertical transport of air masses into the tropical pipe compared to the transport from the monsoon anticyclone into the northern extratropical lower stratosphere. In contrast, Garny and Randel (2016) compares the difference of vertical transport into the lower tropical stratosphere in the anticyclone directly above the tropopause with the isentropic transport from the monsoon anticyclone into the northern extratropical lower stratosphere. Garny and Randel (2016) found only a few percent 3%/8% (360 K/380 K) by isentropic transport, however 15% of trajectories from the Asian monsoon anticyclone reach the northern extratropical lower stratosphere after 60 days. Most of them by upward transport into the tropical stratosphere and subsequent transport into the northern extratropical lower stratosphere. In Vogel et al. (2018), we found a contribution of the India/China tracer up to 16% (at 380 K) in the northern extratropical lower stratosphere during fall 2008. The transport of the India/China tracer within the 3-dimensional CLaMS simulations includes both transport pathways: direct isentropic transport as well as vertical transport in the region of the anticyclone into the tropical stratosphere and subsequent northward transport. Therefore, the value of 15% in Garny and Randel (2016) is comparable with the value of 16% (at 380 K) in Vogel et al. (2018) and therefore in good agreement.

We revised the abstract as follows.

In the upward spiralling range, air masses are uplifted by diabatic heating across the (lapse rate) tropopause, which does not act as a transport barrier under these conditions. Further, in the upward spiralling range air masses from inside the Asian monsoon anticyclone are mixed with air masses convectively uplifted outside the core of the Asian monsoon anticyclone in the tropical adjacent regions. Further, the vertical transport of air masses from the Asian monsoon anticyclone into the tropical pipe is weak in terms of transported air masses compared to the transport from the monsoon anticyclone into the northern extratropical lower stratosphere. Air masses from the Asian monsoon anticyclone (India/China) contribute a minor fraction to the composition of air within the tropical pipe at 550 K (6%), the major fractions are from Southeast Asia (16%) and the tropical Pacific (15%).

The paragraph related to the issue within the Discussion Section 4 is revised as follows.

Vogel et al. (2016) performed a CLaMS simulation for the year 2012 using similar tracers of air mass origin as in this work and found a flooding of the northern extratropical lower stratosphere with young air masses from the region of the Asian monsoon anticyclone. The transport of young air masses (age < 6 months) into the northern extratropical lower stratosphere is calculated, resulting in up to 44% at 360 K (up to 35% at 380 K) end of October 2012, with the highest contribution from India/China up to 15% (14%) (see Fig. 14 in Vogel et al. (2016)). Here, the same analysis is performed for the simulation for 2008 and a slightly higher impact on the northern extratropical lower stratosphere is found for the year 2008, up to 48% young air at 360 K (up to 41% at 380 K) end of October 2008 and up to 18% (16%) from India/China compared to 2012 (see Appendix B). This difference is most likely caused by the interannual variability of the monsoon system. However, within the tropical pipe at 550 K, in 2008 the contributions from India/China are about 6 %, demonstrating that the transport of air masses from the Asian monsoon anticyclone into the northern extratropical lower stratosphere during boreal summer and fall is more effective than the vertical transport into the tropical pipe during the course of one year. This is consistent with Ploeger et al. (2017), who found maximum anticyclone air mass fractions around 5%

in the tropical pipe and 15% in the northern extratropical lower stratosphere using 3-dimensional CLaMS simulations for 2010-2013. In a study releasing trajectories within the Asian monsoon anticyclone, Garny and Randel (2016) found a similar values of 15% of trajectories released in the anticyclone that reach the northern extratropical lower stratosphere after 60 days (for 2006).

P3 L7-10: Regarding the connection of El Nino and La Nina with the Indian summer monsoon. You argue that 2008 was (in terms of rainfall) normal because of La Nina in the winter before, although, in the previous sentence you claim that El Nino and La Nina events tend to be connected to unusual rainfall in the following Indian summer monsoon season. This seems contradictory to me! Further, Kumar et al. (2006) show a relation of concurrent SSTs with rainfall in India (during a quick search I could not find that they are stating a connection with previous winter SSTs). Also, in Webster et al. (1998) I could not easily find to which SST anomaly they refer, i.e. previous/following winter or concurrent summer. Please comment on this and revise if necessary.

Thanks for the comment, we revised these sentences as follows and introduced a further reference to the connection between ENSO to Indian rainfall.

Further, in 2008 there was a normal monsoon season in terms of normal rainfall over India in summer 2008¹. It is established that the Indian monsoon is influenced by the El Niño Southern Oscillation (ENSO) (e.g., Kumar et al., 2006). There is evidence that a strong La Niña in winter (e.g. 2007/08 (DJF) according to the Oceanic Niño Index²) in combination with La Niña conditions during the subsequent summer (as in 2008) is correlated with normal rainfall over India with a certain variability in precipitation between different Indian regions (e.g., Chakraborty, 2018).

P5 L3-5: Is the sum of the tracers for all parcels in the boundary layer really always equal to 1 as you describe on page 5 L3-4. What if unmarked parcels from above the BL are transported into the BL? Are they removed? Otherwise, they might not be marked in the BL as marking takes place every 24h, only. Does the time step of 24h release play an important role? As

¹see e.g. <http://www.tropmet.res.in/~kolli/mol/Monsoon/Historical/air.html>

²see e.g. <http://ggweather.com/enso/oni.htm>

an example, Bergman et al (2013) use backward- trajectories started every 6 hours. Why don't you mark/emmit the tracer "continuously", i.e. at every time step of the simulation? Is there a scientific or technical reason for this setup

Thanks for the comment, in fact we have to be more precise at this point and revised the sentence as follows. We adapted also Table 1 by introducing the emission tracer for the background.

Within the model boundary layer, the sum of all the different emission tracers (Ω_i) including the emission tracer for the background (remaining surface) is equal to 1 ($\Omega = \sum_{i=1}^n \Omega_i = 1$, see Table 1) .

Air parcels in the free troposphere and stratosphere are not unmarked. They are marked with 'zero' in contrast to air parcels in the model boundary that are marked with 'one'. If air parcels from the free troposphere are transported downward into the model boundary layer, they will be overwritten by the boundary conditions every 24 hours. The setting of the emission tracers is adjusted to the mixing in CLaMS which is every 24 hours. The mixing in CLaMS is coupled to the integral deformations in the flow over the time step of transport. The critical deformation parameter λ_c can also be expressed in terms of a critical Lyapunov exponent γ_c (with $\gamma_c = \lambda_c \times \Delta t$) which depends on the advection times step (Δt). The mixing procedure in CLaMS is optimised using a γ_c equal to 1.5 for a $\Delta t = 24$ h (Konopka et al., 2007), therefore we use here a time step of 24 hours to set the boundary emission tracers. It is possible that an air parcel from the free troposphere is transported downwards into the model boundary layer and subsequently upwards out of the model boundary layer into the free troposphere within a time period lower than 24 hours without mixing. In that case the air parcel is not marked by an emission tracer. However, we think the impact of this issue is small compared to the uncertainties of the trajectory calculations itself at the lowest model levels.

P6 L1: Please add whether the trajectories described in this section are calculated using heating rates (as I would assume) or kinematic vertical velocities.

Yes, we use heating rates. We revised the sentence to be more precise as follows. Moreover, we added some further information to the vertical transport

in the model within the general CLaMS description in Sect. 2.0 (see above).

Within this study, 20-day and 40-day backward trajectories are calculated driven by wind data (with a horizontal resolution of $1^\circ \times 1^\circ$) from the ERA-Interim reanalysis (Dee et al., 2011) and using the diabatic approach to analyse the transport pathways of air parcels at the top of the Asian monsoon anticyclone and beyond into the tropical pipe.

P7 L6-9: Has the same method for interpolating MIPAS HCFC-22 data been used in Vogel et al. 2016? Then you could add a note so it is clear.

The same synoptic interpolation of MIPAS HCFC data has been used in Vogel et al. (2016) (see Fig 13). However, in Fig. 13a in Vogel et al. (2016) three-monthly mean values of HCFC for July, August and September 2008 are shown in contrast to the Figures in Vogel et al. (2018). In Vogel et al. (2018), MIPAS HCFC-22 data are shown synoptically interpolated for 18 August 2018 (see Fig. 3 and Fig. 11). Because of this difference, we think here it is better to make no reference to Vogel et al. (2016) to avoid any misunderstanding.

P8 L16 and following as well as P9 L26-27: Either in the description of Fig. 2 2nd row and Fig. 3 2nd row left or in the discussion you should draw a relation to Pan et al. (2016), who showed that upward transport (e.g. of CO) is mainly focused on the eastern side of the AC.

We added the following sentence in Sect. 3.1.1 to the discussion of Fig. 2 (2nd row):

The horizontal transport of air masses from the eastern to the western mode of the anticyclone indicated by the India/China tracer is consistent with simulations of carbon monoxide (CO) using the Whole-Atmosphere Community Climate Model (WACCM4-SD) (Pan et al., 2016).

P10 L13: Please state that you are starting trajectories only on 18 August 2018 for the analyses in Sect. 3.2.1. Or have you analysed other dates as well?

In our paper (Vogel et al., 2018), 40-day backward trajectories started on

18 August 2018 are only presented. We add the date (see below). For your information, we also performed for other days 40-day backward trajectories with similar results as for 18 August 2018. However, we decided to only present the results for the 18 August 2018 as a case study.

To analyse the transport pathways to the top of the anticyclone in more detail, 40-day backward trajectories are calculated starting in the western (20–50°N, 0–70°E) and eastern (20–50°N, 70–140°E) modes of the anticyclone. The trajectories are started at the position of the air parcels from the 3-dimensional CLaMS simulation at different levels of potential temperature ($\Theta = 380, 400, 420, 440 \text{ K} \pm 0.25 \text{ K}$) on 18 August 2018. Note that the air parcels in the 3-dimensional CLaMS simulation are distributed on an irregular grid. To take into account the distribution of the boundary emission tracer at the top of the Asian monsoon anticyclone, only air parcels are selected with contributions of young air masses (age < 6 months, Summer 08) larger than 70% (380 K), 50% (400 K), 20% (420 K), and 5% (440 K) (not all levels of potential temperature are presented here). The percentages are chosen in a way to obtain a number of trajectories (less than 30) that can be reasonably visualised. The results of the 40-day backward trajectories are similar at different levels of potential temperature; therefore we show a selection of trajectories to demonstrate the main transport pathway to the top of the Asian monsoon. A larger set of 20-day backward trajectories analysed statistically will be discussed below in Section 3.2.2.

P10 L22-23: How do you know that the transport occurs above the Tibetan Plateau? From Fig. 5 only the longitudinal range is visible but not where in latitude the parcels ascend. If you have made additional analyses to check that they are indeed from the Tibetan Plateau just note that you have analysed this but chose to not include a figure or the analysis here.

Fig. 2 (of this author comment), shows the location of the strongest updraft along the 40-day backward trajectories shown in Fig. 5 of the revised version of the manuscript. There is a cluster of trajectories in the region of the south slope of Himalayas and the Tibetan Plateau as well as in the western Pacific. We revised the sentence as follows.

Our 40-day backward trajectories show that preferred regions for fast uplift are continental Asia (mainly the region of the south slope of Himalayas and

the Tibetan Plateau) and the western Pacific (not shown here).

P10 L32: At some instances (e.g. here at P10 L32) you refer to inside or outside the anticyclone but do not give a reliable definition or state what you consider as inside or outside. Would it be an option to include PV contours for that purpose? Also on P11 L5 you should probably rephrase to "entire Asian monsoon region" because you do not start only within the anticyclone.

It is known that the Asian monsoon anticyclone has a strong horizontal transport barrier at about 380 K (e.g., Ploeger et al., 2015), however this transport barrier is missing at higher levels of potential temperature. Therefore, it is difficult to define inside/outside the anticyclone for all levels above 380 K. Here we use the emission tracer for India/China as a proxy for the location and shape of the Asian monsoon anticyclone as introduced as follows in the manuscript.

Vogel et al. (2015) showed that the emission tracer for India/China is a good proxy for the location and shape of the Asian monsoon anticyclone using pattern correlations with potential vorticity (PV), and MLS O₃ and CO satellite measurements between 360 K and 400 K. Therefore here we use the India/China tracer as proxy for the location of the anticyclone.

P11 L14: Maybe you should rephrase this part stating "At 380..." instead of "Above 380K,..." because at 400K the structures are not as inhomogeneous anymore and above 400K there is also considerable upward transport in the tropics.

As proposed we revised this paragraph as following including also comments by reviewer #1.

Above 360 K, air parcels that experienced strong upward transport larger than 20–30 K within 20 day (corresponding to a mean value of 1–1.5 K per day) are largely found in the region of the anticyclone. This rate of upwelling is much slower compared to convective upwelling shown at 360 K. Air parcels that experienced strong upward transport are mainly grouped in curved elongated filaments, reflecting a rotating movement of the air parcels at the top of the anticyclone. Often air parcels with strong $\Delta\Theta$ above 360 K are located more at the edge of the eastern and western modes of the anticyclone

and at the edge of the eastward-migrating eddy at the eastern flank of the anticyclone. Thus the upward transport in the region of the anticyclone is inhomogeneous and not homogeneously distributed over the entire anticyclone as suggested from climatological studies (e.g., Randel et al., 2010; Ploeger et al., 2017). This is consistent with results presented above in Sect. 3.2.1 demonstrating that for single selected trajectories the transport at the top of the Asian monsoon anticyclone is a slow upward transport of about 1–1.5 K per day in a large-scale spiral above the anticyclone caused by diabatic heating. In the backward trajectory calculations mixing processes are not included, however the results of the trajectory calculations are consistent with patterns found in the 3-dimensional CLaMS simulation including mixing as discussed in Sect. 3.1.3, demonstrating that young air masses above 400 K are found at the edge of the anticyclone. Above 400 K, air masses in the tropics also experienced upward transport, but the vertical uplift is in general lower than 20 K within 20 day, (i.e. lower than 1 K per day).

P. 12 L14 and L17: Two times 25% instead of 15% is mentioned, as I assume would be correct. If I am correct, the 25% are the contribution of the winter pulse (W07) at 450K, right?

Yes, we agree. However, we changed Fig. 9 (of the manuscript) showing TAR instead of SEA. For TAR 25% is correct. We changed this sentence as follows (see Figure 9 in the revised version of the manuscript).

Many thanks for this comment. 15% is correct. We corrected the percentages in the manuscript.

P14 L6-8: Do you really mean "Asian monsoon air masses from the anticyclone" or rather air masse from your India/China tracer? I think your findings show the claimed relation only for the latter.

We agree that the India/China tracer and air masses from the anticyclone are not the same, however we found in Vogel et al. (2015), that India/China tracer is a good proxy for the location and shape of the Asian monsoon anticyclone using pattern correlations with potential vorticity (PV), and MLS O₃ and CO satellite measurements as explained in Sect. 2.1 in Vogel et al. (2018). We clarified the sentence as follows:

Further, our findings show that air masses from India/China, thus mainly from the Asian monsoon anticyclone, contribute to a smaller fraction of the composition of air within the tropical pipe at 550 K; the major part is from Southeast Asia and the tropical Pacific.

P14 L30-31: I think slow upward transport has been proposed earlier (see my general comment). Please clarify if you are referring to some specific point of the upward transport process that was not published earlier.

We revised the Discussion Section 4 as discussed above and clarified that our focus is the relation of transport of air masses from inside the Asian monsoon anticyclone to air masses uplifted outside the anticyclone in an altitude range higher than 380 K potential temperature (≈ 100 hPa) up to 460 K (≈ 60 hPa).

Here, in contrast to earlier studies, we focus on transport at the top of the anticyclone at altitudes greater than 380 K potential temperature (≈ 100 hPa) reaching up to 460 K (≈ 60 hPa). Further, in addition to previous studies (e.g., Garny and Randel, 2016; Ploeger et al., 2017), we relate the transport of air masses from inside the Asian monsoon anticyclone to air masses uplifted outside the anticyclone. Subsequently these air masses are jointly transported upwards to the top of the anticyclone at ≈ 460 K.

Further we added in Sect. 3.3.1 the following discussion.

It is known that the radiative heating rates in the tropical UTLS are different in current reanalysis models (e.g., Wright and Fueglistaler, 2013) and are most likely overestimated in ERA-Interim (e.g., Ploeger et al., 2012; Schoeberl et al., 2012). Therefore, the rates of diabatic heating in the upward spiralling range found in our study are most likely somewhat too high, however slow upward transport in the UTLS in the region of the Asian monsoon anticyclone associated with positive heating has been addressed previously (e.g., Park et al., 2007; Bergman et al., 2012; Garny and Randel, 2016; Ploeger et al., 2017).

I think it would be good to label all panels of all figures with (a), (b), (c) and so on as you do for example in Fig. 3 but not in Figs. 4, 5 etc. This is just a suggestion, but would definitely help to increase the readability. Then you could refer directly to the individual panels of the figures and it would be

consitent throughout the manuscript.

done

Also, consider to add additional references to the individual panels in the text when you draw a conclusion or describe something that is based on the respective panel.

done

Minor suggestions/corrections:

1. *P1 L11: Either change to "Second, these air masses..." or "Second, air masses are uplifted within the anticyclone..." or something similar.*

done

2. *P1 L14: As before, maybe clarify by changing your sentence to something like: "Third, transport of air masses affected by the Asian monsoon (anticyclone)..." or something similar.*

done

3. *P2. L1: This probably needs some additional restriction to where the the Asian monsoon is the "most pronounced circulation pattern". Do you refer here to the tropospheric flow or the UTLS anticyclone?*

We revised the sentence as follows:

The Asian summer monsoon is associated with deep convection over the Indian subcontinent and is the most pronounced circulation pattern in boreal summer with an anticyclonic flow that extends from the upper troposphere into the lower stratosphere (UTLS) region (e.g., Li

et al., 2005; Randel and Park, 2006; Park et al., 2007).

4. *P2 L21-22: Order references according to year of publication.*

done

5. *P3 L1: Would it be better to change "defined regions" to "specific regions"?*

We prefer 'defined regions'.

6. *P3 L2: Shouldn't this read: "covering Earth's entire surface". Then it would need to be changed throughout the manuscript.*

We don't think so.

7. *P3 L32-33: Maybe change to "...a total simulation period of 18 months)."*

done

8. *P4 L2-6: The two sentences starting with "With this approach..." and "This model setup..." seem somehow repetitive. If they are not, please try to clarify.*

done

9. *P9 L4-5: Repetition of "in particular". Please rephrase.*

done

10. *P13 L6: "exists" should be "exist". Also consider to rephrase, e.g. to "... pathways exist. On these horizontal pathways, air masses are transported isentropically..."*

done

11. *P13 L10: I would suggest to shift the first sentence of the paragraph ("On 18 August...") behind the current second sentence ("To analyse...") or/and adapt as it seems to be doubled at the moment.*

no

12. *P13 L33: Probably this should be "...from the tropical..."*

done

13. *P14 L13: Are "Asian monsoon anticyclone" and "Asian monsoon" switched here?*

done

14. *P32: In the caption of Fig. 8 it should state "... (1 May 2007 - 18 August 2008) ..." instead of "... (1 May 2007 - 31 October 2008) ...", because you show the tracer distribution on 18 August 2008. This is also how you describe the figure in the text.*

done

References

Bergman, J. W., Jensen, E. J., Pfister, L., and Yang, Q.: Seasonal differences of vertical-transport efficiency in the tropical tropopause layer: On the

- interplay between tropical deep convection, large-scale vertical ascent, and horizontal circulations, *J. Geophys. Res.*, 117, <https://doi.org/10.1029/2011JD016992>, 2012.
- Bergman, J. W., Fierli, F., Jensen, E. J., Honomichl, S., and Pan, L. L.: Boundary layer sources for the Asian anticyclone: Regional contributions to a vertical conduit, *J. Geophys. Res.*, 118, 2560–2575, <https://doi.org/10.1002/jgrd.50142>, 2013.
- Chakraborty, A.: Preceding winter La Niña reduces Indian summer monsoon rainfall, *Environmental Research Letters*, 13, 054 030, URL <http://stacks.iop.org/1748-9326/13/i=5/a=054030>, 2018.
- Chen, B., Xu, X. D., Yang, S., and Zhao, T. L.: Climatological perspectives of air transport from atmospheric boundary layer to tropopause layer over Asian monsoon regions during boreal summer inferred from Lagrangian approach, *Atmos. Chem. Phys.*, pp. 5827–5839, <https://doi.org/10.5194/acp-12-5827>, 2012.
- Dee, D. P., Uppala, S. M., Simmons, A. J., Berrisford, P., Poli, P., Kobayashi, S., Andrae, U., Balmaseda, M. A., Balsamo, G., Bauer, P., Bechtold, P., Beljaars, A. C. M., van de Berg, L., Bidlot, J., Bormann, N., Delsol, C., Dragani, R., Fuentes, M., Geer, A. J., Haimberger, L., Healy, S. B., Hersbach, H., Holm, E. V., Isaksen, L., Kallberg, P., Koehler, M., Matricardi, M., McNally, A. P., Monge-Sanz, B. M., Morcrette, J.-J., Park, B.-K., Peubey, C., de Rosnay, P., Tavolato, C., Thepaut, J.-N., and Vitart, F.: The ERA-Interim reanalysis: configuration and performance of the data assimilation system, *Q. J. R. Meteorol. Soc.*, 137, 553–597, <https://doi.org/10.1002/qj.828>, 2011.
- Devasthale, A. and Fueglistaler, S.: A climatological perspective of deep convection penetrating the TTL during the Indian summer monsoon from the AVHRR and MODIS instruments, *Atmos. Chem. Phys.*, 10, 4573–4582, <https://doi.org/10.5194/acp-10-4573-2010>, URL <https://www.atmos-chem-phys.net/10/4573/2010/>, 2010.
- Fadnavis, S., Schultz, M. G., Semeniuk, K., Mahajan, A. S., Pozzoli, L., Sonbawne, S., Ghude, S. D., Kiefer, M., and Eckert, E.: Trends in

- peroxyacetyl nitrate (PAN) in the upper troposphere and lower stratosphere over southern Asia during the summer monsoon season: regional impacts, *Atmos. Chem. Phys.*, 14, 12 725–12 743, <https://doi.org/10.5194/acp-14-12725-2014>, 2014.
- Garny, H. and Randel, W. J.: Transport pathways from the Asian monsoon anticyclone to the stratosphere, *Atmos. Chem. Phys.*, 16, 2703–2718, <https://doi.org/10.5194/acp-16-2703-2016>, 2016.
- Konopka, P., Günther, G., Müller, R., dos Santos, F. H. S., Schiller, C., Ravegnani, F., Ulanovsky, A., Schlager, H., Volk, C. M., Viciani, S., Pan, L. L., McKenna, D.-S., and Riese, M.: Contribution of mixing to upward transport across the tropical tropopause layer (TTL), *Atmos. Chem. Phys.*, 7, 3285–3308, 2007.
- Kumar, K. K., Rajagopalan, B., Hoerling, M., Bates, G., and Cane, M.: Unraveling the Mystery of Indian Monsoon Failure During El Niño, *Science*, 314, 115–119, <https://doi.org/10.1126/science.1131152>, 2006.
- Li, Q., Jiang, J. H., Wu, D. L., Read, W. G., Livesey, N. J., Waters, J. W., Zhang, Y., Wang, B., Filipiak, M. J., Davis, C. P., Turquety, S., Wu, S., Park, R. J., Yantosca, R. M., and Jacob, D. J.: Convective outflow of South Asian pollution: A global CTM simulation compared with EOS MLS observations, *Geophys. Res. Lett.*, 32, L14 826, <https://doi.org/10.1029/2005GL022762>, 2005.
- Pan, L. L., Honomichl, S. B., Kinnison, D. E., Abalos, M., Randel, W. J., Bergman, J. W., and Bian, J.: Transport of chemical tracers from the boundary layer to stratosphere associated with the dynamics of the Asian summer monsoon, *Journal of Geophysical Research: Atmospheres*, 121, 14,159–14,174, <https://doi.org/10.1002/2016JD025616>, URL <https://agupubs.onlinelibrary.wiley.com/doi/abs/10.1002/2016JD025616>, 2016.
- Park, M., Randel, W. J., Gettleman, A., Massie, S. T., and Jiang, J. H.: Transport above the Asian summer monsoon anticyclone inferred from Aura Microwave Limb Sounder tracers, *J. Geophys. Res.*, 112, D16309, <https://doi.org/10.1029/2006JD008294>, 2007.

- Park, M., Randel, W. J., Emmons, L. K., and Livesey, N. J.: Transport pathways of carbon monoxide in the Asian summer monsoon diagnosed from Model of Ozone and Related Tracers (MOZART), *J. Geophys. Res.*, 114, D08303, <https://doi.org/10.1029/2008JD010621>, 2009.
- Ploeger, F., Konopka, P., Müller, R., Fueglistaler, S., Schmidt, T., Manners, J. C., Groß, J.-U., Günther, G., Forster, P. M., and Riese, M.: Horizontal transport affecting trace gas seasonality in the Tropical Tropopause Layer (TTL), *J. Geophys. Res.*, 117, D09303, <https://doi.org/10.1029/2011JD017267>, 2012.
- Ploeger, F., Gottschling, C., Griebbach, S., Groß, J.-U., Günther, G., Konopka, P., Müller, R., Riese, M., Stroh, F., Tao, M., Ungermann, J., Vogel, B., and von Hobe, M.: A potential vorticity-based determination of the transport barrier in the Asian summer monsoon anticyclone, *Atmos. Chem. Phys.*, 15, 13 145–13 159, <https://doi.org/doi:10.5194/acp-15-13145-2015>, 2015.
- Ploeger, F., Konopka, P., Walker, K., and Riese, M.: Quantifying pollution transport from the Asian monsoon anticyclone into the lower stratosphere, *Atmos. Chem. Phys.*, 17, 7055–7066, <https://doi.org/10.5194/acp-17-7055-2017>, URL <https://www.atmos-chem-phys.net/17/7055/2017/>, 2017.
- Randel, W. J. and Park, M.: Deep convective influence on the Asian summer monsoon anticyclone and associated tracer variability observed with Atmospheric Infrared Sounder (AIRS), *J. Geophys. Res.*, 111, D12314, <https://doi.org/10.1029/2005JD006490>, 2006.
- Randel, W. J., Park, M., Emmons, L., Kinnison, D., Bernath, P., Walker, K. A., Boone, C., and Pumphrey, H.: Asian Monsoon Transport of Pollution to the Stratosphere, *Science*, 328, 611–613, <https://doi.org/10.1126/science.1182274>, 2010.
- Schoeberl, M. R., Dessler, A. E., and Wang, T.: Simulation of stratospheric water vapor and trends using three reanalyses, *Atmos. Chem. Phys.*, 12, 6475–6487, <https://doi.org/10.5194/acp-12-6475-2012>, 2012.
- Tissier, A.-S. and Legras, B.: Convective sources of trajectories traversing the tropical tropopause layer, *Atmos. Chem. Phys.*, 16, 3383–3398, <https://doi.org/10.5194/acp-16-3383-2016>, 2016.

- Vogel, B., Günther, G., Müller, R., Groß, J.-U., and Riese, M.: Impact of different Asian source regions on the composition of the Asian monsoon anticyclone and of the extratropical lowermost stratosphere, *Atmos. Chem. Phys.*, 15, 13 699–13 716, <https://doi.org/10.5194/acp-15-13699-2015>, URL <http://www.atmos-chem-phys.net/15/13699/2015/>, 2015.
- Vogel, B., Günther, G., Müller, R., Jens-Uwe Groß, A. A., Bozem, H., Hoor, P., Krämer, M., Müller, S., Riese, M., Rolf, C., Spelten, N., Stiller, G. P., Ungermann, J., and Zahn, A.: Long-range transport pathways of tropospheric source gases originating in Asia into the northern lower stratosphere during the Asian monsoon season 2012, *Atmos. Chem. Phys.*, 16, 15 301–15 325, <https://doi.org/10.5194/acp-16-15301-2016>, URL <http://www.atmos-chem-phys.net/16/15301/2016/>, 2016.
- Vogel, B., Müller, R., Günther, G., Spang, R., Hanumanthu, S., Li, D., Riese, M., and Stiller, G. P.: Lagrangian simulations of the transport of young air masses to the top of the Asian monsoon anticyclone and into the tropical pipe, *Atmos. Chem. Phys. Discuss.*, 2018, 1–38, <https://doi.org/10.5194/acp-2018-724>, URL <https://www.atmos-chem-phys-discuss.net/acp-2018-724/>, 2018.
- Wright, J. S. and Fueglistaler, S.: Large differences in reanalyses of diabatic heating in the tropical upper troposphere and lower stratosphere, *Atmos. Chem. Phys.*, 13, 9565–9576, <https://doi.org/10.5194/acp-13-9565-2013>, 2013.
- Wright, J. S., Fu, R., Fueglistaler, S., Liu, Y. S., and Zhang, Y.: The influence of summertime convection over Southeast Asia on water vapor in the tropical stratosphere, *J. Geophys. Res.*, 116, D12302, <https://doi.org/10.1029/2010JD015416>, 2011.

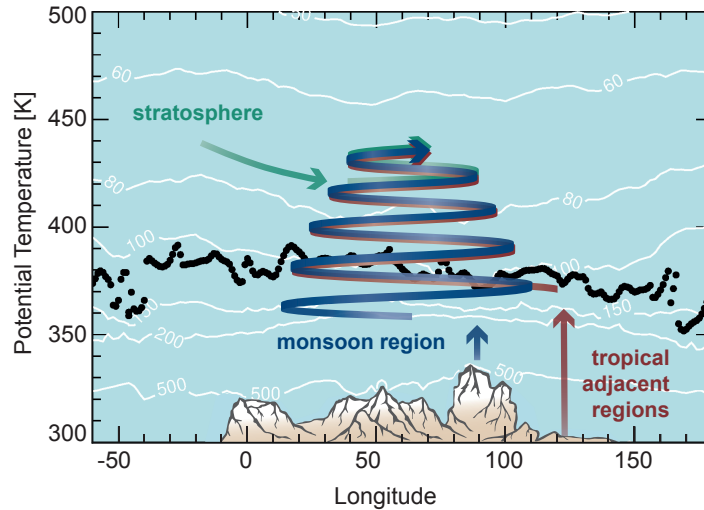


Figure 1: Longitude-theta cross section at 30°N: At the top of the Asian monsoon anticyclone (above ≈ 360 K) air masses circulate around the anticyclone in a large-scale upward spiral extending from northern Africa to the western Pacific. In the upward spiralling range air masses from inside the Asian monsoon anticyclone (shown in blue) are mixed with air masses convectively uplifted outside the core of the Asian monsoon anticyclone in the tropical adjacent regions e.g. uplifted by tropical cyclones in the western Pacific ocean (shown in red). The higher above the thermal tropopause the larger is the contribution of air masses from outside the Asian monsoon anticyclone from the stratospheric background coming into the upward spiralling flow (shown in green). The levels of pressure are marked by thin white lines and the thermal tropopause is shown by black dots.

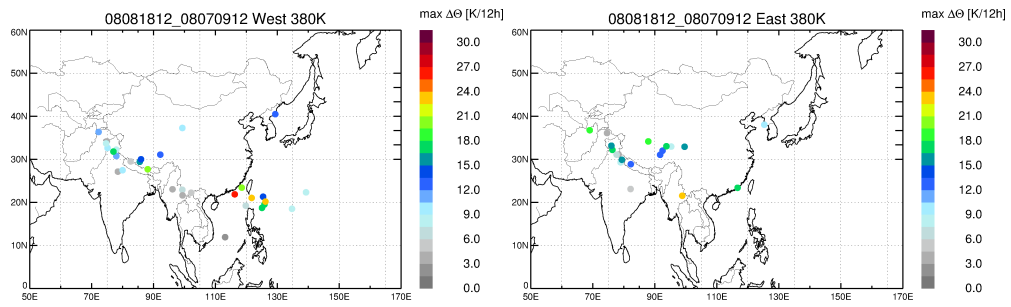


Figure 2: The geographical position of the strongest updraft along the 40-day backward trajectories in the western and eastern mode of the anticyclone (started at 380 K) shown in Fig. 5 of the revised version of the manuscript.

Author Comment to Referee #3

ACP Discussions doi: 10.5194/acp-2018-724

(Editor - Peter Haynes)

‘Lagrangian simulations of the transport of young air masses to the top of the Asian monsoon anticyclone and into the tropical pipe’

We thank Referee #3 for further guidance on how to revise our paper. Following the reviewers advice we have elaborated the relation of our findings to previously published work regarding the ‘longstanding debate’ and introduced an extended discussion of the presented results with respect to previous publications. Our reply to the reviewer comments is listed in detail below. Questions and comments of the referee are shown in italics. Passages from the revised version of the manuscript are shown in blue.

The manuscript ‘Lagrangian simulations of the transport of young air masses to the top of the Asian monsoon anticyclone and into the tropical pipe’ investigates transport pathways in the monsoon region from the boundary layer into the stratosphere. The authors use both Lagrangian backward trajectory calculations and three-dimensional simulations including irreversible mixing with the Lagrangian transport model CLaMS. Artificial tracers of air mass origin are compared to measurements of chlorodifluoromethane (HCFC-22; CHClF₂) by the Michelson Interferometer for Passive Atmospheric Sounding (MIPAS). The methods are similar to those in Vogel et al. (2016) but in addition to horizontal transport they address vertical transport pathways out of the Asian monsoon anticyclone and subsequent upward transport into the lower stratosphere. The chosen period is a normal monsoon season in terms of medium rainfall over India in summer 2008. The paper presents an interesting description of the ‘spiralling staircase’. Consistency with MIPAS data supports the model results. The paper is well written and I support publication after a few comments have been addressed. The heavy focus on a particular day is didactical, but the analysis of different meteorological situations would provide stronger evidence. In certain passages the phrasing could be improved in order to more clearly distinguish what is the particular contribution of this

study to the ‘longstanding debate about the transport mechanisms at the top of the Asian monsoon anticyclone and beyond into the stratosphere’. The debate is mentioned again in the discussion but the different arguments about ‘the exact transport mechanism’ could be more clearly stated. Otherwise it is difficult to distinguish if some very general assertions have been stated before in the literature or are novel to this work. The figures could be improved and the description thereof clarified in the text.

We revised the paper following the referee’s advice and added an extended discussion section to the revised manuscript to point out the relation of our findings to the existing literature.

Minor comments:

1. *p1 l19 ‘However, this upward transport’: Make ‘this’ more clear (the upward spiralling range).*

We revised this part in the abstract as follows.

Moreover, the vertical transport of air masses from the Asian monsoon anticyclone into the tropical pipe is weak in terms of transported air masses compared to the transport from the monsoon anticyclone into the northern extratropical lower stratosphere.

2. *p2 l20 Briefly mention the sides in the debate and state where the authors stand.*

We revised this part in the introduction as follows.

The Asian monsoon circulation provides an effective pathway for tropospheric trace gases such as pollutants, gaseous aerosol precursors, as well as aerosol particles into the lower stratosphere which could play an important role in the formation of ATAL layer (e.g., Vernier et al., 2015, 2018; Höpfner et al., 2016; Brunamonti et al., 2018). There is also export of monsoon air quasi-isentropically out of the monsoon and

a certain fraction of monsoon air may reach greater altitudes in the stratosphere. There is a longstanding debate about the transport mechanisms at the top of the Asian monsoon anticyclone and beyond into the stratosphere (e.g., Bannister et al., 2004; Park et al., 2009; Randel et al., 2010; Bergman et al., 2012, 2013; Randel and Jensen, 2013; Uma et al., 2014; Orbe et al., 2015; Garny and Randel, 2016; Tissier and Legras, 2016; Ploeger et al., 2017). In the literature different aspects of the complex interplay between convection, large-scale upward transport (driven by radiative heating), and the anticyclonic flow in the UTLS are highlighted. Randel et al. (2010) pointed out that the monsoon circulation provides an effective pathway for pollution from Asia to enter the global stratosphere. Vertical upward transport into the deep stratosphere occurs within the tropical pipe, where tropical air masses are isolated to some extent from isentropic mixing with mid-latitude air (e.g., Plumb, 1996; Volk et al., 1996). Bourassa et al. (2012) analysed the eruption of the Nabro volcano in northeastern Africa and reported that the volcanic aerosol enhancement from the Nabro eruption was not injected directly into the stratosphere. They conclude that volcanic aerosol only attained stratospheric altitudes through subsequent transport processes associated with deep convection in the region of the Asian monsoon anticyclone. Pan et al. (2016) highlight that the Asian monsoon anticyclone is an isolated ‘bubble’ of tropospheric air above the global mean tropical tropopause that isentropically sheds tropospheric air into the stratosphere. Further, they argue that the vertical transport of Asian monsoon air into the deep stratosphere is inefficient during summer..

3. *p5 l3 $\zeta < 120K$? p5 l 17 ‘is quantified.’ What will be the quantitative measure?*

In CLaMS a pressure-based coordinate system (σ coordinates) is used for pressure levels greater than 300 hPa with a hybrid vertical coordinate (ζ) (for more details, see Konopka et al., 2012; Pommrich et al., 2014). The model boundary layer is defined ≈ 2 –3 km above the surface following orography corresponding to $\zeta < 120$ K. The emission tracers are set in the model boundary layer every 24 hours and are transported (advection and mixing) into the free troposphere and stratosphere during the course of the simulation. The fraction of different emission

tracers of an air parcel, e. g. in the tropical pipe, is a measure to quantify the transport from the source region into the tropical pipe during the course of the simulation.

4. *p6 l8 Dee et al. (2011) already cited in the first reference to ERAI in p4 l11*

Yes, Dee et al. is cited twice. However, for clarification we think it is good to cite once again Dee et al. in Sect. 2.2.

5. *p7 l20 make more explicit the dates of the monsoon and the pulse releases to clarify the 6 month age.*

We revised the sentence as follows.

To analyse the transport pathways at the top of the Asian monsoon anticyclone during the monsoon season 2008, we use only the tracers of air mass origin for the time pulse for Summer 08 (started on 1 May 2008 until end of October 2008).

6. *l22 'have strong variability from day to day' please rephrase*

The geographic position and shape of the Asian monsoon anticyclone show a strong day-to-day variability.

7. *p8 l1 mention the 360 theta level before in the text to streamline the reading*

Thanks for the this comment. We agree that the 360 K level was introduced too abruptly. We added the following paragraph at the beginning of Sect. 3.1.1.

It is known that the Asian monsoon anticyclone has a strong horizontal transport barrier at about 380 K (e.g., Ploeger et al., 2015), however this transport barrier is not well defined at higher levels of potential temperature. The less strong transport barrier at higher levels has consequences on the vertical transport at the top of the anticyclone. Before the transport at the top is discussed we show the horizontal distribution of different emission tracers at 360 K and then their subsequent transport to the top of the anticyclone up to 460 K. Vogel et al. (2015) showed that the emission tracer for India/China is a good proxy for the location and shape of the Asian monsoon anticyclone using pattern correlations with potential vorticity (PV), and MLS O₃ and CO satellite measurements between 360 K and 400 K. Therefore here we use the India/China tracer as a proxy for the location of the anticyclone.

8. *p8 l10 'simulated horizontal gradients': is there an objective metric or visual inspection? How is the top of the asian monsoon precisely defined?*

We removed this statement about tracer gradients. The objective metric is the tracer distribution of air masses released by the time pulse for Summer08 (India/China tracer and tropical adjacent regions). A precise definition of the top of the Asian monsoon does not exist in the literature. In our simulations we use the contribution of the emission tracers for India/China and the tropical adjacent regions to infer the top of the Asian monsoon.

9. *p8 l17 Fig. 2 (3rd row), to be consistent with previous paragraph.*

done

10. *p10 l15 When are the trajectories started? How many? What release pattern? It would help for understanding what was done to state this clearly in the text. 40 days could be analysed statistically, bur for individual trajectories is a little bit too long.*

We agree that the description of the initialisation procedure of the trajectories is a bit short. The 40-day backward trajectories are presented to illustrate the main transport pathways. A more statistical analysis is presented in Sect. 3.2.2 for global 20-day backward trajectories. We revised this paragraph as follows.

To analyse the transport pathways to the top of the anticyclone in more detail, 40-day backward trajectories are calculated starting in the western (20–50°N, 0–70°E) and eastern (20–50°N, 70–140°E) modes of the anticyclone. The trajectories are started at the position of the air parcels from the 3-dimensional CLaMS simulation at different levels of potential temperature ($\Theta = 380, 400, 420, 440 \text{ K} \pm 0.25 \text{ K}$) on 18 August 2018. Note that the air parcels in the 3-dimensional CLaMS simulation are distributed on an irregular grid. To take into account the distribution of the boundary emission tracer at the top of the Asian monsoon anticyclone, only air parcels are selected with contributions of young air masses (age < 6 months, Summer 08) larger than 70% (380 K), 50% (400 K), 20% (420 K), and 5% (440 K) (not all levels of potential temperature are presented here). The percentages are chosen in a way to obtain a number of trajectories (less than 30) that can be reasonably visualised. The results of the 40-day backward trajectories are similar at different levels of potential temperature; therefore we show a selection of trajectories to demonstrate the main transport pathway to the top of the Asian monsoon. A larger set of 20-day backward trajectories analysed statistically will be discussed below in Section 3.2.2.

11. *p10 l20 describe the panels of fig 5 in the text.*

We revised the text as follows. Note that Fig. 5 from the ACPD version of the manuscript is Fig. 6 in the revised version.

Fig. 6 shows trajectories started in the eastern and western part of the Asian monsoon anticyclone around the thermal tropopause at 380 K on 18 August 2018. Air masses are uplifted to approximately 360 K very rapidly by various convective events occurring at different times and locations. Our 40-day backward trajectories show that preferred regions

for fast uplift are continental Asia (mainly the region of the south slope of Himalayas and the Tibetan Plateau) and the western Pacific (not shown here). A lower fraction of trajectories originates in the free troposphere. The trajectories in Fig. 6 demonstrating convection below 380 K are only a snapshot for 18 August 2018. There are several previous studies (e.g., Randel and Park, 2006; Park et al., 2007, 2009; Wright et al., 2011; Chen et al., 2012; Bergman et al., 2013; Fadnavis et al., 2014; Tissier and Legras, 2016) quantifying the contribution of different source regions to the composition of the Asian monsoon anticyclone during the course of the monsoon season (see discussion in Sect. 4).

12. *p10 last paragraph. At this point the reader would feel satisfied with a statistical analysis of a larger number of days to support the case study results. Maybe some additional results such as those later presented in A1 could be mentioned.*

As mentioned above a statistical analysis of 20-day backward trajectories for the 18 August 2018 is presented in Sect. 3.2.2.

13. *p11 l4 what do you mean with ‘single selected trajectories’?*

We revised the text as follows:

In the previous section, the transport pathways for a restricted number of trajectories were discussed. Here, for a broader view 20-day backward trajectories for the entire region of the Asian monsoon anticyclone are presented.

14. *p11 l32 ‘In the previous sections, we could show that the Asian monsoon is an effective circulation pattern in the UTLS that transports very young air masses (< 6 months) from the surface into the lower stratosphere up to ≈ 460 K.’ This may have been mentioned before in the literature. You could rephrase this as ‘we could show how the effective circulation pattern in the UTLS can be seen with CLaMS and MIPAS data’, for example. Also it seems that all your conclusions will be drawn*

from a single day case study. Additional statistical evidence from more modelling cases could help.

As proposed by referee #3, we revised the text as follows.

In the previous sections using CLaMS model simulations and MIPAS HCFC-22 measurements, we could show that the circulation of the Asian monsoon is effective in transporting very young air masses (< 6 months) from the surface into the lower stratosphere up to ≈ 460 K.

We agree that the most of the analysis is focused on 18 August 2008 as a case study. However, the results of the 3-dimensional CLaMS simulation for 18 August 2008 is a result of the interplay between convection, large-scale upward transport (driven by radiative heating), and the anticyclonic flow in the UTLS during the last weeks of the simulation. The same is true for the 40-day and 20-day backward trajectories as well as for the MIPAS measurements. Thus our results are representative for August 2008. To give a broader view, we already include 20-day backward trajectories showing different days during the monsoon season 2008 within the Appendix.

15. *12 4 is it a CLaMS simulation?*

Yes, it is a CLaMS simulation as described in Sect. 2.1.

16. *Fig 8. The figure is difficult to read. The label at the color bar is very small and takes time to find. You could replace the title of the subplots '08081812 at 90 E' that is the same for all and put it in the caption. 'horizontal winds (black lines)', do you mean horizontal wind absolute value isolines? 'corresponding levels of pressure' corresponding to what? 'Pressure levels as white lines' would be better. Are the values really zero in W07 (lower left panel) or is the color scale?*

Following the referee's advice we revised the figure caption as shown in Fig. 1 of this author comment (= Fig. 9 of the revised version of this

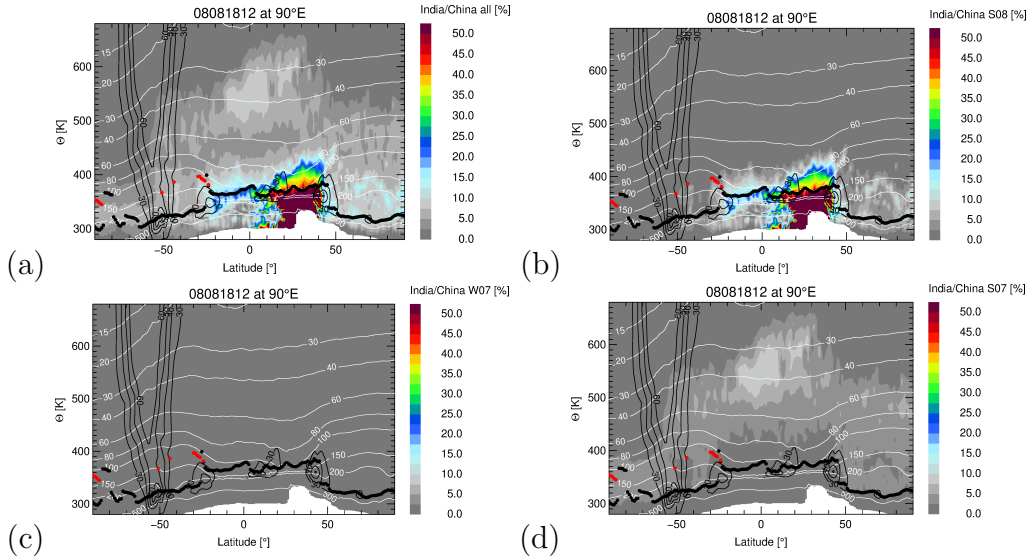


Figure 1: Latitude–theta cross sections at 90°E for the fraction of the India/China tracer for the simulation period (1 May 2007 - 18 August 2008 labeled as ‘all’) (a), for the Summer 08 (S08) pulse (b), for the Winter 07/08 (W07) pulse (c), and for the Summer 07 (S07) pulse (d) on 18 August 2008. The thermal tropopause (primary in black dots and secondary in red dots) and absolute horizontal winds (black lines for 30, 40, 50, and 60 m/s) are shown. The levels of pressure are marked by thin white lines. Note that the maximum value for the Winter 07/08 (W07) pulse (c) is 2.4%.

manuscript).

Further we removed ‘corresponding’ in all figure captions of the revised manuscript. The ‘horizontal winds (black lines)’ are calculated by $\sqrt{u^2 + v^2}$ and isolines for 30, 40, 50, and 60 m/s are shown and labelled. The maximum value for W07 is 2.4%.

17. *‘demonstrating’ may sound a bit strong for this context. ‘Suggesting’ or ‘indicating’ could fit better.*

We revised the sentence as follows.

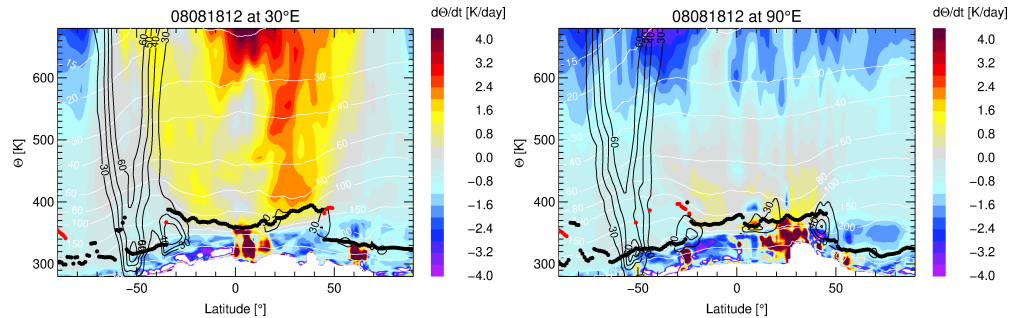


Figure 2: Latitude–theta cross section of $d\Theta/dt$ showing the radiative heating above the Asian monsoon anticyclone for the western (30°E) and eastern mode (90°E) of the anticyclone on 18 August 2008. The thermal tropopause (primary in black dots and secondary in red dots) and absolute horizontal winds (black lines for 30, 40, 50, and 60 m/s) are shown. The pressure levels are marked by thin white lines.

Fractions of air from the India/China tracer for the time pulse for Winter 07/08 are below 2.4%, indicating that during winter in the absence of the Asian monsoon anticyclone the transport of boundary layer emissions from India/China into the stratosphere is insignificant weak.

18. *p12 l14 If still describing Fig. 9 better to keep the same paragraph.*

done

19. *Figure 10: again, wind speed contours, ‘pressure levels’ instead of ‘corresponding levels of pressure’*

Following the referee’s advice we revised the figure caption as shown in Fig. 1 of this author comment (= Fig. 11 of the revised version of this manuscript).

20. *p13 l11: attract the attention of the reader to the vertical dashed line immediately here.*

We added in the figure caption of Fig. 12 of the ACPD version (=Fig. 13 of the revised manuscript) the following explanation.

Top: The contribution of the three different time pulses S07, W07, and S08 (each set for a time period of 6 months marked the vertical dotted lines) for the entire Earth's surface (Ω_{S07} , Ω_{W07} , Ω_{S08}) to the tropical pipe between 30°S and 30°N at 550 K potential temperature from 1 October 2007 until the end of the simulation period (31 October 2008) (top, black lines).

21. *Fig 13 what is the dashed line?*

The dashed line marks the tropical pipe as described in the revised figure caption as follows.

The dashed line marks the tropical pipe which isolates tropical air masses largely from isentropic mixing with mid-latitude air (e.g., Plumb, 1996; Volk et al., 1996).

22. *p15 l12 please refer to the published version.*

The paper Hanumanthu et al., 2018 is not as yet published, therefore we refer here to Vernier et al. (2015, 2018); Brunamonti et al. (2018).

23. *p16 l17 'Thus, air masses in the upward spiral range are uplifted by diabatic heating across the (lapse rate) tropopause, which does not act as a transport barrier against this diabatic vertical transport process.': This assertion is likely to be 'consistent with previous studies'.*

We added the following references in the revised version of the paper.

Thus, air masses in the upward spiralling range are uplifted by diabatic heating across the (lapse rate) tropopause, which does not act

as a transport barrier against this diabatic vertical transport process. This transport across the tropopause is consistent with previous studies (e.g., Bergman et al., 2012; Garny and Randel, 2016; Ploeger et al., 2017).

24. *p16 l 22 occurs where?*

We revised this paragraph as follows:

Above 380 K, within the upward spiralling range above the anticyclone, young air masses from along the edge of the anticyclone originating in the tropical adjacent regions are mixed with air masses from inside the anticyclone mainly originating in India/China. Therefore, a significant fraction of air masses from the tropical adjacent regions is found within a widespread area around the anticyclone and above caused by the large-scale anticyclonic flow in this region, acting as a large-scale stirrer. This transport pattern up to 460 K is consistent with previous results focused on lower levels of potential temperature (up to ≈ 400 K (Vogel et al., 2014, 2016; Li et al., 2017)).

25. *The last paragraph is a nice summary of the mechanism but it undoubtedly draws from the conclusions of many previous studies. This should somehow be acknowledged.*

We added within the conclusions in the revised version of the manuscript some additional references.

References

Bannister, R. N., O'Neill, A., Gregory, A. R., and Nissen, K. M.: The role of the south-east Asian monsoon and other seasonal features in creating the 'tape-recorder' signal in the Unified Model, Q. J. R. Meteorol. Soc., 130, 1531–1554, 2004.

- Bergman, J. W., Jensen, E. J., Pfister, L., and Yang, Q.: Seasonal differences of vertical-transport efficiency in the tropical tropopause layer: On the interplay between tropical deep convection, large-scale vertical ascent, and horizontal circulations, *J. Geophys. Res.*, 117, <https://doi.org/10.1029/2011JD016992>, 2012.
- Bergman, J. W., Fierli, F., Jensen, E. J., Honomichl, S., and Pan, L. L.: Boundary layer sources for the Asian anticyclone: Regional contributions to a vertical conduit, *J. Geophys. Res.*, 118, 2560–2575, <https://doi.org/10.1002/jgrd.50142>, 2013.
- Bourassa, A. E., Robock, A., Randel, W. J., Deshler, T., Rieger, L. A., Lloyd, N. D., Llewellyn, E. J. T., and Degenstein, D. A.: Large Volcanic Aerosol Load in the Stratosphere Linked to Asian Monsoon Transport, *Science*, 337, 78–81, <https://doi.org/10.1126/science.1219371>, 2012.
- Brunamonti, S., Jorge, T., Oelsner, P., Hanumanthu, S., Singh, B. B., Kumar, K. R., Sonbawne, S., Meier, S., Singh, D., Wienhold, F. G., Luo, B. P., Boettcher, M., Poltera, Y., Jauhiainen, H., Kayastha, R., Karmacharya, J., Dirksen, R., Naja, M., Rex, M., Fadnavis, S., and Peter, T.: Balloon-borne measurements of temperature, water vapor, ozone and aerosol backscatter on the southern slopes of the Himalayas during StratoClim 2016–2017, *Atmos. Chem. Phys.*, 18, 15 937–15 957, <https://doi.org/10.5194/acp-18-15937-2018>, URL <https://www.atmos-chem-phys.net/18/15937/2018/>, 2018.
- Chen, B., Xu, X. D., Yang, S., and Zhao, T. L.: Climatological perspectives of air transport from atmospheric boundary layer to tropopause layer over Asian monsoon regions during boreal summer inferred from Lagrangian approach, *Atmos. Chem. Phys.*, pp. 5827–5839, <https://doi.org/10.5194/acp-12-5827>, 2012.
- Fadnavis, S., Schultz, M. G., Semeniuk, K., Mahajan, A. S., Pozzoli, L., Sonbawne, S., Ghude, S. D., Kiefer, M., and Eckert, E.: Trends in peroxyacetyl nitrate (PAN) in the upper troposphere and lower stratosphere over southern Asia during the summer monsoon season: regional impacts, *Atmos. Chem. Phys.*, 14, 12 725–12 743, <https://doi.org/10.5194/acp-14-12725-2014>, 2014.

- Garny, H. and Randel, W. J.: Transport pathways from the Asian monsoon anticyclone to the stratosphere, *Atmos. Chem. Phys.*, 16, 2703–2718, <https://doi.org/10.5194/acp-16-2703-2016>, 2016.
- Höpfner, M., Volkamer, R., Grabowski, U., Grutter, M., Orphal, J., Stiller, G., von Clarmann, T., and Wetzel, G.: First detection of ammonia (NH₃) in the Asian summer monsoon upper troposphere, *Atmos. Chem. Phys.*, 16, 14 357–14 369, <https://doi.org/10.5194/acp-16-14357-2016>, URL <https://www.atmos-chem-phys.net/16/14357/2016/>, 2016.
- Konopka, P., Ploeger, F., and Müller, R.: Entropy- and static stability-based Lagrangian model grids, in: *Geophysical Monograph Series: Lagrangian Modeling of the Atmosphere*, edited by Lin, J., vol. 200, pp. 99–109, American Geophysical Union, <https://doi.org/10.1029/2012GM001253>, 2012.
- Li, D., Vogel, B., Bian, J., Müller, R., Pan, L. L., Günther, G., Bai, Z., Li, Q., Zhang, J., Fan, Q., and Vömel, H.: Impact of typhoons on the composition of the upper troposphere within the Asian summer monsoon anticyclone: the SWOP campaign in Lhasa 2013, *Atmos. Chem. Phys.*, 17, 4657–4672, <https://doi.org/10.5194/acp-17-4657-2017>, URL <https://www.atmos-chem-phys.net/17/4657/2017/>, 2017.
- Orbe, C., Waugh, D. W., and Newman, P. A.: Air-mass origin in the tropical lower stratosphere: The influence of Asian boundary layer air, *Geophys. Res. Lett.*, 42, 2015GL063937, <https://doi.org/10.1002/2015GL063937>, URL <http://dx.doi.org/10.1002/2015GL063937>, 2015.
- Pan, L. L., Honomichl, S. B., Kinnison, D. E., Abalos, M., Randel, W. J., Bergman, J. W., and Bian, J.: Transport of chemical tracers from the boundary layer to stratosphere associated with the dynamics of the Asian summer monsoon, *Journal of Geophysical Research: Atmospheres*, 121, 14,159–14,174, <https://doi.org/10.1002/2016JD025616>, URL <https://agupubs.onlinelibrary.wiley.com/doi/abs/10.1002/2016JD025616>, 2016.
- Park, M., Randel, W. J., Gettleman, A., Massie, S. T., and Jiang, J. H.: Transport above the Asian summer monsoon anticyclone inferred from Aura Microwave Limb Sounder tracers, *J. Geophys. Res.*, 112, D16309, <https://doi.org/10.1029/2006JD008294>, 2007.

- Park, M., Randel, W. J., Emmons, L. K., and Livesey, N. J.: Transport pathways of carbon monoxide in the Asian summer monsoon diagnosed from Model of Ozone and Related Tracers (MOZART), *J. Geophys. Res.*, 114, D08303, <https://doi.org/10.1029/2008JD010621>, 2009.
- Ploeger, F., Gottschling, C., Griebbach, S., Grooß, J.-U., Günther, G., Konopka, P., Müller, R., Riese, M., Stroh, F., Tao, M., Ungermann, J., Vogel, B., and von Hobe, M.: A potential vorticity-based determination of the transport barrier in the Asian summer monsoon anticyclone, *Atmos. Chem. Phys.*, 15, 13 145–13 159, <https://doi.org/doi:10.5194/acp-15-13145-2015>, 2015.
- Ploeger, F., Konopka, P., Walker, K., and Riese, M.: Quantifying pollution transport from the Asian monsoon anticyclone into the lower stratosphere, *Atmos. Chem. Phys.*, 17, 7055–7066, <https://doi.org/10.5194/acp-17-7055-2017>, URL <https://www.atmos-chem-phys.net/17/7055/2017/>, 2017.
- Plumb, R. A.: A “tropical pipe” model of stratospheric transport, *J. Geophys. Res.*, 101, 3957–3972, 1996.
- Pommrich, R., Müller, R., Grooß, J.-U., Konopka, P., Ploeger, F., Vogel, B., Tao, M., Hoppe, C. M., Günther, G., Spelten, N., Hoffmann, L., Pumphrey, H.-C., Viciani, S., D’Amato, F., Volk, C. M., Hoor, P., Schlager, H., and Riese, M.: Tropical troposphere to stratosphere transport of carbon monoxide and long-lived trace species in the Chemical Lagrangian Model of the Stratosphere (CLaMS), *Geosci. Model Dev.*, 7, 2895–2916, <https://doi.org/10.5194/gmd-7-2895-2014>, URL <http://www.geosci-model-dev.net/7/2895/2014/>, 2014.
- Randel, W. and Jensen, E.: Physical processes in the tropical tropopause layer and their role in a changing climate, *Nature Geoscience*, 6, 169–176, <https://doi.org/10.1038/ngeo1733>, 2013.
- Randel, W. J. and Park, M.: Deep convective influence on the Asian summer monsoon anticyclone and associated tracer variability observed with Atmospheric Infrared Sounder (AIRS), *J. Geophys. Res.*, 111, D12314, <https://doi.org/10.1029/2005JD006490>, 2006.

- Randel, W. J., Park, M., Emmons, L., Kinnison, D., Bernath, P., Walker, K. A., Boone, C., and Pumphrey, H.: Asian Monsoon Transport of Pollution to the Stratosphere, *Science*, 328, 611–613, <https://doi.org/10.1126/science.1182274>, 2010.
- Tissier, A.-S. and Legras, B.: Convective sources of trajectories traversing the tropical tropopause layer, *Atmos. Chem. Phys.*, 16, 3383–3398, <https://doi.org/10.5194/acp-16-3383-2016>, 2016.
- Uma, K. N., Das, S. K., and Das, S. S.: A climatological perspective of water vapor at the UTLS region over different global monsoon regions: observations inferred from the Aura-MLS and reanalysis data, *Clim. Dyn.*, 43, 407–420, <https://doi.org/10.1007/s00382-014-2085-9>, 2014.
- Vernier, J. P., Fairlie, T. D., Natarajan, M., Wienhold, F. G., Bian, J., Martinsson, B. G., Crumeyrolle, S., Thomason, L. W., and Bedka, K. M.: Increase in upper tropospheric and lower stratospheric aerosol levels and its potential connection with Asian pollution, *J. Geophys. Res.*, <https://doi.org/10.1002/2014JD022372>, 2015.
- Vernier, J.-P., Fairlie, T. D., Deshler, T., Ratnam, M. V., Gadhavi, H., Kumar, B. S., Natarajan, M., Pandit, A. K., Raj, S. T. A., Kumar, A. H., Jayaraman, A., Singh, A. K., Rastogi, N., Sinha, P. R., Kumar, S., Tiwari, S., Wegner, T., Baker, N., Vignelles, D., Stenchikov, G., Shevchenko, I., Smith, J., Bedka, K., Kesarkar, A., Singh, V., Bhate, J., Ravikiran, V., Rao, M. D., Ravindrababu, S., Patel, A., Vernier, H., Wienhold, F. G., Liu, H., Knepp, T. N., Thomason, L., Crawford, J., Ziemba, L., Moore, J., Crumeyrolle, S., Williamson, M., Berthet, G., Jégou, F., and Renard, J.-B.: BATAL: The Balloon Measurement Campaigns of the Asian Tropopause Aerosol Layer, *Bull. Am. Meteorol. Soc.*, 99, 955–973, <https://doi.org/10.1175/BAMS-D-17-0014.1>, 2018.
- Vogel, B., Günther, G., Müller, R., Groß, J.-U., Hoor, P., Krämer, M., Müller, S., Zahn, A., and Riese, M.: Fast transport from Southeast Asia boundary layer sources to northern Europe: rapid uplift in typhoons and eastward eddy shedding of the Asian monsoon anticyclone, *Atmos. Chem. Phys.*, 14, 12 745–12 762, <https://doi.org/10.5194/acp-14-12745-2014>, URL <http://www.atmos-chem-phys.net/14/12745/2014/>, 2014.

- Vogel, B., Günther, G., Müller, R., Groß, J.-U., and Riese, M.: Impact of different Asian source regions on the composition of the Asian monsoon anticyclone and of the extratropical lowermost stratosphere, *Atmos. Chem. Phys.*, 15, 13 699–13 716, <https://doi.org/10.5194/acp-15-13699-2015>, URL <http://www.atmos-chem-phys.net/15/13699/2015/>, 2015.
- Vogel, B., Günther, G., Müller, R., Jens-Uwe Groß, A. A., Bozem, H., Hoor, P., Krämer, M., Müller, S., Riese, M., Rolf, C., Spelten, N., Stiller, G. P., Ungermann, J., and Zahn, A.: Long-range transport pathways of tropospheric source gases originating in Asia into the northern lower stratosphere during the Asian monsoon season 2012, *Atmos. Chem. Phys.*, 16, 15 301–15 325, <https://doi.org/10.5194/acp-16-15301-2016>, URL <http://www.atmos-chem-phys.net/16/15301/2016/>, 2016.
- Volk, C. M., Elkins, J. W., Fahey, D. W., Salawitch, R. J., Dutton, G. S., Gilligan, J. M., Proffitt, M. H., Loewenstein, M., Podolske, J. R., Minschwaner, K., Margitan, J. J., and Chan, K. R.: Quantifying transport between the tropical and mid-latitude lower stratosphere, *Science*, 272, 1763–1768, 1996.
- Wright, J. S., Fu, R., Fueglistaler, S., Liu, Y. S., and Zhang, Y.: The influence of summertime convection over Southeast Asia on water vapor in the tropical stratosphere, *J. Geophys. Res.*, 116, D12302, <https://doi.org/10.1029/2010JD015416>, 2011.

Lagrangian simulations of the transport of young air masses to the top of the Asian monsoon anticyclone and into the tropical pipe

Bärbel Vogel¹, Rolf Müller¹, Gebhard Günther¹, Reinhold Spang¹, Sreeharsha Hanumanthu¹, Dan Li^{1,2}, Martin Riese¹, and Gabriele P. Stiller³

¹Forschungszentrum Jülich, Institute of Energy and Climate Research - Stratosphere (IEK-7), Jülich, Germany

²Key Laboratory of Middle Atmosphere and Global Environment Observation (LAGEO), Institute of Atmospheric Physics, Chinese Academy of Sciences, Beijing, China

³Institute for Meteorology and Climate Research, Karlsruhe Institute of Technology, Karlsruhe, Germany

Correspondence: Bärbel Vogel (b.vogel@fz-juelich.de)

Abstract.

We have performed backward trajectory calculations and simulations with the 3-dimensional Chemical Lagrangian Model of the Stratosphere (CLaMS) for two succeeding monsoon seasons using artificial tracers of air mass origin. With these tracers we trace back the origin of young air masses (age < 6 months) at the top of the Asian monsoon anticyclone and of air masses within the tropical pipe (6 months < age < 18 months) during summer 2008. The occurrence of young air masses (< 6 months) at the top of the Asian monsoon anticyclone up to ≈ 460 K is in agreement with satellite measurements of chlorodifluoromethane (HCFC-22) by the Michelson Interferometer for Passive Atmospheric Sounding (MIPAS) instrument. HCFC-22 can be considered as a regional tracer for continental eastern Asia and the Near East as it is mainly emitted in this region.

Our findings show that the transport ~~pathway~~ of air masses from boundary ~~layer~~ sources in the region of the Asian monsoon into the tropical pipe occurs in three distinct steps. First, very fast uplift in ‘a convective range’ transports air masses up to 360 K potential temperature within a few days. Second, air masses are uplifted from about 360 K up to 460 K within ‘an upward spiralling range’ within a few months. The large-scale upward spiral extends from northern Africa to the western Pacific. The air masses are transported upwards by diabatic heating with a rate of up to 1–1.5 K per day, implying strong vertical transport above the Asian monsoon anticyclone. Third, transport of air masses occurs within the tropical pipe up to 550 K associated with the large-scale Brewer-Dobson circulation within \sim one year.

In the upward spiralling range, air masses are uplifted by diabatic heating across the (lapse rate) tropopause, which does not act as a transport barrier under these conditions. Further, in the upward spiralling range air masses from inside the Asian monsoon anticyclone are mixed with air masses convectively uplifted outside the core of the Asian monsoon anticyclone in the tropical adjacent regions. ~~However, this upward transport~~ Moreover, the vertical transport of air masses from the Asian monsoon anticyclone into the tropical pipe is weak in terms of transported air masses compared to the ~~quasi-horizontal~~ transport from the monsoon anticyclone into the northern ~~lower stratosphere and tropical tropopause region~~ extratropical lower stratosphere. Air masses from the Asian monsoon anticyclone (India/China) contribute a minor fraction to the composition of air within the tropical pipe at 550 K (6%), the major fractions are from Southeast Asia (16%) and the tropical Pacific (15%).

1 Introduction

The Asian summer monsoon is ~~the most pronounced circulation pattern in boreal summer~~ associated with deep convection over the Indian subcontinent and is the most pronounced circulation pattern in boreal summer with an anticyclonic flow that extends from the upper troposphere into the lower stratosphere (UTLS) region (e.g., Li et al., 2005; Randel and Park, 2006; Park et al., 2007). The strong anticyclonic circulation in the UTLS acts as an effective transport barrier (e.g., Ploeger et al., 2015) causing a confinement of tropospheric trace gases in the anticyclone, isolating them from the surrounding air (stratospheric background) as shown by a variety of satellite measurements (e.g., Rosenlof et al., 1997; Li et al., 2005; Park et al., 2007; Fadnavis et al., 2014; Glatthor et al., 2015; Chirkov et al., 2016; Santee et al., 2017).

~~There is a~~ The transport of tropospheric trace gases by the Asian monsoon anticyclone into the lower stratosphere changes the chemical composition in this part of the Earth's atmosphere. Radiatively active species transported into the lowermost extratropical stratosphere have a significant impact on surface climate (e.g., Solomon et al., 2010; Riese et al., 2012; Hossaini et al., 2015) or can cause regional radiative forcing such as the Asian tropopause aerosol layer (ATAL) (e.g., Vernier et al., 2015).

There is large variability of the spatial extent, strength, and location of the ~~UTLS anticyclone reaching monsoon anticyclone in the UTLS, which reaches~~ from Northeast Africa to East Asia (e.g., Annamalai and Slingo, 2001; Randel and Park, 2006; Garny and Randel, 2013; Vogel et al., 2015; Pan et al., 2016). In particular, the location and the shape of the anticyclone change from day to day caused by ~~the~~ internal dynamical variability, manifesting in an oscillation between a state with one anticyclone and two separated anticyclones (2 modes) often referred to as western (Iranian) and eastern (Tibetan) mode (e.g., Zhang et al., 2002; Vogel et al., 2015; Nützel et al., 2016). In addition, smaller anticyclones characterised by low PV values are breaking off a few times each summer from the main anticyclone, a process which is referred to as “eddy shedding” (Hsu and Plumb, 2001; Popovic and Plumb, 2001; Garny and Randel, 2013; Vogel et al., 2014, 2016; Ungermann et al., 2016).

The Asian monsoon circulation provides an effective pathway for tropospheric trace gases such as pollutants, gaseous aerosol precursors, or aerosols as well as aerosol particles into the lower stratosphere which could play an important role in the formation of ~~the Asian tropopause aerosol layer (ATAL) (e.g., Vernier et al., 2015; Höpfner et al., 2016). However, there~~ ATAL layer (e.g., Vernier et al., 2015, 2018; Höpfner et al., 2016; Brunamonti et al., 2018). There is also export of monsoon air quasi-isentropically out of the monsoon and a certain fraction of monsoon air may reach greater altitudes in the stratosphere. There is a longstanding debate about the transport mechanisms at the top of the Asian monsoon anticyclone and beyond into the stratosphere (e.g., Bannister et al., 2004; Park et al., 2009; Randel et al., 2010; Randel and Jensen, 2013; Bergman et al., 2012, 2013; Uma et al., 2014; Bannister et al., 2004; Park et al., 2009; Randel et al., 2010; Bergman et al., 2012, 2013; Randel and Jensen, 2013; Uma et al., 2014). In the literature different aspects of the complex interplay between convection, large-scale upward transport (driven by radiative heating), and the anticyclonic flow in the UTLS are highlighted. Randel et al. (2010) pointed out that the monsoon circulation provides an effective pathway for pollution from Asia to enter the global stratosphere. Vertical upward transport into the deep stratosphere occurs within the tropical pipe, where tropical air masses are isolated to some extent from isentropic mixing with mid-latitude air (e.g., Plumb, 1996; Volk et al., 1996).

~~The transport of tropospheric trace gases by~~ Bourassa et al. (2012) analysed the eruption of the Nabro volcano in northeastern Africa and reported that the volcanic aerosol enhancement from the Nabro eruption was not injected directly into the stratosphere. They conclude that volcanic aerosol only attained stratospheric altitudes through subsequent transport processes associated with deep convection in the region of the Asian monsoon anticyclone ~~into the lower stratosphere changes the chemical composition in~~
5 ~~this part of the Earth's atmosphere. Radiatively active species transported into the lowermost extra-tropical stratosphere have a significant impact on surface climate (e.g., Solomon et al., 2010; Riese et al., 2012; Hossaini et al., 2015) or can cause regional radiative forcing such as the ATAL layer (e.g., Vernier et al., 2015).~~ Pan et al. (2016) highlight that the Asian monsoon anticyclone is an isolated 'bubble' of tropospheric air above the global mean tropical tropopause that isentropically sheds tropospheric air into the stratosphere. Further, they argue that the vertical transport of Asian monsoon air into the deep stratosphere is inefficient
10 ~~during summer.~~

Here, we investigate ~~the following~~ two main questions: First, what are the transport pathways at the top of the Asian monsoon anticyclone into the stratosphere? Second, how do boundary layer source regions in Asia affect the composition of the lower/middle stratosphere within the tropical pipe?

To ~~answer address~~ these questions we performed both backward trajectory calculations and three-dimensional simulations
15 including irreversible mixing (Konopka et al., 2007) with the Lagrangian transport model CLaMS (McKenna et al., 2002b, a; Pommrich et al., 2014, and references therein). Artificial tracers of air mass origin that mark defined regions in the Earth's boundary layer (covering the entire Earth's surface) are introduced in the CLaMS model (Vogel et al., 2015, 2016) and are compared to measurements of the Michelson Interferometer for Passive Atmospheric Sounding (MIPAS) instrument onboard the European Environmental Satellite (~~EnviSat~~ Envisat) (Fischer et al., 2008; Chirkov et al., 2016) to study transport processes
20 and pathways at the top of the Asian monsoon anticyclone and beyond into the tropical pipe. We conduct a case study for the monsoon season 2008. The monsoon season 2008 is chosen because MIPAS measurements have very good data coverage in summer 2008 over Asia. Further, in 2008 there was a normal monsoon season in terms of normal rainfall over India in summer 2008¹. It is established that ~~a strong relation between the Indian monsoon is influenced by the~~ El Niño ~~and Southern Oscillation (ENSO) (e.g., Kumar et al., 2006). There is evidence that a strong~~ La Niña ~~events in winter influence the rainfall~~
25 ~~abundance (droughts or floods) during the following Indian summer monsoon (e.g., Webster et al., 1998; Kumar et al., 2006) in winter in winter (e.g., 2007/08 (DJF), there was a strong La Niña~~ according to the Oceanic Niño Index² ~~causing a normal monsoon season in terms of medium~~ in combination with La Niña conditions during the subsequent summer (as in 2008) is correlated with normal rainfall over India ~~in summer 2008~~³ with a certain variability in precipitation between different Indian regions (e.g., Chakraborty, 2018).

30 We compare the distribution of tracers of air mass origin found in the CLaMS model with ~~observations of~~ global chlorodifluoromethane (HCFC-22; CHClF₂) measurements ~~of from~~ the MIPAS satellite instrument (Chirkov et al., 2016). Chirkov et al. (2016) found enhanced values of HCFC-22 in the region of the Asian monsoon anticyclone at 16 km altitude in July,

¹ see e.g. <http://www.tropmet.res.in/~kolli/mol/Monsoon/Historical/air.html>

² see e.g. <http://ggweather.com/enso/oni.htm>

³ see e.g.

August, and September (JAS) averaged over the MIPAS measurement period from 2005 until 2011. In the last few decades, HCFC-22 has been used as a substitute for more potent ozone-depleting substances such as chlorofluorocarbons (CFCs) in the chemical industry, in particular as a refrigerant, in some regions of the Earth, e.g., in continental eastern Asia and in the Near East (Fortems-Cheiney et al., 2013; Simmonds et al., 2018). In contrast, the production and utilisation of HCFC-22 has been phased out in developed countries regulated by the Montreal Protocol and its amendments and adjustments. As a consequence, HCFC-22 is emitted in locally restricted regions, in particular in the region of the Asian monsoon. Simmonds et al. (2018) estimate that between 55% and 65% of the global HCFC-22 emissions within the last decade are from Chinese production.

Therefore, HCFC-22 is a good tracer for studying transport processes in the region of the Asian monsoon anticyclone and for comparing with CLaMS artificial tracers of air mass origin (e.g., Vogel et al., 2016). In this paper similar methods as in Vogel et al. (2016), namely three-dimensional CLaMS simulations with artificial tracers of air mass origin as well as MIPAS HCFC-22, are used, however the model setup and the scientific objectives are different. In Vogel et al. (2016) horizontal transport pathways out of the ~~the~~-Asian monsoon anticyclone ~~between~~-from 360 K up to 400 K were analysed in a simulation for the monsoon season 2012. Vogel et al. (2016) found, in agreement with MIPAS HCFC-22 measurements, two main horizontal transport pathways from the Asian monsoon anticyclone: one to the east along the subtropical jet and subsequent transport into the northern lower stratosphere, a second horizontal transport pathway to the west into the tropical tropopause layer (TTL).

Here, a more sophisticated model setup is used with the focus on vertical transport pathways out of the Asian monsoon anticyclone and subsequent upward transport into the lower stratosphere up to 550 K. Two consecutive monsoon seasons in summer 2007 and 2008 are simulated. In this two-monsoon-season simulation, the different emission tracers are released during three different time periods each with a length of 6 months (i.e., we use a three-pulse-approach with a total simulation period of 18 months). This allows ~~as~~-us to infer the different transport times of air parcels from the Earth's surface to the top of the anticyclone and beyond in contrast to the approach of a one-monsoon-season simulation (one-pulse-approach with a simulation period of 6 months) used earlier (Vogel et al., 2015, 2016). With this approach it is possible to quantify the impact of the monsoon season of the year before (2007), the winter time 2007/2008, and the monsoon season 2008 on the lower stratosphere and in particular on the tropical pipe at the end of August 2008. ~~This~~-Furthermore, this model setup allows us to identify the origin of air masses found at the top of the Asian monsoon and within the tropical pipe as well as the transport times from the model boundary layer into the stratosphere including irreversible mixing processes.

2 CLaMS model simulations and MIPAS HCFC-22 measurements

We conduct model simulations with the three-dimensional chemistry transport model CLaMS (McKenna et al., 2002a, b; Pommrich et al., 2014, and references therein) and pure backward trajectory calculations with the CLaMS trajectory model covering the Asian monsoon season 2008.

The model simulations and trajectory calculations are driven by horizontal winds from ERA-Interim reanalysis (Dee et al., 2011) provided by the European Centre for Medium-Range Weather Forecasts (ECMWF). For the vertical velocities, the diabatic approach (with contributions to vertical velocities from radiative heating including the effects of clouds, latent heat

release, mixing, and diffusion) was applied using diabatic heating rate as the vertical velocity including latent heat release (for details, see Ploeger et al., 2010). Further, CLaMS employs a hybrid vertical coordinate (ζ), which transforms from a strictly isentropic coordinate Θ to a pressure-based coordinate system (σ coordinates) below a certain reference level (in this study 300 hPa) (for more details, see Konopka et al., 2012; Pommrich et al., 2014). ~~Previous-~~

5 The upward transport and convection in CLaMS (in both three-dimensional simulations as well as in trajectory calculations) is driven by ERA-Interim reanalysis data in which changes are implemented to improve deep and mid-level convection compared to previous reanalysis data (Dee et al., 2011). However, small-scale rapid uplift in convective cores is not included. Therefore convection over Asia is most likely underestimated in ERA-Interim. However, the focus of our paper is to understand the main transport pathways at the top of the anticyclone greater than 380 K and up to 460 K (≈ 100 -60 hPa) which is above the
10 main level of tropical deep convection (e.g., Devasthale and Fueglistaler, 2010; Bergman et al., 2012). Further, previous studies demonstrated that the vertical transport in CLaMS allows the spatio-temporal distribution of CO within the Asian monsoon anticyclone measured by the Aura Microwave Limb Sounder (MLS) to be reproduced (Vogel et al., 2015; Ploeger et al., 2017) (Vogel et al., 2015; Ploeger et al., 2017).

2.1 Three-dimensional CLaMS simulations

15 The three-dimensional CLaMS simulations include irreversible mixing accounting for wind shear (Konopka et al., 2007) and are therefore capable of reproducing strong gradients of atmospheric trace gases found in regions with strong transport barriers, such as the edge of the Asian monsoon anticyclone (e.g., Konopka et al., 2010; Vogel et al., 2015, 2016; Ploeger et al., 2015, 2017), the extratropical tropopause in the vicinity of the subtropical jet (e.g., Pan et al., 2006; Vogel et al., 2011, 2016), and the polar vortex (e.g., Günther et al., 2008; Vogel et al., 2008).

20 The three-dimensional global CLaMS simulations employed here cover an altitude range from the surface up to 900 K potential temperature (≈ 37 km altitude) with a horizontal resolution of 100 km and a maximum vertical resolution of approximately 400 m near the tropopause. A two-monsoon-season simulation is performed covering the time period from 1 May 2007 to 31 October 2008, including both the 2007 and 2008 Asian monsoon seasons to study the upwelling of surface air characterised by local emissions into the lower stratosphere and into the tropical pipe during the course of two succeeding monsoon
25 seasons.

In the two-monsoon-season simulation, artificial tracers of air mass origin, referred to as “emission tracers”, that mark defined regions in the Earth’s boundary layer (covering the entire Earth’s surface) are implemented (≈ 2 -3 km above the surface following orography corresponding to $\zeta < 120$ K), as shown in Fig. 1 and Table 1. Within the model boundary layer, the sum of all the different emission tracers (Ω_i) including the emission tracer for the background (remaining surface) is equal
30 to 1 ($\Omega = \sum_{i=1}^n \Omega_i = 1$, see Table 1). Air masses in the model boundary layer are marked by different emission tracers every 24 hours (the time step for mixing in CLaMS) (for details see Vogel et al., 2016).

In the two-monsoon-season simulation, we used a three-pulse-approach and released the different emission tracers Ω_i in 3 different time periods (pulses) from t_j until $t_j + \Delta t_j$ with Δt_j equal to 6 months. For each pulse, the different emission tracers are continuously released (every 24 hours) at the model boundary between t_j and $t_j + \Delta t_j$. The three pulses start at

1 May 2007 for the summer/fall season 2007 (Summer 07 = S07; $\Omega_{S07} = \sum_{i=1}^n \Omega_{i,S07}$), 1 November 2007 for the winter/spring season 2007/2008 (Winter 07/08 = W07; $\Omega_{W07} = \sum_{i=1}^n \Omega_{i,W07}$), and 1 May 2008 for the summer/fall season 2008 (Summer 08 = S08; $\Omega_{S08} = \sum_{i=1}^n \Omega_{i,S08}$). The summer pulses were chosen to start a few weeks prior to the onset of the Asian monsoon. With this approach it is possible to quantify the impact of the monsoon season of the year before, namely Summer 07, on the lower stratosphere and in particular on the tropical pipe in summer 2008 in addition to the impact of younger air masses of Summer 08 (one-monsoon-season simulation) with an age lower than 6 months. Furthermore, with this approach also the impact of the strong upwelling above the Maritime Continent (the region between Indian and Pacific oceans) and the western Pacific (emission tracers for Southeast Asia and the tropical Pacific Ocean) during Winter 07/08 on the tropical pipe in summer 2008 is quantified.

10 In our two-monsoon-season simulation, the composition of an air mass in the free atmosphere (outside of the model boundary layer) will be a combination of air masses younger than 1 May 2007 ($\Omega_{S08} + \Omega_{W07} + \Omega_{S07}$) and aged air masses (A_{aged}) older than 1 May 2007 originating in the free troposphere or stratosphere ($\Omega_{S08} + \Omega_{W07} + \Omega_{S07} + A_{aged} = 1$).

In a one-monsoon-season simulation for the year 2012, Vogel et al. (2015) showed that the emission tracers for northern India plus southern India plus eastern China (in the following referred to as ‘India/China’ tracer) are a good proxy for the location and shape of the Asian monsoon anticyclone using pattern correlations with potential vorticity (PV), and MLS O₃ and CO satellite measurements. Young air masses that are convectively uplifted outside the core of the Asian monsoon anticyclone and subsequently transported clockwise around the outer edge of the Asian monsoon mainly originate in Southeast Asia, the tropical Pacific, northwestern Pacific, and in northern Africa. Therefore, in this study the sum of these emission tracers is summarised in one emission tracer referred to as the tropical adjacent regions ‘~~tropical-AR~~’-‘TAR’. Note that in this paper a new emission tracer for the northwestern Pacific (NWP) is introduced in the CLaMS simulation compared to previous studies (Vogel et al., 2015, 2016) because it was demonstrated that tropical cyclones in the Pacific and their interaction with the Asian monsoon anticyclone play an important role in the chemical composition of air masses found at the edge of the anticyclone (Vogel et al., 2014; Li et al., 2017).

25 We note that also minor fractions of the emission tracers from the tropical adjacent regions (in particular from Southeast Asia) are found inside the Asian monsoon. This is due to the south-north shift and east-west oscillations of the monsoon anticyclone itself (Vogel et al., 2015).

2.2 CLaMS backward trajectory calculations

The three-dimensional CLaMS simulations including mixing simulate the contribution of different source regions within the model boundary layer to an air parcel in the free atmosphere. Pure trajectory calculations consider only the advective transport neglecting mixing processes entirely. However, backward trajectories are very well suited to analyse the detailed transport pathway of an air parcel and therefore provide an added value compared to three-dimensional CLaMS simulations (e.g., Vogel et al., 2014; Li et al., 2017).

Within this study, 20-day and 40-day backward trajectories are calculated ~~using wind data from the ERA-Interim reanalysis (Dee et al., 2011) driven by wind data~~ (with a horizontal resolution of $1^\circ \times 1^\circ$) ~~from the ERA-Interim reanalysis (Dee et al., 2011) and using the diabatic approach~~ to analyse the transport pathways of air parcels at the top of the Asian monsoon anticyclone and beyond into the tropical pipe.

5

2.3 Calculation of thermal tropopause

An accurate tropopause height determination is crucial to analyse to what extent the thermal tropopause acts as a vertical transport barrier at the top of the Asian monsoon anticyclone. In the extra-tropics, the tropopause acts as a chemical transport boundary in contrast to the tropics.

10 Here, we use an improved determination of the lapse rate tropopause for ERA-Interim data developed by Spang et al. (2015). The vertical resolution of the retrieved tropopause height cannot be better than the vertical grid resolution of the temperature data and hence can produce a significant positive bias for analyses with tropopause related altitude coordinates (Pan and Munchak, 2011). To partly compensate for this effect a vertical spline interpolation with 30 m vertical resolution is applied to the temperature profile around the actual tropopause height computed with the original vertical resolution. The tropopause
15 height computation is repeated with the artificially higher vertical resolution and a weighted mean with distance of the four surrounding grid points of the observation point represents now the so-called high resolution tropopause height. This approach delivers a more realistic lapse rate tropopause, because the single tropopause height values are no longer associated ~~to~~ with the altitude grid points of the analysis data ~~anymore~~. Moreover, Spang et al. (2015) found with this approach smaller bias and standard deviation between ERA-Interim and radiosonde-based tropopause heights.

20 2.4 MIPAS HCFC-22 measurements

To compare the spatial distribution of CLaMS emission tracers with observations in the region of the ~~Asia~~ Asian monsoon anticyclone, we compare results of the CLaMS simulation with global HCFC-22 measurements of the MIPAS satellite instrument (Data Version V5R) (Chirkov et al., 2016). ~~HCFC-22 is emitted in locally restricted regions, in particular in the region of the Asian monsoon (Fortems-Cheiney et al., 2013; Simmonds et al., 2018), and is therefore very well suited for comparison with CLaMS emission tracers.~~

25 For MIPAS-CLaMS intercomparisons, the data density of HCFC-22 measurements is improved by synoptic interpolation of multiple days of MIPAS measurements using CLaMS 3-dimensional trajectory calculations, making use of the relatively long lifetime of HCFC-22 near the tropopause. For a specific day at the end of August 2008, trajectories were computed from the time of measurements in a time window of 4 days (i.e., ± 2 days) to 12:00 UTC (Universal Time Coordinated) of the
30 selected day. Over a period of a few days, there is practically no chemical destruction of HCFC-22 because of its global total atmospheric lifetime of about 12 years (SPARC Report 2013 'Lifetimes of Stratospheric Ozone-Depleting Substances', Ko et al., 2013).

A trajectory length of 2 days for the ~~synoptical-synoptic~~ interpolation gives sufficient coverage of the MIPAS data in the region of the Asian monsoon. An even longer interpolation would give a higher data density, however by calculating solely trajectories mixing processes are neglected. Thus a time window of 4 days for the ~~synoptical-synoptic~~ interpolation is a good compromise between sufficient data coverage and neglecting mixing processes.

5 The limited vertical resolution of the MIPAS HCFC-22 data needs to be taken into account in comparisons to model results. The precision of an individual data point in the altitude region of the Asian monsoon tropopause is 7 to 8 pptv in terms of measurement noise. Parameter errors contribute to a total uncertainty of about 15 pptv in this region for each data point. Thus, the scatter of the HCFC-22 data points (e.g. as shown in Fig. 4) is consistent to the total error. According to Chirkov et al. (2016), the vertical resolution ~~is typically 3 km at 10 km altitude, linearly increasing to 7 km at 30 km altitude. At the altitudes~~
10 ~~relevant for this study, it is typically about 5 km~~ (in terms of the full width at half maximum of the vertical averaging kernel) increases from about 3.3 km at 12 km to 5.5 km at 20 km altitude (see Fig. 2 in Chirkov et al., 2016). ~~However, given~~ The horizontal resolution (in terms of the full width at half maximum of the horizontal averaging kernel) increases from 300 km at 15 km altitude to 600 km at 20 km altitude. Given the rather smooth profiles expected in this study, the limited altitude resolution has a minor effect only; in contrast, it turns out to be crucial when highly structured profiles, such as typically occur
15 at the edge of the polar vortex, are analysed. Further it has to be noted that tropical HCFC-22 profiles from MIPAS seem to have a high bias below 30 km, that, however, is ~~broadly~~ constant with altitude (Chirkov et al., 2016); thus, it does not affect the comparisons made here.

3 Results

3.1 Impact of emission tracers of the Summer 08 pulse

20 3.1.1 Contribution of different emission tracers to the top of the Asian monsoon anticyclone

It is known that the Asian monsoon anticyclone has a strong horizontal transport barrier at about 380 K (e.g., Ploeger et al., 2015), however this transport barrier is not well defined at higher levels of potential temperature. The less strong transport barrier at higher levels has consequences on the vertical transport at the top of the anticyclone. Before the transport at the top is discussed we show the horizontal distribution of different emission tracers at 360 K and then their subsequent transport to the top of the
25 anticyclone up to 460 K. Vogel et al. (2015) showed that the emission tracer for India/China is a good proxy for the location and shape of the Asian monsoon anticyclone using pattern correlations with potential vorticity (PV), and MLS O₃ and CO satellite measurements between 360 K and 400 K. Therefore here we use the India/China tracer as a proxy for the location of the anticyclone.

To analyse the transport pathways at the top of the Asian monsoon anticyclone during the monsoon season 2008, we use
30 only the tracers of air mass origin for the time pulse for Summer 08 (~~age < 6 started on 1 months~~-

May 2008 until end of October 2008). The geographic position and shape of the Asian monsoon anticyclone ~~have strong variability from day to day~~ show a strong day-to-day variability (e.g., Garny and Randel, 2013; Ploeger et al., 2015; Vogel

et al., 2015). In this paper, we focus on 18 August 2008 during the monsoon season 2008 as a case study. On that day, the anticyclone has two modes, the western mode located over the Near East and the eastern Mediterranean Basin and the eastern mode over India and western China as shown in Fig. 2a. Further, a smaller anticyclone (eddy shedding event) is found over the northwestern Pacific. We selected ~~the~~ 18 August 2008 for this study because first this day is dynamically very interesting and
5 second on this day there is very good data coverage of the MIPAS HCFC-22 measurements.

To analyse the transport of young air masses to the top of the Asian monsoon anticyclone, we distinguish between air masses that experienced strong upward transport mainly inside (India/China) and mainly outside (tropical adjacent regions) of the Asian monsoon anticyclone. Fig. 2(~~top~~) a/b shows the horizontal distribution of the fraction of the emission tracer for India/China (~~left~~Fig. 2a) and for tropical adjacent regions (~~right~~Fig. 2b) at 360 K potential temperature. It is evident in Fig. 2
10 (top) that at 360 K the CLaMS model simulates very strong horizontal tracer gradients between the tracer for India/China and that for the tropical adjacent regions at the edge of the anticyclone. High fractions of air from India/China up to 90% and low fractions below 10% from the tropical adjacent regions are found in the core of the Asian monsoon anticyclone at 360 K potential temperature. Highest fractions from the tropical adjacent regions of about 40% are found in a belt around the edge of the anticyclone. Towards the north this belt is separated by the subtropical jet from the northern lower stratosphere visible as a
15 very sharp gradient. To the south, air masses from the tropical adjacent regions do not show a strong gradient with air masses within the tropics and therefore are not separated by a strong transport barrier from the TTL at a level of potential temperature of 360 K (e.g., Ploeger et al., 2015; Santee et al., 2017).

~~In this paper, we define inside and outside (= outer edge or belt of) the anticyclone using these simulated horizontal gradients of the tracers for India/China and for tropical adjacent regions at 360 K. In the following, we will show that this separation is
20 not valid for higher levels of potential temperature.~~

Fig. 2(~~2nd row~~) c/d shows the longitude–theta cross sections at 25°N of the fraction from India/China (~~left~~Fig. 2c) and from the tropical adjacent regions (~~right~~Fig. 2d) on 18 August 2008. We would like to emphasise the horizontal transport of air masses with high fractions contributions from India/China (40%–90%) from the eastern part of the anticyclone to both the western part and into the eddy over the western Pacific between ~~350~~≈340 K and ≈380 K. Correspondingly, low ~~values of~~
25 fractions from the tropical adjacent regions (0%–30%) are simulated in these regions. The horizontal transport of air masses from the eastern to the western mode of the anticyclone indicated by the India/China tracer is consistent with simulations of carbon monoxide (CO) using the Whole-Atmosphere Community Climate Model (WACCM4-SD) (Pan et al., 2016).

Fig. 2 shows the latitude–theta cross sections in the eastern mode of the anticyclone at 90°E (~~3rd row~~Fig. 2e/f) and in the western mode of the anticyclone at 30°E (~~bottom~~Fig. 2g/h) on 18 August 2008. Below 360 K, high fractions of air from
30 India/China up to 90% and low fractions from the tropical adjacent regions lower than 5% are found in the eastern mode of the anticyclone (Fig. 2e/f). In the western mode there is still a high ~~fraction from contribution from the~~ India/China ~~between~~
30~~tracer between 20% and 60% and lower fractions about 10%–40% from the tropical adjacent regions (Fig. 2g/h inside the thick white line). Below the western mode, in the tropics below ≈330 K at around 10°N fractions from the tropical adjacent regions (in that case from Northern Africa) are up to 90% caused by local upward transport (Fig. 2h).~~

Further, a strong vertical gradient of the India/China tracer is found at about 360 K. This level is below the thermal tropopause, which is located at around 380 K (≈ 100 hPa) over the eastern mode of the Asian monsoon anticyclone (at 90°E). ~~There (Fig. 2e). At 90°E , there~~ is a layer of young air masses with enhanced fractions from India/China (up to $\approx 20\%$) above the thermal tropopause up to about 420 K potential temperature. An obvious explanation for this model result would be that the tropopause over the Asian monsoon is not a strict vertical transport barrier and weak vertical cross-tropopause transport occurred, in contrast to the extra-tropics (air masses at the polar side of the subtropical jet) where the tropopause acts as a chemical transport boundary.

~~Inside the anticyclone below~~ Below 360 K in the region with high values of the India/China tracer, the fractions from the tropical adjacent regions are below 10%, however above 360 K around the tropopause the fractions are much higher, up to about ~~35~~30%, and up to about 15% around 420 K (see Fig. 2d/f). Thus, at 420 K the contributions of young air masses are about 20% from India/China and 15% from the tropical adjacent regions. From this result the question arises, ‘how can air masses from the outer edge of the anticyclone be transported from 360 K into the lower stratosphere above?’ A straight vertical cross-tropopause transport cannot be the explanation because inside the anticyclone the fraction from the tropical adjacent regions is much lower.

Note that in Fig. 2 the same data range is used for all colour bars for a better comparability between the horizontal and different vertical cross sections. Therefore some features at the horizontal cross section at 360 K are not too prominent for example the thin filament at around 50°E between 40°N and 60°N in Fig. 2a (see next section Fig. 3).

3.1.2 Emission tracer for India/China vs MIPAS HCFC-22

To demonstrate that the spatial distribution of tracers of air mass origin found in the CLaMS model in the region of the Asian monsoon anticyclone is consistent with observations of chemical tracers, we analyse HCFC-22 measurements of the MIPAS instrument (Chirkov et al., 2016). As described in Sect. 1, HCFC-22 is emitted in locally restricted regions in ~~particular in~~ continental eastern Asia, in particular in China, and in the Near East.

Fig. ~~4 (top)-3~~ and Fig. 4a shows the horizontal distribution for the India/China tracer (~~left~~) and of HCFC-22 measurements (~~right~~) synoptically interpolated to 18 August 2008 12:00 UTC at 380 K potential temperature (for details see Sect. 2.4) and ~~latitude-theta cross sections (2nd row) at 30°E~~ longitude-theta cross section at 25°N (Fig. 4b) as well as the latitude-theta cross sections at $90^\circ\text{E} \pm 10^\circ$ and 90°E (Fig. 4c) and at $30^\circ\text{E} \pm 10^\circ$ as well as a longitude-theta cross section at 25°N (bottom (Fig. 4d). The contour line of 20% ~~for percentages~~ of the India/China tracer ~~are marked~~ is marked on the cross sections for better comparison with the CLaMS results shown in Fig. 2.

The horizontal spatial distribution of the India/China tracer (Fig. 3) and HCFC-22 at 380 K (Fig. 4a) show good overall agreement. In particular the strong gradient at the northern flank of the Asian monsoon anticyclone is evident both in the model and in HCFC-22 observations. Enhanced HCFC-22 values up to 240 pptv compared to the stratospheric background (of around 180 to 200 pptv at 16 km altitude in JAS derived from MIPAS measurements (Chirkov et al., 2016)) are found in both the eastern and western mode of the anticyclone, in the smaller eddy at the northeastern flank of the anticyclone as well as in the

thin filament at around 50°E between 40°N and 60°N. Further, as in the CLaMS model in the observations there is no sharp gradient at the southern flank of the anticyclone, which separates anticyclonic air from the surrounding tropics.

The vertical HCFC-22 distributions (Fig. 4, ~~2nd row c/d~~) within the eastern and western ~~mode~~ modes of the anticyclone are broadly consistent with the vertical distribution of the India/China tracer (see Fig. 2e/g). The highest mixing ratios of HCFC-22 are found within the anticyclone below the thermal tropopause. However, also at the top of the anticyclone above the tropopause enhanced HCFC-22 values are measured in agreement with the CLaMS tracer for India/China. Thus, measurements of HCFC-22 are consistent with our model result that young air masses from the region of the Asian monsoon are transported to the top of the anticyclone above the tropopause.

In addition, the vertical HCFC-22 distribution (Fig. 4, ~~2nd row left d~~) for the western mode shows a very steep gradient in the upper troposphere between 350 K and 360 K in agreement with the spatial distribution of the India/China tracer (see Fig. 2g). Thus below 350–360 K ~~lower~~ smaller mixing ratios of HCFC-22 are measured than above, indicating that below the western mode of the anticyclone there exists no upward transport from boundary sources for HCFC-22. The enhanced values of HCFC-22 within the western mode and below the thermal tropopause along the longitude–theta cross sections at 25°N (Fig. 4, ~~bottom b~~) confirm the horizontal westward transport within the Asian monsoon anticyclone as found for the India/China tracer in the CLaMS simulations (see Fig. 2c).

3.1.3 Impact of young air masses on the top of the AMA

In Sect. 3.1.1, it is shown that enhanced fractions of both tracers for India/China and tropical adjacent regions are found above the thermal tropopause at the top of the Asian monsoon anticyclone. Fig. 5 shows the horizontal distribution of the fraction of air originating in India/China (left) and in tropical adjacent regions (right) at different levels of potential temperature between 380 K and 460 K.

Young air masses (age < 6 months) from both India/China and tropical adjacent regions are found up to ≈ 460 K. ~~At 380 K, the highest fractions of air from~~ It was shown earlier that the horizontal distribution of the India/China ~~are found in the core~~ tracer is a good proxy for the location of the anticyclone ~~and~~ (Vogel et al., 2015). The horizontal distribution of the tropical adjacent regions ~~at the edge of the anticyclone.~~ At compared to the horizontal distribution of the India/China tracer strongly differs depending on the level of potential temperature from a nearly disjoint distribution at 360 K (see Fig. 2) to a more coincident distribution from 400 K to 460 K (see Fig. 5).

At 380 K, the highest ~~contributions of both tracers are found within the anticyclone ; however, between 420~~ fractions from tropical adjacent regions are found at the edge of the anticyclone and at 400 K ~~and 460~~ within the anticyclone. Above 400 K ~~highest contributions of both are found around the edge of the anticyclone.~~ This ~~both tracers~~ India/China and tropical adjacent regions show a similar horizontal distribution. We emphasise that at these levels of potential temperature the tracer distributions have the shape of rotating filaments in contrast to the more compact distribution at lower levels. The variation of the distribution of the tracer for the tropical adjacent regions with altitude is an indication that ~~at these altitudes the vertical~~ the upward transport

of young air masses ~~occurred more at the edge at the top~~ of the anticyclone ~~and not~~ occurred more towards the edge and less inside the anticyclone itself.

3.2 Backward trajectory calculations

3.2.1 40-day backward trajectories at the top of the anticyclone and beyond

- 5 To analyse the transport pathways to the top of the anticyclone in more detail, 40-day backward trajectories are calculated ~~started~~ starting in the western (20–50°N, 0–70°E) and eastern (20–50°N, 70–140°E) ~~mode~~ modes of the anticyclone. The trajectories are started at the position of the air parcels from the 3-dimensional CLaMS simulation at different levels of potential temperature ($\Theta \pm 0.25 \text{ K}$). Only $\Theta = 380, 400, 420, 440 \text{ K} \pm 0.25 \text{ K}$ on 18 August 2018. Note that the air parcels in the 3-dimensional CLaMS simulation are distributed on an irregular grid. To take into account the distribution of the boundary
- 10 emission tracer at the top of the Asian monsoon anticyclone, only air parcels are selected with contributions of young air masses (age < 6 months, Summer08) larger than 70% (380 K), 50% (400 K), 20% (420 K), and 5% (440 K) (not all levels of potential temperature are presented ~~within this paper here~~). The ~~results of all percentages are chosen in a way to obtain a number of trajectories (less than 30) that can be reasonably visualised. The results of the~~ 40-day backward trajectories are similar at different levels of potential temperature; therefore we show a selection of trajectories to demonstrate the ~~transport~~
- 15 ~~pathways at main transport pathway to~~ the top of the Asian monsoon. A larger set of 20-day backward trajectories analysed statistically will be discussed below in Section 3.2.2.

Fig. 6 shows trajectories started in the eastern and western part of the Asian monsoon anticyclone around the thermal tropopause at 380 K ~~on 18 August 2018~~. Air masses are uplifted to approximately 360 K very rapidly by various convective events occurring at different times and locations. Our 40-day backward trajectories show that preferred regions for fast

20 uplift are continental Asia (mainly the region of the south slope of Himalayas and the Tibetan Plateau) and the western Pacific

~~(not shown here). A lower fraction of trajectories originates in the free troposphere. The trajectories in Fig. 6 demonstrating convection below 380 K are only a snapshot for 18 August 2018. There are several previous studies (e.g., Randel and Park, 2006; Park et al.,~~

25 of the monsoon season (see discussion in Sect. 4). The backward trajectories demonstrate that above 360 K potential temperature the air masses circulate around the anticyclone in a large-scale upward spiral extending from northern Africa to the western Pacific. Here in the upward spiralling range, the ~~upward~~ vertical transport is much slower than in the convective range.

Fig. 7 shows trajectories started in the western and eastern ~~part~~ parts of the Asian monsoon anticyclone above the thermal tropopause at 400 K and at 440 K. The slow upward transport up to ≈ 1 to 1.5 K per day in a large-scale upward spiral is evident

30 in both the western and eastern ~~part~~ parts of the anticyclone. The 40-day backward trajectories demonstrate that at the top of the anticyclone the upward transport of air masses occurs along a large-scale upward spiral and therefore no straight vertical ~~upward~~ transport from the upper tropopause into the lower stratosphere takes place. The higher above the thermal tropopause the larger is the contribution of trajectories from outside the Asian monsoon anticyclone coming into the upward spiralling

flow above 360 K. Trajectories at other levels of potential temperature (not shown) both in the western and in eastern ~~part~~parts of the anticyclone have a similar behaviour as shown in Figs. 6 and 7 and therefore confirm the presented results.

In general, trajectory calculations have limitations due to trajectory dispersion by errors through interpolation of the wind data to the position of the air parcel at a specific time. Over the timescales in question, mixing can also be relevant (e.g., McKenna et al., 2000).
5 These errors can accumulate depending on the trajectory length over the course of the simulation. However, the frequently employed trajectory length to study transport processes in the Asian monsoon region is ranging from a couple of weeks to a few months (e.g., Chen et al., 2012; Bergman et al., 2013; Vogel et al., 2014; Garny and Randel, 2016; Müller et al., 2016; Li et al., 2017).
In our trajectory analysis, the focus is to demonstrate the large-scale transport pathways of the air parcels at the top of the anticyclone, small changes of the trajectory position will therefore not affect our findings.

10

3.2.2 Global 20-day backward trajectories in the region of the Asian monsoon anticyclone

In the ~~last~~previous section, the transport pathways ~~of single-selected for a restricted number of~~ trajectories were discussed. Here, for a broader view 20-day backward trajectories for the entire region of the Asian monsoon anticyclone are presented. In the region of the Asian monsoon (0–160°E and 10–60°N) on a $1.0^\circ \times 0.5^\circ$ longitude-latitude-grid 20-day backward trajectories
15 are calculated at 360 K, 380 K, 400 K, 420 K, and 440 K starting on 18 August 2008. Each point in Fig. 8 indicates the location of the start position of a 20-day backward trajectory colour-coded by the change in potential temperature ($\Delta\Theta$) during the last 20 days.

At 360 K, air parcels that experienced very strong upward transport by up to ≈ 60 K within the last 20 days were found inside the western and eastern ~~mode~~modes of the anticyclone, within the eddy over the Pacific, and within the tropics south of
20 the anticyclone. The ~~upwelling is~~pattern of $\Delta\Theta$ at 360 K within the anticyclone and in the tropics are very patchy, reflecting that the strong upward transport in this region is caused by single convective events.

Above 360 K, air parcels that experienced ~~substantial upward transport are only~~strong upward transport larger than 20–30 K within 20 day (corresponding to a mean value of 1–1.5 K per day) are largely found in the region of the anticyclone, ~~however~~
25 ~~the upwelling is inhomogeneous and slow, with an uplift of about a maximum of 1–1.5. This rate of upwelling is much slower compared to convective upwelling shown at 360 K~~per day. Air parcels that experienced strong upward transport are mainly grouped in curved elongated filaments, reflecting a rotating movement of the air parcels at the top of the anticyclone. Often air parcels with ~~maximum-strong~~ $\Delta\Theta$ above 360 K are located more at the edge of the eastern and western ~~mode~~modes of the anticyclone and at the edge of the ~~eddy~~eastward-migrating eddy at the eastern flank of the anticyclone. Thus the upward
30 transport in the region of the anticyclone is inhomogeneous and not homogeneously distributed over the entire anticyclone as suggested from climatological studies (e.g., Randel et al., 2010; Ploeger et al., 2017). This is consistent with results presented above in Sect. 3.2.1 demonstrating that for single selected trajectories the transport at the top of the Asian monsoon anticyclone is a slow upward transport of about 1–1.5 K per day in a large-scale spiral above the anticyclone caused by diabatic heating. In the backward trajectory calculations mixing processes are not included, however the results of the trajectory calculations are

consistent with patterns found in the 3-dimensional CLaMS simulation including mixing as discussed in Sect. 3.1.3, demonstrating that young air masses above 400 K are found at the edge of the anticyclone. Above 400 K, air masses in the tropics also experienced upward transport, but the vertical uplift is in general lower than 20 K within 20 day, (i.e. lower than 1 K per day).

In Appendix A, results of global 20-day backward trajectories demonstrate that during the monsoon season above 360 K an uplift of air parcels of about 1–1.5 K per day occurred only in the region of the Asian monsoon anticyclone compared to the rest of the tropics. Even in the tropics the uplift is in general slower at these levels of potential temperature. Further the seasonal variability of this upwelling above the Asian monsoon anticyclone from monsoon-onset until post-monsoon 2008 is discussed in ~~the~~ Appendix A.

10 3.3 Results from the three-pulse-approach

In the previous sections using CLaMS model simulations and MIPAS HCFC-22 measurements, we could show that the circulation of the Asian monsoon is ~~an effective circulation pattern in the UTLS that transports effective in transporting~~ very young air masses (< 6 months) from the surface into the lower stratosphere up to ≈ 460 K. Here, we discuss subsequent transport pathways of air masses from the region of the Asian monsoon and Southeast Asia into the tropical pipe (middle stratosphere).

3.3.1 Transport within the tropical pipe

Fig. 9 shows latitude–theta cross sections at 90°E for the fraction from India/China from the start of the simulation on 1 May 2007 until 18 August 2008, which is a sum of the contributions of each of the three time pulses Summer07, Winter07/08, and Summer08 each set for a time period of 6 months. A signal with enhanced fractions from India/China (up to 10%) is found at around 550 K within the tropics which is from the Summer07 pulse. This shows that air masses from boundary layer regions in India/China are transported into the middle stratosphere within the tropical pipe within a time period of one year. ~~No fractions from~~ Fractions of air from the India/China tracer for the time pulse for Winter07/08 are ~~found on 18 August 2008, demonstrating below 2.4%, indicating~~ that during winter ~~time~~ in the absence of the Asian monsoon anticyclone ~~no boundary the transport of boundary layer~~ emissions from India/China ~~are transported~~ into the stratosphere is insignificant weak.

Fig. ~~??~~ 10 shows the same images as Fig. 9, but for the fractions from ~~Southeast Asia (SEA~~ tropical adjacent regions (TAR). Because of the Summer08 pulse, high fractions from ~~Southeast Asia~~ tropical AR are found at the edge of or outside the Asian monsoon anticyclone below 360 K. At altitudes up to ≈ 460 K, enhanced fractions are found over the region of the Asian monsoon, but also above the entire tropics.

For the Summer07 pulse, an enhanced signal from ~~Southeast Asia~~ TAR (up to 25%) is found at around 550 K within the tropics similar as for India/China tracer. This model result shows that also air masses from outside the Asian monsoon anticyclone (Summer07 pulse) are transported into the middle stratosphere within the tropical pipe within one year. The fraction of air from ~~Southeast Asia~~ tropical AR (up to 25%) is even larger ~~as than~~ from India/China (up to 10%). In contrast to the India/China tracer (~~Winter07/08 pulse~~), ~~the Southeast Asia~~, the TAR tracer shows that also emissions mainly from

Southeast Asia and the tropical Pacific (details see Sect. 3.3.2) released during winter ~~time~~ (Winter 07/08 pulse) are transported into the lower stratosphere via the tropical pipe.

Fig. 11 shows that the upward spiralling transport above 360 K occurs in a field of radiative heating above the Asian monsoon, in particular above the western mode of the anticyclone. Thus, the combination of the anticyclonic flow and the uplift by radiative heating results in an upward spiralling transport like a ‘Spiral Staircase’. Positive radiative heating rates are found in Era-Interim ~~analysis-reanalysis~~ on top of the Asian monsoon anticyclone as well as over the subtropics in the southern hemisphere (see Fig. 11). In these regions, positive radiative heating rates were also reported in a study by Park et al. (2007), using a free-running climate model. They argue that the positive radiative heating rates are the response to very low temperatures around the tropopause ~~which again-~~ which in turn are the response to convective heating near the equator (e.g., Gill, 1980; Highwood and Hoskins, 1998). It is known that the radiative heating rates in the tropical UTLS are different in current reanalysis models (e.g., Wright and Fueglistaler, 2013) and are most likely overestimated in ERA-Interim (e.g., Schoeberl et al., 2012)

(e.g., Ploeger et al., 2012; Schoeberl et al., 2012). Therefore, the rates of diabatic heating in the upward spiralling range found in our study are most likely somewhat too high, however slow upward transport in the UTLS in the region of the Asian monsoon anticyclone associated with positive heating has been addressed previously (e.g., Park et al., 2007; Bergman et al., 2012; Garny et al., 2012)

Fig. 12 shows MIPAS HCFC-22 measurements at the same ~~longitude-theta-latitude-theta~~ cross sections as Fig. ~~??~~ 10 and Fig. 9. The transport pathway of HCFC-22 within the tropical pipe is evident. The transport of HCFC-22 is similar to that of the emission tracer for ~~Southeast Asia~~ tropical adjacent regions, in contrast to the signal for the India/China tracer, which results from a combination of just two signals, one from the Summer 07 pulse and another from the Summer 08 pulse. It was shown in previous studies (Chirkov et al., 2016; Vogel et al., 2016) that HCFC-22 is enhanced in the region of the Asian monsoon anticyclone. There are also HCFC-22 source regions outside the ~~Asia-Asian~~ monsoon region in continental eastern Asia (Fortems-Cheiney et al., 2013), therefore the upward transport of HCFC-22 in the troposphere can also occur during winter ~~time~~. In boreal winter, efficient transport into the stratosphere is found over the west Pacific and Maritime Continent caused by strong convection and in addition by the ascending branch of the Walker Circulation located over the Maritime continent (e.g., Bergman et al., 2012; Hosking et al., 2012). In addition, stronger heating rates (vertical ~~velocity~~ velocities) are found in the TTL during winter compared to summer ~~time~~ (e.g., Bergman et al., 2012).

Figs. 9, ~~??~~ 10, and 12 further show that in addition to the upward transport into the tropical pipe, ~~horizontal transport pathways exists; that~~ transport air masses ~~isentropically~~ out of the region of the Asian monsoon occurs into the northern lower stratosphere and to a much lower extent into the southern hemisphere. ~~These quasi-horizontal transport pathways~~ Details of the transport into the northern lower stratosphere are further discussed in Sect. 4.

3.3.2 Transport times and origin of air within the tropical pipe

On 18 August 2008, enhanced signals for the tracers from India/China and ~~Southeast Asia~~ tropical adjacent regions from the Summer07 pulse are found at around 550 K in the tropics between 30°S and 30°N (see Fig. 139 and Fig. 10). To analyse in more detail the transport times from the model boundary layer into the tropical pipe the contributions of the three different time pulses from different emission tracers are calculated within the tropical pipe at 550 K potential temperature. We use the following approach: for each day between 1 May 2007 and 31 October 2008, a mean value for each emission tracer of all CLaMS air parcels is calculated between 30°S and 30°N at 550 K (± 0.5 K). This is done for the sum of all three time pulses Summer07, Winter07/08, and Summer08 and for each pulse individually.

Fig. 13 (top) shows the contribution of the three different time pulses (Ω_{S07} , Ω_{W07} , Ω_{S08}) for the entire Earth's surface between 1 October 2007 until the end of the simulation period (31 October 2008). The time period between 1 May 2007 and 1 October 2007 is not shown because here the contribution of all emission tracers is zero caused by the fact that the air masses need a certain transport time to reach the level of 550 K potential temperature within the tropical pipe. Air masses from the Summer07 pulse reach this level first in November/December 2007; between January and May there is a steep increase of air masses from the Summer07 pulse with a maximum in June 2008. Air masses from the Winter07 pulse reach the 550 K level of potential temperature during May 2008 and are increasing until the end of the simulation period. No contributions from the Summer08 pulse are found at 550 K, since the transport times are too short to reach the tropical pipe within the simulation period.

The ~~highest~~ largest contributions to the Summer07 pulse are from tropical Pacific, India/China, Southeast Asia, and northern Africa Fig. 13 (top). To the Winter07 pulse contribute mainly the tropical Pacific and Southeast Asia. Here, the contribution of India/China and northern Africa is insignificant, demonstrating that during the absence of the monsoon anticyclone in winter no vertical transport into the tropical pipe occurred.

Fig. 13 (bottom) shows that on the 550 K level, the contributions of all ~~boundary~~ emission tracers (age < 18 months) to the tropical pipe is up to 55% by the end of October 2008. The contributions from Southeast Asia and the tropical Pacific are 16% and 15%, respectively. The contribution from India/China, which is mostly monsoon air, is much lower, around 6%. Lower fractions are from tropical the Indian Ocean (4%), Northern Africa (3%), and South America (4%). The contributions of all other regions of the Earth's surface are lower than 3% and are summarised in the tracer referred to as residual surface (8%) shown in grey.

The black and the white lines in Fig. 13 (bottom) mark the ~~the~~ contribution of the Summer07 and Winter07/08 pulses for each emission tracer, respectively (as shown in Fig. 13 (top)). For the tracer from India/China as well as for northern Africa, the black and the white lines are overlapping, implying that there is no contribution from India/China or northern Africa from the Winter07/08 pulse in the tropical pipe (as shown above). Further, our findings show that air masses from India/China, thus mainly from the Asian monsoon anticyclone, contribute to a ~~lower~~ smaller fraction of the composition of air within the tropical pipe at 550 K; the major part is from Southeast Asia and the tropical Pacific. We would like to point out that the CLaMS emission tracer for Southeast Asia ~~include~~ includes both the land masses of Southeast Asia and parts of the western

Pacific including the Maritime Continent, which is known to also have intense deep convection during summer (e.g., Pan and Munchak, 2011).

4 Discussion

5 ~~It has been proposed that the~~

~~It is well known that the composition of the~~ Asian monsoon anticyclone ~~constitutes an effective transport pathway from~~ the surface, through the Asian monsoon, and deep into the tropical pipe using satellite observations of hydrogen cyanide (HCN) (Randel et al., 2010). HCN is a tropospheric pollutant produced by biomass burning with a strong sink on ocean surfaces. Therefore tropical ocean regions cannot be the source for HCN found in the tropical pipe. Ploeger et al. (2017) ~~confirm using CLAMS simulations marking air masses within~~ is strongly affected by convection over continental Asia (e.g. the south slope of the Himalayas and the Tibetan Plateau), Bay of Bengal, and the western Pacific, (e.g., Randel and Park, 2006; Park et al., 2006). However there is a debate about the contribution of different source regions to the composition of the Asian monsoon anticyclone by a PV-gradient criterion (Ploeger et al., 2015) that the air mass fraction from the anticyclone correlates well with satellite HCN within the tropical pipe. Further, there are differences in the conclusions in the literature about the contribution ~~of different source regions depending on the used reanalysis data (e.g., Wright et al., 2011; Bergman et al., 2013). Findings by Vogel et al. (2015) show that there is a strong intraseasonal variability of boundary source regions to the composition of the Asian monsoon anticyclone during a particular monsoon season. We would like to emphasise that the trajectories presented in Fig. 6 demonstrating convection below 380 K are only a snapshot for 18 August 2018 with convection over the western Pacific and continental Asia mainly in the region of the south slope of the Himalayas and the Tibetan Plateau.~~

20 ~~In our study, we found a similar behaviour for contributions of the India/China tracer within the tropical pipe as Randel et al. (2010) and Ploeger et al. (2017) for HCN and the simulated anticyclone air mass fraction. However in addition, we show that the contributions from emissions from Southeast Asia and the tropical Pacific during summer are larger than the contribution from India/China within the tropical pipe. This demonstrates that~~ Here, in contrast to earlier studies, we focus on transport at the top of the anticyclone at altitudes greater than 380 K potential temperature (≈ 100 hPa) reaching up to 460 K (≈ 60 hPa). Further, ~~in addition to previous studies (e.g., Garny and Randel, 2016; Ploeger et al., 2017), we relate the transport of air masses from inside the Asian monsoon anticyclone is a more effective transport pathway for the tropical adjacent regions from which air masses can be transported to the edge of the Asian monsoon anticyclone and then further into the tropical pipe than for air masses from inside the anticyclone itself (India/China) to air masses uplifted outside the anticyclone. Subsequently these air masses are jointly transported upwards to the top of the anticyclone at ≈ 460 K.~~

30 4.1 Transport pathways at the top of the anticyclone

It has been demonstrated by satellite observations that the Asian monsoon anticyclone affects the transport of sulphate aerosol and its precursor SO_2 injected by volcanic eruptions within the adjacent regions of the Asian monsoon (e.g., Bourassa et al.,

2012; Griessbach et al., 2013; Fairlie et al., 2014; Fromm et al., 2014; Wu et al., 2017). However, there is a debate about the exact transport mechanism. The observed transport into the stratosphere of air masses injected into the upper troposphere by volcanoes located at the edge of the Asian monsoon (~~e.g., Griessbach et al., 2013; Fairlie et al., 2014; Fromm et al., 2014; Wu et al., 2017~~) (e.g., Griessbach et al., 2013; Fairlie et al., 2014; Fromm et al., 2014; Wu et al., 2017) can be explained by the vertical transport concept of upward spiralling above the ~~the~~ Asian monsoon, proposed here. It has been found in several satellite measurements (Griessbach et al., 2013; Fromm et al., 2014; Fairlie et al., 2014) that polluted air masses from the Nabro eruption in Eritrea, northeastern Africa, in June 2011 are transported around the anticyclone and at higher levels are found above the anticyclone, consistent with the CLaMS tracer for the tropical adjacent regions. Wu et al. (2017) show that the Asian monsoon anticyclone causes the transport of air masses emitted by the June 2009 eruption of the volcano Sarychev around the anticyclone southwards into the TTL, isolating aerosol-free air masses inside the anticyclone from aerosol-rich air outside.

Furthermore, the concept of the upward spiralling range transporting air masses from the adjacent regions of the Asian monsoon can also explain the impact of air masses uplifted by tropical cyclones in the western Pacific ocean on air masses observed by balloon measurements over Lhasa (China) (Li et al., 2017). Tropical cyclones rapidly loft marine air masses outside the Asian monsoon into the upper troposphere. The interplay between the location of the Asian monsoon anticyclone and the tropical cyclone controls the transport pathways of the air parcels from the boundary layer. Air parcels injected by a tropical cyclone into the outer anticyclonic flow of the anticyclone follow the flow around the anticyclone.

Moreover, the concept of the upward spiralling range including air mass transport from sources in the tropical adjacent regions could be a transport pathway to understand the formation of the Asian tropopause aerosol layer (ATAL) (e.g., Vernier et al., 2015) observed above the Asian monsoon region (~~Hanumanthu et al., 2018, in preparation~~) (e.g., Vernier et al., 2015, 2018; Brunamonti et al., 2018).

4.2 Contributions to the tropical pipe

It has been proposed that the Asian monsoon constitutes an effective transport pathway from the surface, through the Asian monsoon anticyclone, and deep into the tropical pipe based on satellite observations of hydrogen cyanide (HCN) (Randel et al., 2010). HCN is a tropospheric pollutant produced mainly by biomass burning with a strong sink on ocean surfaces. Therefore tropical ocean regions cannot be the source for HCN found in the tropical pipe. Ploeger et al. (2017) addressed this issue using CLaMS simulations marking air masses within the Asian monsoon anticyclone by a PV-gradient criterion (Ploeger et al., 2015). They find that the air mass fraction from the anticyclone correlates well with satellite measurements of HCN within the tropical pipe. However, we In our study, we found a similar behaviour for contributions of the India/China tracer within the tropical pipe as Randel et al. (2010) for HCN and Ploeger et al. (2017) for the simulated anticyclone air mass fraction. Ploeger et al. (2017) found a maximum anticyclone air mass fractions around 5% in the tropical pipe using 3-dimensional CLaMS simulations for 2010-2013. This is consistent to our simulations finding about 6% contributions of the India/China tracer within the tropical pipe at 550 K in 2008.

5 However in addition to Randel et al. (2010) and Ploeger et al. (2017), we show that the contributions from emissions from Southeast Asia and the tropical Pacific during summer are larger than the contribution from India/China within the tropical pipe. This demonstrates that the Asian monsoon anticyclone is a more effective transport pathway for the tropical adjacent regions than for air masses from inside the anticyclone itself (India/China). From the tropical adjacent regions air masses can be transported to the edge of the Asian monsoon anticyclone and then further into the tropical pipe.

4.3 Transport to the northern extratropical lower stratosphere

10 We would like to emphasise that ~~this the~~ vertical transport of air masses ~~is much slower at the top of the anticyclone is less effective~~ than the horizontal isentropic transport by eastward eddy shedding events transporting air from the Asian monsoon anticyclone and from the tropical adjacent regions into the northern lower stratosphere or westward shedding transporting air into the TTL (e.g., Garny and Randel, 2016; Orbe et al., 2015; Vogel et al., 2016; Ploeger et al., 2017)(e.g., Orbe et al., 2015; Garny and Randel, 2016). The impact of the quasi-horizontal transport on the chemical composition of the northern lower stratosphere ~~is already has already been~~ discussed in detail in previous studies (e.g., Dethof et al., 1999; Ploeger et al., 2013; Müller et al., 2016; Vogel et al., 2014, 2016; Dethof et al., 1999; Ploeger et al., 2013, 2017; Garny and Randel, 2016; Müller et al., 2016; Vogel et al., 2014, 2016; Rolf et al., 2016).

15 Vogel et al. (2016) performed a CLaMS simulation for the year 2012 using similar tracers of air mass origin as in this work and found a flooding of the ~~lower northern northern extratropical lower~~ stratosphere with young air masses from the region of the Asian monsoon anticyclone. ~~Horizontal~~The transport of young air masses (age < 6 months) ~~into the northern extratropical lower stratosphere~~ is calculated, resulting in up to 44% at 360 K (up to 35% at 380 K) ~~end of October 2012~~, with the highest contribution from India/China up to 15% (14%) (see Fig. 14 in Vogel et al. (2016)). ~~In this paper~~Here, the same analysis is performed for the simulation for 2008 and a slightly higher impact on the ~~extratropical northern northern extratropical~~ lower stratosphere is found for the year 2008, up to 48% young air at 360 K (up to 41% at 380 K) ~~end of October 2008~~ and up to 18% (16%) from India/China compared to 2012 (see Appendix B). This difference is most likely caused by the interannual variability of the monsoon system. However, within the tropical pipe at 550 K, in 2008 the contributions from India/China are ~~much smaller than 10~~about 6 %, demonstrating that the ~~horizontal isentropic~~ transport of air masses from the Asian monsoon anticyclone into the ~~stratosphere northern extratropical lower stratosphere during boreal summer and fall~~ is more effective than the vertical transport ~~-into the tropical pipe during the course of one year. This is consistent with Ploeger et al. (2017), who found maximum anticyclone air mass fractions around 5% in the tropical pipe and 15% in the northern extratropical lower stratosphere using 3-dimensional CLaMS simulations for 2010-2013. In a study releasing trajectories within the Asian monsoon anticyclone, Garny and Randel (2016) found a similar value of 15% of trajectories released in the anticyclone that reach the northern extratropical lower stratosphere after 60 days (for 2006).~~

5 Conclusions

In this paper, the transport mechanisms of young air masses at the top of the Asian monsoon and subsequent transport into the tropical pipe are analysed using 3-dimensional CLaMS simulations as well as CLaMS backward trajectory calculations. Tracers of air mass origin are introduced in the 3-dimensional CLaMS simulation to trace back the origin of young air masses (age < 6 months) found at the top of the Asian monsoon anticyclone and of air masses found within the tropical pipe (6 months < age < 18 months).

Young air masses with an age lower than 6 months are found at the top of the Asian monsoon anticyclone up to altitudes of about 460 K (≈ 60 hPa) by the end of August 2008. MIPAS satellite measurements of HCFC-22, a regional tracer emitted especially in continental eastern Asia and in the Near East, confirm our model result that young air masses from the region of the Asian monsoon are transported to the top of the anticyclone above the tropopause up to around 460 K.

A trajectory analysis in combination with the 3-dimensional CLaMS simulation shows that air masses from the lower troposphere are rapidly lofted by convective events up to approximately 360 K potential temperature (**convective range**) (see Fig. 14) consistent to previous results (e.g., Randel and Park, 2006; Park et al., 2007, 2009; Chen et al., 2012; Bergman et al., 2013; Fadnavis et al., 2013). Strong convection occurs both directly below the Asian monsoon anticyclone in continental Asia (India and China) and outside the anticyclone region over Southeast Asia and the Pacific Ocean (see Fig. 15).

Above 360 K and up to ≈ 460 K, our findings from trajectory analysis demonstrate that air masses are uplifted in an anticyclonic large-scale upward spiral around the anticyclone extending from northern Africa to the western Pacific by diabatic heating of ≈ 1 – 1.5 K per day (**upward spiralling range**) (see Figs. 14 and 15). A straight homogeneous vertical cross-tropopause transport is not found in our backward trajectories, rather a very inhomogeneous horizontal distribution of tracers of air mass origin is found within and at the edge of the anticyclone, resulting in filamentary structures. Within the upward spiralling range strong horizontal transport of air masses from the eastern mode to the western mode of the anticyclone occurs. The altitude of the thermal tropopause is located within this upward spiralling range. Thus, air masses in the upward spiral spiralling range are uplifted by diabatic heating across the (lapse rate) tropopause, which does not act as a transport barrier against this diabatic vertical transport process. This transport across the tropopause is consistent with previous studies (e.g., Bergman et al., 2012; Garny and Randel, 2016; Ploeger et al., 2017). Diabatic heating rates within the tropical transition layer have strong seasonal variability. Diabatic heating rates of up to ≈ 1 – 1.5 K per day are in particular found between July and October 2008 over the region of the Asian monsoon anticyclone. In other regions within the tropical transition layer the heating rates are in general smaller (≈ 0.5 – 1.0 K per day).

Above 380 K mixing occurs between young air masses from inside (India/China) and outside (Southeast Asia/Pacific Ocean) the edge of the anticyclone. Between 420 K and 460 K highest contributions of young air masses are found around the edge of the anticyclone.

Thus, within the upward spiralling range above the anticyclone, young air masses from along the edge of the anticyclone originating in the tropical adjacent regions are mixed with air masses from inside the anticyclone mainly originating in India/China within the upward spiralling range above the anticyclone (see Fig. 15). Therefore, a significant fraction of air masses

from the tropical adjacent regions is found within a widespread area around the anticyclone and above caused by the large-scale anticyclonic flow in this region, acting as a large-scale stirrer, ~~which is consisted with our previous results~~. This transport pattern up to 460 K is consistent with previous results focused on lower levels of potential temperature up to ≈ 400 K (Vogel et al., 2014, 2016; Li et al., 2017).

5 Further between 420 K and 460 K, highest contributions from young air masses are found around the edge of the anticyclone, indicating a spatially strongly inhomogeneous ascent in the monsoon with strongest ascent at the edge. The higher in the upward spiralling range the more air masses from the stratospheric background are mixed with the young air masses transported upwards within this upward spiralling range –

~~To analyse the impact of air masses influenced by the region~~ (see Fig. 15). Thus in this paper, we answer the question of what are the transport pathways of young air masses at the top of the Asian monsoon ~~on~~ into the stratosphere by the concept of the upward spiralling range.

To answer our second question of how boundary layer source regions in Asia affect the composition of ~~air masses the middle stratosphere~~ within the tropical pipe at 550 K, the transport times from the Earth's surface up to this level of potential temperature need to be taken into account. In a two-monsoon-season simulation tracing back air masses that are released at the Earth's surface since 1 May 2007 (age < 18 months) only air masses older than 6 months are found within the tropical pipe at 550 K. Consequently, fresh emissions from the Asian monsoon season 2008 do not contribute to the distribution within the tropical pipe at 550 K. ~~before October 2008~~. Air masses released during the monsoon season 2007 and during Winter 2007/2008 contribute up to 55% to the signal within the tropical pipe at 550 K. ~~in October 2008~~. Air masses from India/China, mainly from inside the Asian monsoon anticyclone, contribute a minor fraction (6%) to the composition of air within the tropical pipe at 550 K; the major fraction is from Southeast Asia (16%) and the tropical Pacific (15%).

In summary, the transport ~~pathway~~ of air masses from the region of the Asian monsoon into the tropical pipe occurs in three distinct steps: first, very fast uplift within the convective range up to ≈ 360 K within the Asian monsoon anticyclone and outside in the tropical adjacent regions (within a few days). ~~Second;~~ second, uplift above 360 K up to ≈ 460 K within the upward spiralling range (within a few months) and third, above 460 K transport within the tropical pipe associated with the large-scale Brewer-Dobson circulation (within \sim one year). Furthermore, we emphasise that in addition to air masses from ~~within~~ the Asian monsoon region, a substantial percentage of air masses from the tropical adjacent regions (Southeast Asia/tropical Pacific/northern Africa/northwestern Pacific) ~~are transported in a substantial percentage is transported~~ by this pathway into the tropical pipe.

Data availability. The complete MIPAS data are available at <http://www.imk-asf.kit.edu/english/308.php>. The CLaMS model data may be requested from Bärbel Vogel (b.vogel@fz-juelich.de).

Appendix A: Intraseasonal variability of upwelling above Asian monsoon anticyclone

Global 20-day backward trajectories are calculated at 360 K, 380 K, 400 K, 420 K, 440 K potential temperature on a $2.5^\circ \times 2.0^\circ$ longitude-latitude-grid from 1 June until 31 October 2008 covering the time period from monsoon-onset until post-monsoon to discuss the intraseasonal variability of upward transport at the top of the Asian monsoon anticyclone. Some chosen days
5 (1 June, 1 July, 1 August, 1 September, and 1 October 2008) are shown in Fig. A1. During the monsoon season in July, August and September an upward transport of about 1–1.5 K per day is mainly found in the regions of the Asian monsoon anticyclone, in contrast to monsoon-onset in June. In June, an upward transport of about 1–1.5 K per day is found in the entire tropics, however the patterns are very inhomogeneous; in particular maximum values are found in the region of the northern subtropical jet stream.

10

Appendix B: Impact on the northern extratropical lower stratosphere

The accumulation of young air masses (age < 6 months) from the region of the Asian monsoon since 1 May 2008 in the northern extratropical lower stratosphere is calculated using a climatological isentropic barrier derived by Kunz et al. (2015) that separates tropical tropospheric air from ~~extra-tropical~~extratropical stratospheric air depending on potential temperature and
15 season. To calculate the percentages of different emission tracers within the ~~lower-extratropical~~extratropical lower stratosphere at 360 K and at 380 K, the mean value for each emission tracer of all CLaMS air parcels is calculated for PV values larger than those of the transport barrier (5.5 PVU at $360 \text{ K} \pm 0.5 \text{ K}$ and 7.2 PVU at $380 \text{ K} \pm 0.5 \text{ K}$) and poleward of 30°N for each day between 1 May and 31 October 2008. Fig. A2 shows that at the end of October 2008, the contributions of young air masses to the composition of northern extratropical lower stratosphere is up to 48% at 360 K (up to 41% at 380 K not shown here). The
20 contribution from India/China is up to 18% (16%) and from tropical Pacific and Southeast Asia up to 18% (16%).

Competing interests. The authors declare that they have no conflict of interest.

Acknowledgements. The authors sincerely thank ~~Michael Volk (University Wuppertal), and~~ William J. Randel (NCAR, Boulder), and Michael Volk (University Wuppertal) for very helpful discussions. We gratefully acknowledge the European Centre of Medium-Range Weather Forecasts (ECMWF) for providing the ERA-Interim reanalysis data. Our activities were partly funded by the European Commu-
25 nity's Seventh Framework Programme (FP7/2007-2013) under the project StratoClim (grant agreement no. 603557) and by the German Science Foundation (Deutsche Forschungsgemeinschaft, DFG) under the DFG project AMOS (HALO-SPP 1294/VO 1276/5-1). The authors would also like to thank three anonymous reviewers for their very helpful comments.

References

- Annamalai, H. and Slingo, J. M.: Active/break cycles: diagnosis of the intraseasonal variability of the Asian Summer Monsoon, *Clim. Dyn.*, 18, 85–102, 2001.
- Bannister, R. N., O'Neill, A., Gregory, A. R., and Nissen, K. M.: The role of the south-east Asian monsoon and other seasonal features in creating the 'tape-recorder' signal in the Unified Model, *Q. J. R. Meteorol. Soc.*, 130, 1531–1554, 2004.
- Bergman, J. W., Jensen, E. J., Pfister, L., and Yang, Q.: Seasonal differences of vertical-transport efficiency in the tropical tropopause layer: On the interplay between tropical deep convection, large-scale vertical ascent, and horizontal circulations, *J. Geophys. Res.*, 117, <https://doi.org/10.1029/2011JD016992>, 2012.
- Bergman, J. W., Fierli, F., Jensen, E. J., Honomichl, S., and Pan, L. L.: Boundary layer sources for the Asian anticyclone: Regional contributions to a vertical conduit, *J. Geophys. Res.*, 118, 2560–2575, <https://doi.org/10.1002/jgrd.50142>, 2013.
- Bourassa, A. E., Robock, A., Randel, W. J., Deshler, T., Rieger, L. A., Lloyd, N. D., Llewellyn, E. J. T., and Degenstein, D. A.: Large Volcanic Aerosol Load in the Stratosphere Linked to Asian Monsoon Transport, *Science*, 337, 78–81, <https://doi.org/10.1126/science.1219371>, 2012.
- Brunamonti, S., Jorge, T., Oelsner, P., Hanumanthu, S., Singh, B. B., Kumar, K. R., Sonbawne, S., Meier, S., Singh, D., Wienhold, F. G., Luo, B. P., Boettcher, M., Poltera, Y., Jauhiainen, H., Kayastha, R., Karmacharya, J., Dirksen, R., Naja, M., Rex, M., Fadnavis, S., and Peter, T.: Balloon-borne measurements of temperature, water vapor, ozone and aerosol backscatter on the southern slopes of the Himalayas during StratoClim 2016–2017, *Atmos. Chem. Phys.*, 18, 15 937–15 957, <https://doi.org/10.5194/acp-18-15937-2018>, <https://www.atmos-chem-phys.net/18/15937/2018/>, 2018.
- Chakraborty, A.: Preceding winter La Niña reduces Indian summer monsoon rainfall, *Environmental Research Letters*, 13, 054 030, <http://stacks.iop.org/1748-9326/13/i=5/a=054030>, 2018.
- Chen, B., Xu, X. D., Yang, S., and Zhao, T. L.: Climatological perspectives of air transport from atmospheric boundary layer to tropopause layer over Asian monsoon regions during boreal summer inferred from Lagrangian approach, *Atmos. Chem. Phys.*, pp. 5827–5839, <https://doi.org/10.5194/acp-12-5827>, 2012.
- Chirkov, M., Stiller, G. P., Laeng, A., Kellmann, S., von Clarmann, T., Boone, C. D., Elkins, J. W., Engel, A., Glatthor, N., Grabowski, U., Harth, C. M., Kiefer, M., Kolonjari, F., Krummel, P. B., Linden, A., Lunder, C. R., Miller, B. R., Montzka, S. A., Mühle, J., O'Doherty, S., Orphal, J., Prinn, R. G., Toon, G., Vollmer, M. K., Walker, K. A., Weiss, R. F., Wiecele, A., and Young, D.: Global HCFC-22 measurements with MIPAS: retrieval, validation, global distribution and its evolution over 2005-2012, *Atmos. Chem. Phys.*, 16, 3345–3368, <https://doi.org/10.5194/acp-16-3345-2016>, www.atmos-chem-phys.net/16/3345/2016/, 2016.
- Dee, D. P., Uppala, S. M., Simmons, A. J., Berrisford, P., Poli, P., Kobayashi, S., Andrae, U., Balmaseda, M. A., Balsamo, G., Bauer, P., Bechtold, P., Beljaars, A. C. M., van de Berg, L., Bidlot, J., Bormann, N., Delsol, C., Dragani, R., Fuentes, M., Geer, A. J., Haimberger, L., Healy, S. B., Hersbach, H., Holm, E. V., Isaksen, I., Kallberg, P., Koehler, M., Matricardi, M., McNally, A. P., Monge-Sanz, B. M., Morcrette, J.-J., Park, B.-K., Peubey, C., de Rosnay, P., Tavolato, C., Thepaut, J.-N., and Vitart, F.: The ERA-Interim reanalysis: configuration and performance of the data assimilation system, *Q. J. R. Meteorol. Soc.*, 137, 553–597, <https://doi.org/10.1002/qj.828>, 2011.
- Dethof, A., O'Neill, A., Slingo, J. M., and Smit, H. G. J.: A mechanism for moistening the lower stratosphere involving the Asian summer monsoon, *Q. J. R. Meteorol. Soc.*, 556, 1079–1106, 1999.

- Devasthale, A. and Fueglistaler, S.: A climatological perspective of deep convection penetrating the TTL during the Indian summer monsoon from the AVHRR and MODIS instruments, *Atmos. Chem. Phys.*, 10, 4573–4582, <https://doi.org/10.5194/acp-10-4573-2010>, <https://www.atmos-chem-phys.net/10/4573/2010/>, 2010.
- Fadnavis, S., Schultz, M. G., Semeniuk, K., Mahajan, A. S., Pozzoli, L., Sonbawne, S., Ghude, S. D., Kiefer, M., and Eckert, E.: Trends in peroxyacetyl nitrate (PAN) in the upper troposphere and lower stratosphere over southern Asia during the summer monsoon season: regional impacts, *Atmos. Chem. Phys.*, 14, 12 725–12 743, <https://doi.org/10.5194/acp-14-12725-2014>, 2014.
- Fairlie, D., Vernier, J.-P., Natarajan, M., and Bedka, K. M.: Dispersion of the Nabro volcanic plume and its relation to the Asian summer monsoon, *Atmos. Chem. Phys.*, 14, 7045–7057, <https://doi.org/10.5194/acp-14-7045-2014>, 2014.
- Fischer, H., Birk, M., Blom, C., Carli, B., Carlotti, M., von Clarmann, T., Delbouille, L., Dudhia, A., Ehhalt, D., Endemann, M., Flaud, J. M., Gessner, R., Kleinert, A., Koopmann, R., Langen, J., López-Puertas, M., Mosner, P., Nett, H., Oelhaf, H., Perron, G., Remedios, J., Ridolfi, M., Stiller, G., and Zander, R.: MIPAS: An instrument for atmospheric and climate research, *Atmos. Chem. Phys.*, 8, <https://doi.org/10.5194/acp-8-2151-2008>, 2008.
- Fortems-Cheiney, A., Chevallier, F., Saunio, M., Pison, I., Bousquet, Cressot, C., Wang, H. J., Yokouchi, Y., and Artuso, F.: HCFC-22 emissions at global and regional scales between 1995 and 2010: Trends and variability, *J. Geophys. Res.*, 118, 7379–7388, <https://doi.org/10.1002/jgrd.50544>, 2013.
- Fromm, M., Kablick III, G., Nedoluha, G., Carboni, E., Grainger, R., Campbell, J., and Lewis, J.: Correcting the record of volcanic stratospheric aerosol impact: Nabro and Sarychev Peak, *J. Geophys. Res.*, 119, 10 343–10 364, <https://doi.org/10.1002/2014JD021507>, <http://dx.doi.org/10.1002/2014JD021507>, 2014.
- Garny, H. and Randel, W. J.: Dynamic variability of the Asian monsoon anticyclone observed in potential vorticity and correlations with tracer distributions, *J. Geophys. Res.*, 118, 13 421–13 433, <https://doi.org/10.1002/2013JD020908>, 2013.
- Garny, H. and Randel, W. J.: Transport pathways from the Asian monsoon anticyclone to the stratosphere, *Atmos. Chem. Phys.*, 16, 2703–2718, <https://doi.org/10.5194/acp-16-2703-2016>, 2016.
- Gill, A. E.: Some simple solutions for heat-induced tropical circulation, *Q. J. R. Meteorol. Soc.*, 106, 447–462, 1980.
- Glatthor, N., Höpfner, M., Stiller, G. P., von Clarmann, T., Funke, B., Lossow, S., Eckert, E., Grabowski, U., Kellmann, S., Linden, A., Walker, K. A., and Wiegeler, A.: Seasonal and interannual variations in HCN amounts in the upper troposphere and lower stratosphere observed by MIPAS, *Atmos. Chem. Phys.*, 15, 563–582, <https://doi.org/10.5194/acp-15-563-2015>, 2015.
- Griessbach, S., Hoffmann, L., Spang, R., von Hobe, M., Müller, R., and Riese, M.: MIPAS Volcanic Sulfate Aerosol Observations of the Nabro Eruption, in: *Stratospheric Sulfur and its Role in Climate (SSiRC)*, Atlanta, Georgia, USA, October 2013, SPARC, <http://www.sparc-ssirc.org/downloads/Griessbach.pdf>, 2013.
- Günther, G., Müller, R., von Hobe, M., Stroh, F., Konopka, P., and Volk, C. M.: Quantification of transport across the boundary of the lower stratospheric vortex during Arctic winter 2002/2003, *Atmos. Chem. Phys.*, 8, 3655–3670, <http://www.atmos-chem-phys.net/8/3655/2008/>, 2008.
- Highwood, E. J. and Hoskins, B. J.: The tropical tropopause, *Q. J. R. Meteorol. Soc.*, 124, 1579 – 1604, 1998.
- Höpfner, M., Volkamer, R., Grabowski, U., Grutter, M., Orphal, J., Stiller, G., von Clarmann, T., and Wetzel, G.: First detection of ammonia (NH₃) in the Asian summer monsoon upper troposphere, *Atmos. Chem. Phys.*, 16, 14 357–14 369, <https://doi.org/10.5194/acp-16-14357-2016>, <https://www.atmos-chem-phys.net/16/14357/2016/>, 2016.
- Hosking, J. S., Russo, M. R., Braesicke, P., and Pyle, J. A.: Tropical convective transport and the Walker circulation, *Atmos. Chem. Phys.*, 12, 9791–9797, <https://doi.org/10.5194/acp-12-9791-2012>, <https://www.atmos-chem-phys.net/12/9791/2012/>, 2012.

- Hossaini, R., Chipperfield, M., Montzka, M. P., Rap, S. A., Dhomse, S., and Feng, W.: Efficiency of short-lived halogens at influencing climate through depletion of stratospheric ozone, *Nature Geoscience*, 8, 186–190, <https://doi.org/10.1038/ngeo2363>, 2015.
- Hsu, C. J. and Plumb, R. A.: Nonaxisymmetric Thermally Driven Circulations and Upper-Tropospheric Monsoon Dynamics, *J. Atmos. Sci.*, 57, 1255–1276, 2001.
- 5 Ko, M., Newman, P., Reimann, S., and Strahan, S., eds.: Lifetimes of Stratospheric Ozone-Depleting Substances, Their Replacements, and Related Species, SPARC Report No. 6, WCRP-15/2013, SPARC 6, 2013.
- Konopka, P., Günther, G., Müller, R., dos Santos, F. H. S., Schiller, C., Ravegnani, F., Ulanovsky, A., Schlager, H., Volk, C. M., Viciani, S., Pan, L. L., McKenna, D.-S., and Riese, M.: Contribution of mixing to upward transport across the tropical tropopause layer (TTL), *Atmos. Chem. Phys.*, 7, 3285–3308, 2007.
- 10 Konopka, P., Groöß, J.-U., Günther, G., Ploeger, F., Pommrich, R., Müller, R., and Livesey, N.: Annual cycle of ozone at and above the tropical tropopause: observations versus simulations with the Chemical Lagrangian Model of the Stratosphere (CLaMS), *Atmos. Chem. Phys.*, 10, 121–132, <https://doi.org/10.5194/acp-10-121-2010>, <http://www.atmos-chem-phys.net/10/121/2010/>, 2010.
- Konopka, P., Ploeger, F., and Müller, R.: Entropy- and static stability-based Lagrangian model grids, in: *Geophysical Monograph Series: Lagrangian Modeling of the Atmosphere*, edited by Lin, J., vol. 200, pp. 99–109, American Geophysical Union, <https://doi.org/10.1029/2012GM001253>, 2012.
- 15 Kumar, K. K., Rajagopalan, B., Hoerling, M., Bates, G., and Cane, M.: Unraveling the Mystery of Indian Monsoon Failure During El Niño, *Science*, 314, 115–119, <https://doi.org/10.1126/science.1131152>, 2006.
- Kunz, A., Sprenger, M., and Wernli, H.: Climatology of potential vorticity streamers and associated isentropic transport pathways across PV gradient barriers, *J. Geophys. Res.*, 120, 3802–3821, <https://doi.org/10.1002/2014JD022615>, <http://dx.doi.org/10.1002/2014JD022615>, 2014JD022615, 2015.
- 20 Li, D., Vogel, B., Bian, J., Müller, R., Pan, L. L., Günther, G., Bai, Z., Li, Q., Zhang, J., Fan, Q., and Vömel, H.: Impact of typhoons on the composition of the upper troposphere within the Asian summer monsoon anticyclone: the SWOP campaign in Lhasa 2013, *Atmos. Chem. Phys.*, 17, 4657–4672, <https://doi.org/10.5194/acp-17-4657-2017>, <https://www.atmos-chem-phys.net/17/4657/2017/>, 2017.
- Li, Q., Jiang, J. H., Wu, D. L., Read, W. G., Livesey, N. J., Waters, J. W., Zhang, Y., Wang, B., Filipiak, M. J., Davis, C. P., Turquety, S., Wu, S., Park, R. J., Yantosca, R. M., and Jacob, D. J.: Convective outflow of South Asian pollution: A global CTM simulation compared with EOS MLS observations, *Geophys. Res. Lett.*, 32, L14 826, <https://doi.org/10.1029/2005GL022762>, 2005.
- 25 McKenna, D. S., Groöß, J.-U., Günther, G., Konopka, P., Müller, R., Carver, G., and Sasano, Y.: A new Chemical Lagrangian Model of the Stratosphere (CLaMS): 2. Formulation of chemistry scheme and initialization, *J. Geophys. Res.*, 107, 4256, <https://doi.org/10.1029/2000JD000113>, 2002a.
- 30 McKenna, D. S., Konopka, P., Groöß, J.-U., Günther, G., Müller, R., Spang, R., Offermann, D., and Orsolini, Y.: A new Chemical Lagrangian Model of the Stratosphere (CLaMS): 1. Formulation of advection and mixing, *J. Geophys. Res.*, 107, 4309, <https://doi.org/10.1029/2000JD000114>, 2002b.
- Müller, S., Hoor, P., Bozem, H., Gute, E., Vogel, B., Zahn, A., Bönisch, H., Keber, T., Krämer, M., Rolf, C., Riese, M., Schlager, H., and Engel, A.: Impact of the Asian monsoon on the extratropical lower stratosphere: trace gas observations during TACTS over Europe 2012, *Atmos. Chem. Phys.*, 16, 10 573–10 589, <https://doi.org/10.5194/acp-16-10573-2016>, 2016.
- 35 Nützel, M., Dameris, M., and Garny, H.: Movement, drivers and bimodality of the South Asian High, *Atmos. Chem. Phys.*, 16, 14 755–14 774, <https://doi.org/10.5194/acp-16-14755-2016>, <https://www.atmos-chem-phys.net/16/14755/2016/>, 2016.

- Orbe, C., Waugh, D. W., and Newman, P. A.: Air-mass origin in the tropical lower stratosphere: The influence of Asian boundary layer air, *Geophys. Res. Lett.*, 42, 2015GL063937, <https://doi.org/10.1002/2015GL063937>, <http://dx.doi.org/10.1002/2015GL063937>, 2015.
- Pan, L. L. and Munchak, L. A.: Relationship of cloud top to the tropopause and jet structure from CALIPSO data, *J. Geophys. Res.*, 116, D12201, <https://doi.org/10.1029/2010JD015462>, 2011.
- 5 Pan, L. L., Konopka, P., and Browell, E. V.: Observations and model simulations of mixing near the extratropical tropopause, *J. Geophys. Res.*, 111, D05106, <https://doi.org/10.1029/2005JD006480>, 2006.
- Pan, L. L., Honomichl, S. B., Kinnison, D. E., Abalos, M., Randel, W. J., Bergman, J. W., and Bian, J.: Transport of chemical tracers from the boundary layer to stratosphere associated with the dynamics of the Asian summer monsoon, *Journal of Geophysical Research: Atmospheres*, 121, 14,159–14,174, <https://doi.org/10.1002/2016JD025616>, <https://agupubs.onlinelibrary.wiley.com/doi/abs/10.1002/2016JD025616>, 2016.
- 10 Park, M., Randel, W. J., Gettleman, A., Massie, S. T., and Jiang, J. H.: Transport above the Asian summer monsoon anticyclone inferred from Aura Microwave Limb Sounder tracers, *J. Geophys. Res.*, 112, D16309, <https://doi.org/10.1029/2006JD008294>, 2007.
- Park, M., Randel, W. J., Emmons, L. K., and Livesey, N. J.: Transport pathways of carbon monoxide in the Asian summer monsoon diagnosed from Model of Ozone and Related Tracers (MOZART), *J. Geophys. Res.*, 114, D08303, <https://doi.org/10.1029/2008JD010621>, 2009.
- 15 Ploeger, F., Konopka, P., Günther, G., Groöß, J.-U., and Müller, R.: Impact of the vertical velocity scheme on modeling transport across the tropical tropopause layer, *J. Geophys. Res.*, 115, D03301, <https://doi.org/10.1029/2009JD012023>, 2010.
- Ploeger, F., Konopka, P., Müller, R., Fueglistaler, S., Schmidt, T., Manners, J. C., Groöß, J.-U., Günther, G., Forster, P. M., and Riese, M.: Horizontal transport affecting trace gas seasonality in the Tropical Tropopause Layer (TTL), *J. Geophys. Res.*, 117, D09303, <https://doi.org/10.1029/2011JD017267>, 2012.
- 20 Ploeger, F., Günther, G., Konopka, P., Fueglistaler, S., Müller, R., Hoppe, C., Kunz, A., Spang, R., Groöß, J.-U., and Riese, M.: Horizontal water vapor transport in the lower stratosphere from subtropics to high latitudes during boreal summer, *J. Geophys. Res.*, 118, 8111–8127, <https://doi.org/10.1002/jgrd.50636>, 2013.
- Ploeger, F., Gottschling, C., Griebach, S., Groöß, J.-U., Günther, G., Konopka, P., Müller, R., Riese, M., Stroh, F., Tao, M., Ungermann, J., Vogel, B., and von Hobe, M.: A potential vorticity-based determination of the transport barrier in the Asian summer monsoon anticyclone, *Atmos. Chem. Phys.*, 15, 13 145–13 159, <https://doi.org/doi:10.5194/acp-15-13145-2015>, 2015.
- 25 Ploeger, F., Konopka, P., Walker, K., and Riese, M.: Quantifying pollution transport from the Asian monsoon anticyclone into the lower stratosphere, *Atmos. Chem. Phys.*, 17, 7055–7066, <https://doi.org/10.5194/acp-17-7055-2017>, <https://www.atmos-chem-phys.net/17/7055/2017/>, 2017.
- Plumb, R. A.: A “tropical pipe” model of stratospheric transport, *J. Geophys. Res.*, 101, 3957–3972, 1996.
- 30 Pommrich, R., Müller, R., Groöß, J.-U., Konopka, P., Ploeger, F., Vogel, B., Tao, M., Hoppe, C. M., Günther, G., Spelten, N., Hoffmann, L., Pumphrey, H.-C., Viciani, S., D’Amato, F., Volk, C. M., Hoor, P., Schlager, H., and Riese, M.: Tropical troposphere to stratosphere transport of carbon monoxide and long-lived trace species in the Chemical Lagrangian Model of the Stratosphere (CLaMS), *Geosci. Model Dev.*, 7, 2895–2916, <https://doi.org/10.5194/gmd-7-2895-2014>, <http://www.geosci-model-dev.net/7/2895/2014/>, 2014.
- Popovic, J. M. and Plumb, R. A.: Eddy Shedding from the Upper-Tropospheric Asian Monsoon Anticyclone, *J. Atmos. Sci.*, 58, 93–104, 2001.
- 35 Randel, W. and Jensen, E.: Physical processes in the tropical tropopause layer and their role in a changing climate, *Nature Geoscience*, 6, 169–176, <https://doi.org/10.1038/ngeo1733>, 2013.

- Randel, W. J. and Park, M.: Deep convective influence on the Asian summer monsoon anticyclone and associated tracer variability observed with Atmospheric Infrared Sounder (AIRS), *J. Geophys. Res.*, 111, D12314, <https://doi.org/10.1029/2005JD006490>, 2006.
- Randel, W. J., Park, M., Emmons, L., Kinnison, D., Bernath, P., Walker, K. A., Boone, C., and Pumphrey, H.: Asian Monsoon Transport of Pollution to the Stratosphere, *Science*, 328, 611–613, <https://doi.org/10.1126/science.1182274>, 2010.
- 5 Riese, M., Ploeger, F., Rap, A., Vogel, B., Konopka, P., Dameris, M., and Forster, P.: Impact of uncertainties in atmospheric mixing on simulated UTLS composition and related radiative effects, *J. Geophys. Res.*, 117, D16305, <https://doi.org/10.1029/2012JD017751>, 2012.
- Rolf, C., Vogel, B., Hoor, P., Afchine, A., Günther, G., Krämer, M., Müller, R., Müller, S., Spelten, N., and Riese, M.: Water vapor increase in the lower stratosphere of the Northern Hemisphere due to the Asian monsoon anticyclone observed during the TACTS/ESMVal campaigns, *Atmospheric Chemistry and Physics*, 18, 2973–2983, <https://doi.org/10.5194/acp-18-2973-2018>, [https://www.atmos-chem-phys.net/18/](https://www.atmos-chem-phys.net/18/2973/2018/)
10 2973/2018/, 2018.
- Rosenlof, K. H., Tuck, A. F., Kelly, K. K., Russell III, J. M., and McCormick, M. P.: Hemispheric asymmetries in the water vapor and inferences about transport in the lower stratosphere, *J. Geophys. Res.*, 102, 13 213–13 234, <https://doi.org/10.1029/97JD00873>, 1997.
- Santee, M. L., Manney, G. L., Livesey, N. J., Schwartz, M. J., Neu, J. L., and Read, W. G.: A comprehensive overview of the climatological composition of the Asian summer monsoon anticyclone based on 10 years of Aura Microwave Limb Sounder measurements, *Journal of Geophysical Research: Atmospheres*, 122, 5491–5514, <https://doi.org/10.1002/2016JD026408>, <https://agupubs.onlinelibrary.wiley.com/doi/abs/10.1002/2016JD026408>, 2017.
- 15 Schoeberl, M. R., Dessler, A. E., and Wang, T.: Simulation of stratospheric water vapor and trends using three reanalyses, *Atmos. Chem. Phys.*, 12, 6475–6487, <https://doi.org/10.5194/acp-12-6475-2012>, 2012.
- Simmonds, P. G., Rigby, M., McCulloch, A., Vollmer, M. K., Henne, S., Mühle, J., O’Doherty, S., Manning, A. J., Krummel, P. B., Fraser, P. J., Young, D., Weiss, R. F., Salameh, P. K., Harth, C. M., Reimann, S., Trudinger, C. M., Steele, L. P., Wang, R. H. J., Ivy, D. J., Prinn, R. G., Mitrevski, B., and Etheridge, D. M.: Recent increases in the atmospheric growth rate and emissions of HFC-23 (CHF₃) and the link to HCFC-22 (CHClF₂) production, *Atmospheric Chemistry and Physics*, 18, 4153–4169, <https://doi.org/10.5194/acp-18-4153-2018>, <https://www.atmos-chem-phys.net/18/4153/2018/>, 2018.
- 20 Solomon, S., Rosenlof, K., Portmann, R., Daniel, J., Davis, S., Sanford, T., and Plattner, G.-K.: Contributions of stratospheric water vapor to decadal changes in the rate of global warming, *Science*, 327, 1219–1223, <https://doi.org/10.1126/science.1182488>, 2010.
- Spang, R., Günther, G., Riese, M., Hoffmann, L., Müller, R., and Griessbach, S.: Satellite observations of cirrus clouds in the Northern Hemisphere lowermost stratosphere, *Atmospheric Chemistry and Physics*, 15, 927–950, <https://doi.org/10.5194/acp-15-927-2015>, <http://www.atmos-chem-phys.net/15/927/2015/>, 2015.
- Tissier, A.-S. and Legras, B.: Convective sources of trajectories traversing the tropical tropopause layer, *Atmos. Chem. Phys.*, 16, 3383–3398, <https://doi.org/10.5194/acp-16-3383-2016>, 2016.
- 30 Uma, K. N., Das, S. K., and Das, S. S.: A climatological perspective of water vapor at the UTLS region over different global monsoon regions: observations inferred from the Aura-MLS and reanalysis data, *Clim. Dyn.*, 43, 407–420, <https://doi.org/10.1007/s00382-014-2085-9>, 2014.
- Ungermann, J., Ern, M., Kaufmann, M., Müller, R., Spang, R., Ploeger, F., Vogel, B., and Riese, M.: Observations of PAN and its confinement in the Asian summer monsoon anticyclone in high spatial resolution, *Atmos. Chem. Phys.*, 16, 8389–8403, <https://doi.org/10.5194/acp-16-8389-2016>, 2016.
- 35

- Vernier, J. P., Fairlie, T. D., Natarajan, M., Wienhold, F. G., Bian, J., Martinsson, B. G., Crumeyrolle, S., Thomason, L. W., and Bedka, K. M.: Increase in upper tropospheric and lower stratospheric aerosol levels and its potential connection with Asian pollution, *J. Geophys. Res.*, <https://doi.org/10.1002/2014JD022372>, 2015.
- Vernier, J.-P., Fairlie, T. D., Deshler, T., Ratnam, M. V., Gadhavi, H., Kumar, B. S., Natarajan, M., Pandit, A. K., Raj, S. T. A., Kumar, A. H., Jayaraman, A., Singh, A. K., Rastogi, N., Sinha, P. R., Kumar, S., Tiwari, S., Wegner, T., Baker, N., Vignelles, D., Stenchikov, G., Shevchenko, I., Smith, J., Bedka, K., Kesarkar, A., Singh, V., Bhate, J., Ravikiran, V., Rao, M. D., Ravindrababu, S., Patel, A., Vernier, H., Wienhold, F. G., Liu, H., Knepp, T. N., Thomason, L., Crawford, J., Ziemba, L., Moore, J., Crumeyrolle, S., Williamson, M., Berthet, G., Jégou, F., and Renard, J.-B.: BATAL: The Balloon Measurement Campaigns of the Asian Tropopause Aerosol Layer, *Bull. Am. Meteorol. Soc.*, 99, 955–973, <https://doi.org/10.1175/BAMS-D-17-0014.1>, 2018.
- 5 Vogel, B., Konopka, P., Groöß, J.-U., Müller, R., Funke, B., López-Puertas, M., Reddman, T., Stiller, G., von Clarmann, T., and Riese, M.: Model simulations of stratospheric ozone loss caused by enhanced mesospheric NO_x during Arctic Winter 2003/2004, *Atmos. Chem. Phys.*, 8, 5279–5293, 2008.
- 10 Vogel, B., Pan, L. L., Konopka, P., Günther, G., Müller, R., Hall, W., Campos, T., Pollack, I., Weinheimer, A., Wei, J., Atlas, E. L., and Bowman, K. P.: Transport pathways and signatures of mixing in the extratropical tropopause region derived from Lagrangian model simulations, *J. Geophys. Res.*, 116, D05306, <https://doi.org/10.1029/2010JD014876>, 2011.
- 15 Vogel, B., Günther, G., Müller, R., Groöß, J.-U., Hoor, P., Krämer, M., Müller, S., Zahn, A., and Riese, M.: Fast transport from Southeast Asia boundary layer sources to northern Europe: rapid uplift in typhoons and eastward eddy shedding of the Asian monsoon anticyclone, *Atmos. Chem. Phys.*, 14, 12 745–12 762, <https://doi.org/10.5194/acp-14-12745-2014>, <http://www.atmos-chem-phys.net/14/12745/2014/>, 2014.
- 20 Vogel, B., Günther, G., Müller, R., Groöß, J.-U., and Riese, M.: Impact of different Asian source regions on the composition of the Asian monsoon anticyclone and of the extratropical lowermost stratosphere, *Atmos. Chem. Phys.*, 15, 13 699–13 716, <https://doi.org/10.5194/acp-15-13699-2015>, <http://www.atmos-chem-phys.net/15/13699/2015/>, 2015.
- Vogel, B., Günther, G., Müller, R., Jens-Uwe Groöß, A. A., Bozem, H., Hoor, P., Krämer, M., Müller, S., Riese, M., Rolf, C., Spelten, N., Stiller, G. P., Ungermann, J., and Zahn, A.: Long-range transport pathways of tropospheric source gases originating in Asia into the northern lower stratosphere during the Asian monsoon season 2012, *Atmos. Chem. Phys.*, 16, 15 301–15 325, <https://doi.org/10.5194/acp-16-15301-2016>, <http://www.atmos-chem-phys.net/16/15301/2016/>, 2016.
- 25 Volk, C. M., Elkins, J. W., Fahey, D. W., Salawitch, R. J., Dutton, G. S., Gilligan, J. M., Proffitt, M. H., Loewenstein, M., Podolske, J. R., Minschwaner, K., Margitan, J. J., and Chan, K. R.: Quantifying transport between the tropical and mid-latitude lower stratosphere, *Science*, 272, 1763–1768, 1996.
- 30 Webster, P. J., Magaña, V. O., Palmer, T. N., Shukla, J., Tomas, R. A., Yanai, M., and Yasunari, T.: Monsoon: Processes, predictability, and the prospects for prediction, *J. Geophys. Res.*, 103, 14.451–14.510, 1998.
- Wright, J. S. and Fueglistaler, S.: Large differences in reanalyses of diabatic heating in the tropical upper troposphere and lower stratosphere, *Atmos. Chem. Phys.*, 13, 9565–9576, <https://doi.org/10.5194/acp-13-9565-2013>, 2013.
- Wright, J. S., Fu, R., Fueglistaler, S., Liu, Y. S., and Zhang, Y.: The influence of summertime convection over Southeast Asia on water vapor in the tropical stratosphere, *J. Geophys. Res.*, 116, D12302, <https://doi.org/10.1029/2010JD015416>, 2011.
- 35 Wu, X., Griessbach, S., and Hoffmann, L.: Equatorward dispersion of a high-latitude volcanic plume and its relation to the Asian summer monsoon: a case study of the Sarychev eruption in 2009, *Atmos. Chem. Phys.*, 17, 13 439–13 455, <https://doi.org/10.5194/acp-17-13439-2017>, <https://www.atmos-chem-phys.net/17/13439/2017/>, 2017.

Table 1. Latitude and longitude range of artificial boundary layer sources in the CLaMS model, also referred to as “emission tracers”. The geographical position of each emission tracer is shown in Fig. 1 (adapted from Vogel et al. (2015, 2016))

Emission tracer (Ω_i)	Latitude	Longitude
Northern India (NIN)	20–40° N	55–90° E
Southern India (SIN)	0–20° N	55–90° E
Eastern China (ECH)	20–40° N	90–125° E
Southeast Asia (SEA)	12° S–20° N	90–155° E
Northwestern Pacific (NWP)	20–40° N	125–180° E
Siberia (SIB)	40–75° N	55–180° E
Europe (EUR)	45–75° N	20° W–55° E
Mediterranean (MED)	35–45° N	20° W–55° E
Northern Africa (NAF)	0–35° N	20° W–55° E
Southern Africa (SAF)	36° S–0° N	7–42° E
Madagascar (MDG)	27–12° S	42–52° E
Australia (AUS)	40–12° S	110–155° E
North America (NAM)	15–75° N	160–50° W
South America (SAM)	55° S–15° N	80–35° W
Tropical Pacific Ocean (TPO)	20° S–20° N	see Fig. 1
Tropical Atlantic Ocean (TAO)	20° S–20° N	see Fig. 1
Tropical Indian Ocean (TIO)	20° S–20° N	see Fig. 1
<u>Background</u>	<u>remaining surface</u>	<u>see Fig. 1</u>
<u>ALL ($\Omega = \sum_{i=1}^n \Omega_i$)</u>	entire surface	
India/China	NIN+SIN+ECH	
tropical adjacent regions (TAR)	SEA+TPO+NAF+NWP	
ALL -height		

Zhang, Q., Wu, G., and Qian, Y.: The Bimodality of the 100 hPa South Asia High and its Relationship to the Climate Anomaly over East Asia in Summer, *J. Meteorol. Soc. Jpn.*, 80, 733–744, 2002.

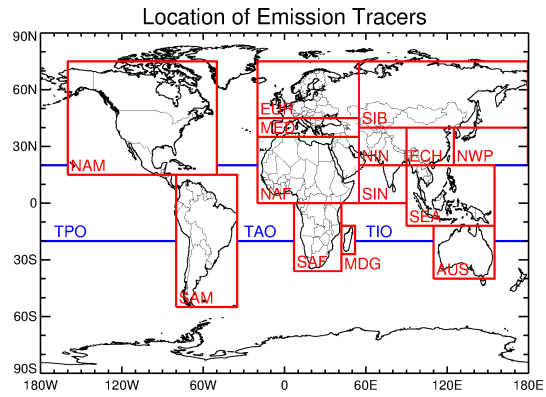


Figure 1. Global geographical location of artificial boundary layer source regions in the CLaMS model, also referred to as ‘emission tracers’ adapted from Vogel et al. (2015). The latitude and longitude range for each emission tracer is listed in Table 1.



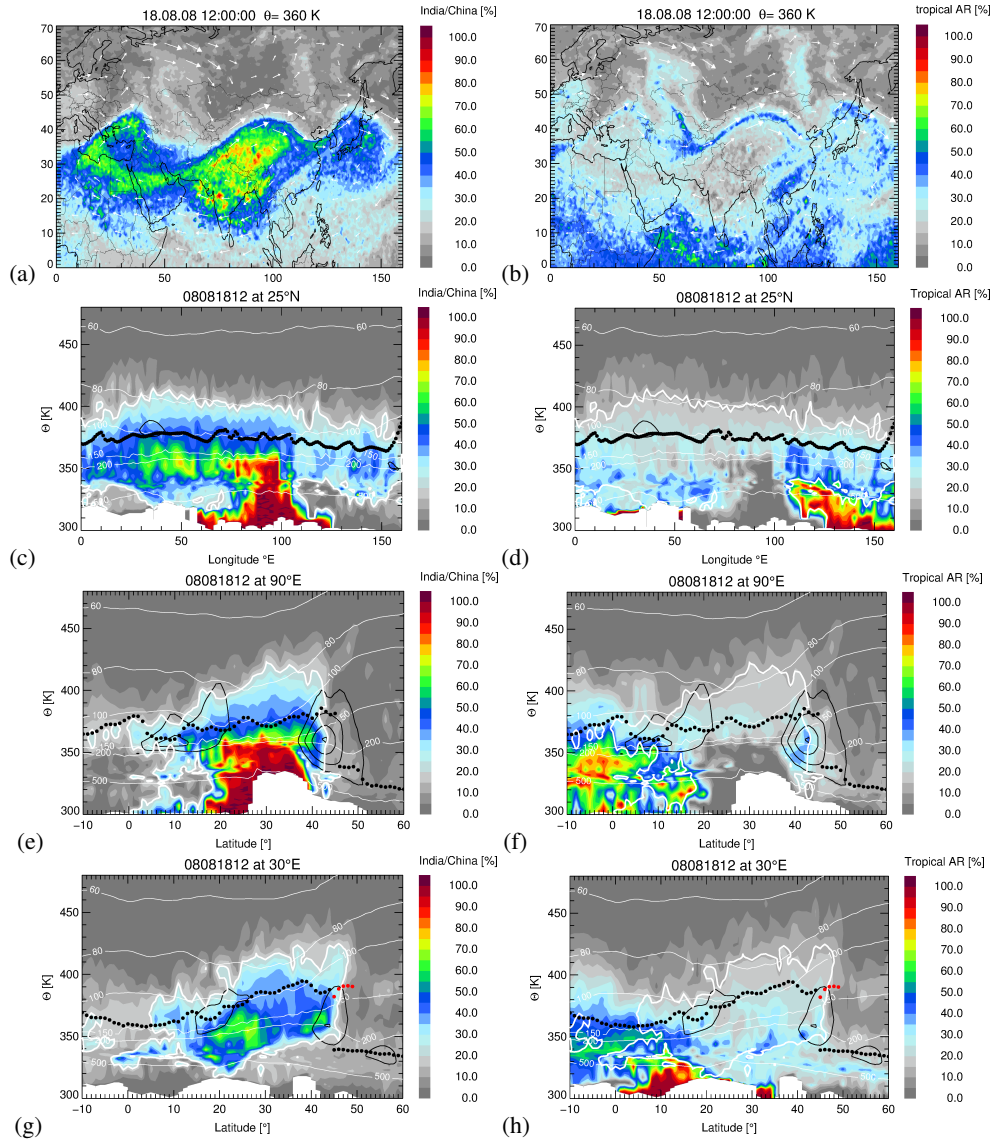


Figure 2. Horizontal distribution of the fraction of air originating in India/China (left) and in tropical adjacent regions (right) at 360 K potential temperature, longitude–theta cross sections at 25°N and latitude–theta cross sections at 90°E (eastern part of the anticyclone) and 30°E (western part of the anticyclone) on 18 August 2008. The horizontal winds are indicated by white arrows (maps) or by black thin lines (cross sections) (shown are 30, 40, 50, and 60 m/s). The first-primary thermal tropopause is marked by black dots, the second-secondary thermal tropopause by red dots, and the corresponding levels of pressure are marked by thin white lines. The contour line of 20% percentages of the India/China tracer is shown by thick white lines (cross sections).

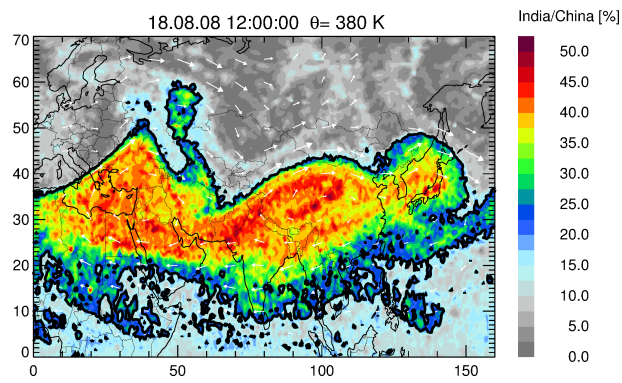


Figure 3. Horizontal distribution of the fraction of air originating in India/China at 380 K potential temperature. The contour line of 20% of the India/China tracer is shown by thick black line.

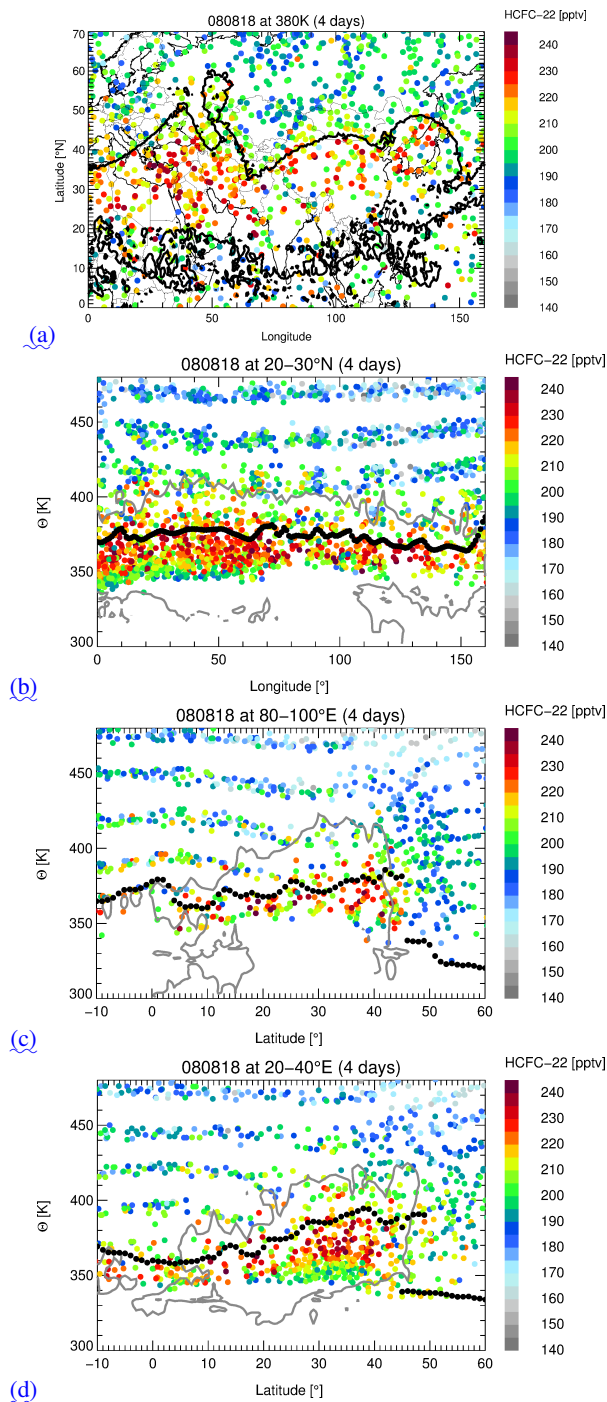


Figure 4. Horizontal distribution of **the fraction of air originating in India/China (left) and of MIPAS HCFC-22 measurements (right)** at 380 K potential temperature (**topa**). The MIPAS measurements are synoptically interpolated within 4 days (for details see Sect. 2.4). **Latitude–theta Longitude–theta cross section at 25°N (b) is shown as well as latitude–theta cross sections at 3090°E (western-eastern part of the anticyclone) (c) and 90at 30°E (eastern-western part of the anticyclone) (d) on 18 August 2008 are shown (2nd row) as well as a longitude–theta cross section at 25°N (bottom)–2008.** The contour line of 20% of the India/China tracer is shown by thick black (**maps**) or grey (**cross sections**) lines as shown in **FigFigs. 3 and 2.** The thermal tropopause is marked by black dots.

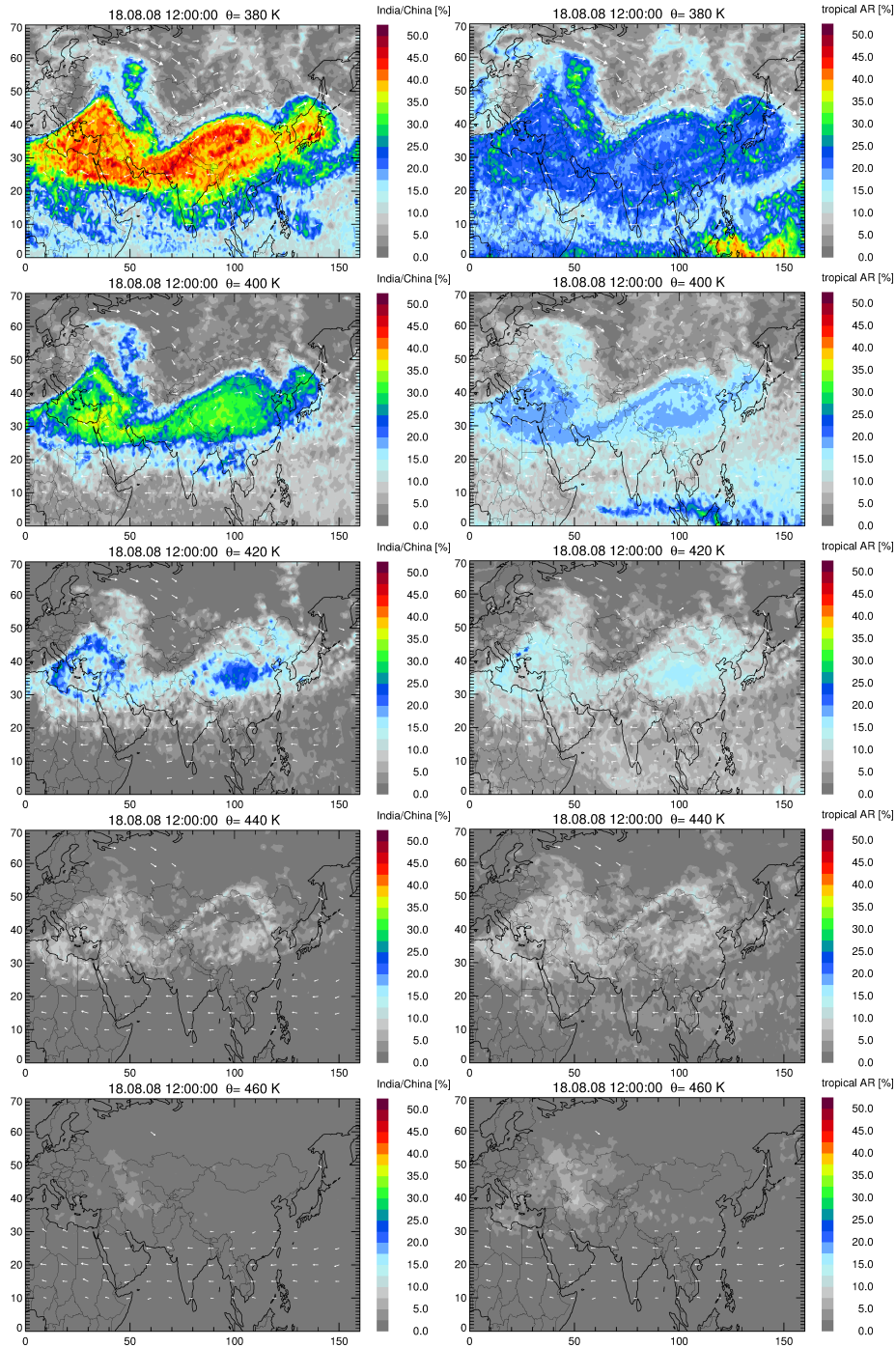


Figure 5. Horizontal distribution of the fraction of air originating in India/China (left) and in tropical adjacent regions (right) at 380 K, 400 K, 420 K, 440 K, and 460 K potential temperature.

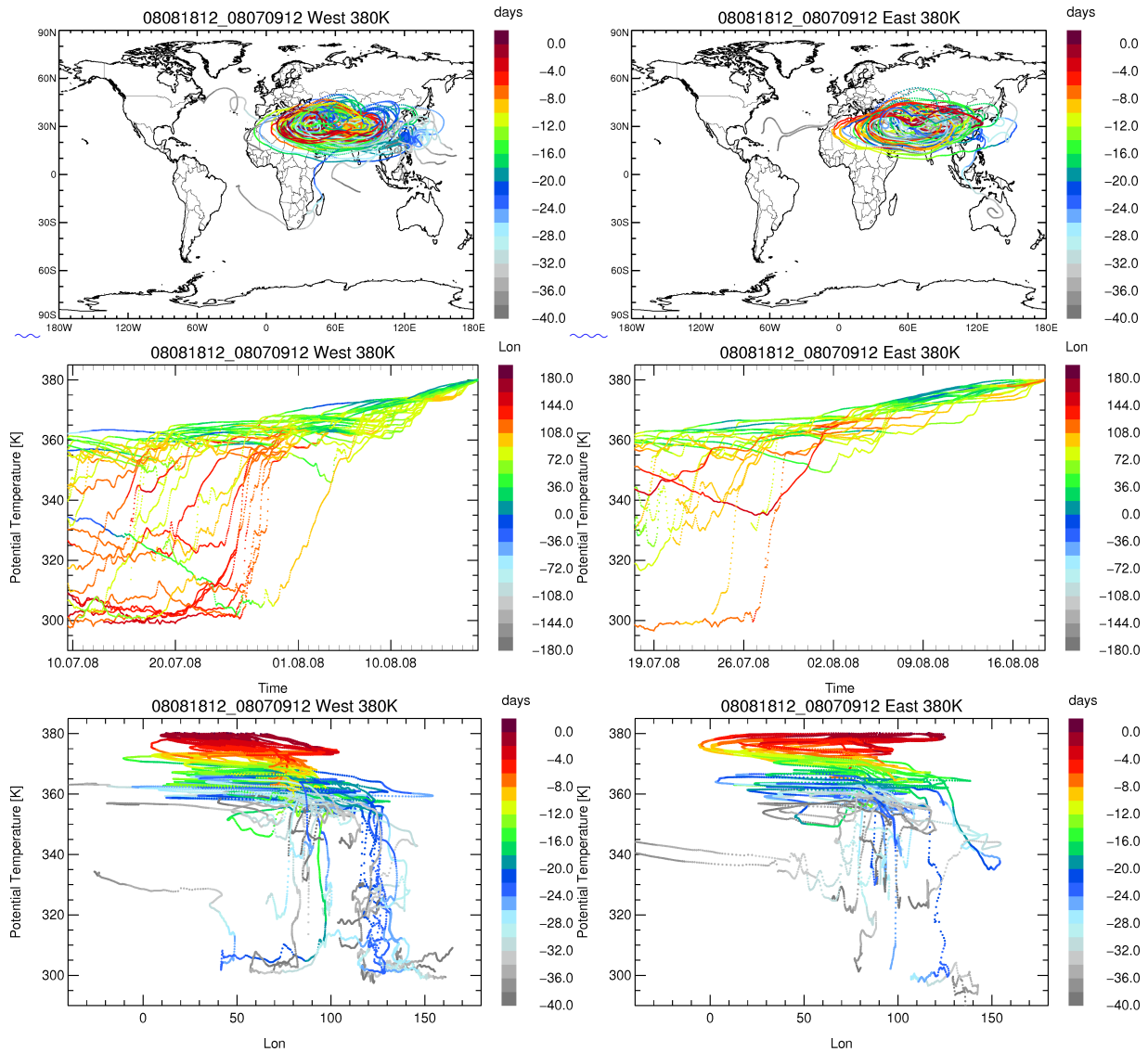


Figure 6. Different 40-day backward trajectories started at 380K in the western (left) and eastern (right) mode of the Asian monsoon anticyclone are shown colour-coded by days back from 18 August 2008 (top). Further, potential temperature versus time (in UTC) along 40-day backward trajectories colour-coded by longitude (middle) and potential temperature versus longitude colour-coded by days reversed back from 18 August 2008 (bottom) are shown. The trajectory positions are plotted every hour (coloured dots). Large distances between single successive positions indicate rapid uplift.

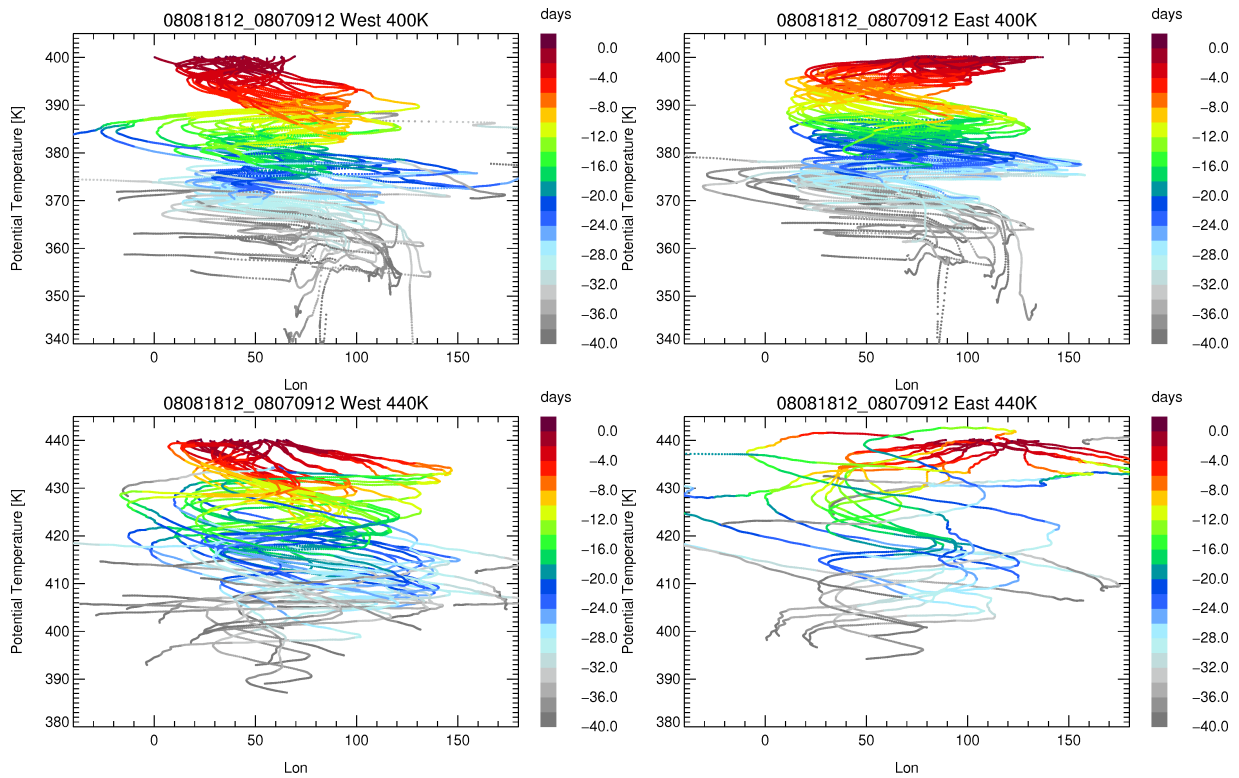


Figure 7. Potential temperature of different 40-day backward trajectories started at 400 K (top) and 440 K (bottom) in the western (left) and eastern ~~mode~~ (right) ~~mode~~ of the Asian monsoon anticyclone are shown versus longitude colour-coded by days ~~reversed~~ ~~back~~ from 18 August 2008

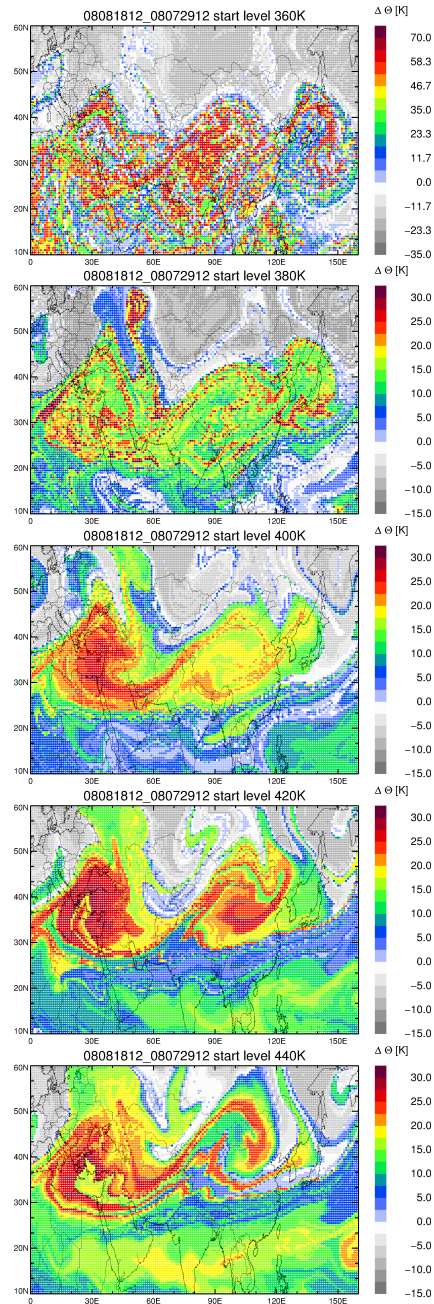


Figure 8. The change in potential temperature ($\Delta\Theta$) along 20-day backward trajectories initialised on 18 August 2008 are shown for different levels of potential temperature (360 K, 380 K, 400 K, 420 K, and 440 K). Note that the range of the colour bar in the 1st row panel is much larger than in the other rows panels. At the lower potential temperature levels (360 K, 380 K), some 20-day backward trajectories exist that reach the model boundary layer within a time period shorter than 20 days (in cases of very strong uplift by convection). For these trajectories $\Delta\Theta$ is shown for the shorter time period.

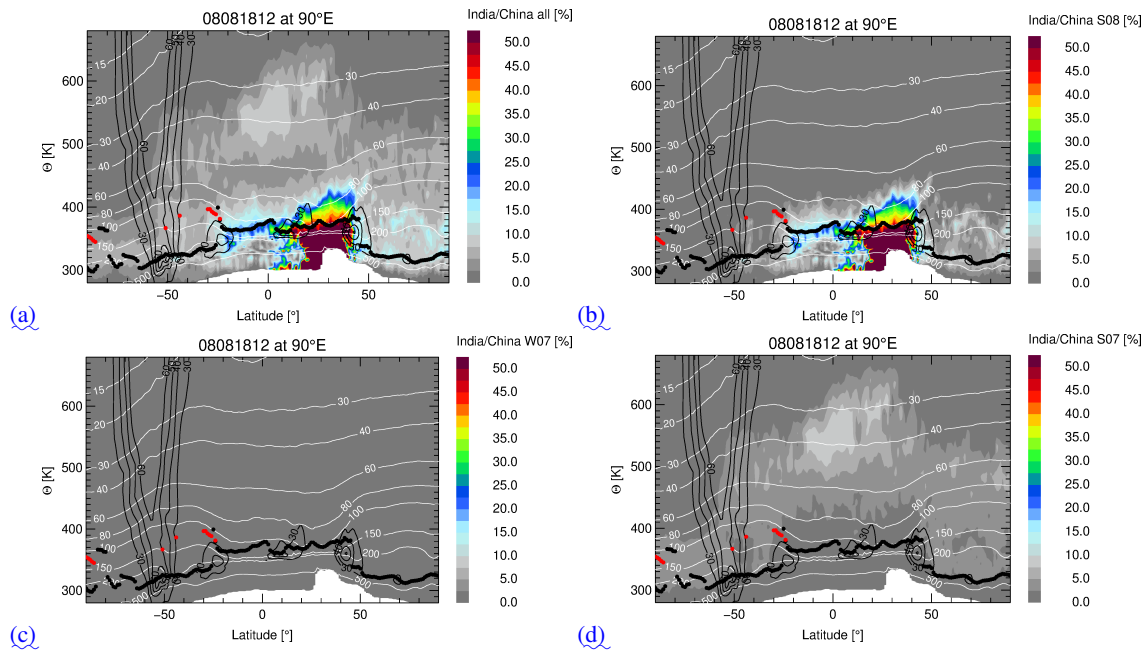


Figure 9. Latitude–theta cross sections at 90°E for the fraction of the India/China tracer for the **entire**-simulation period (1 May 2007 - ~~31 October~~ 18 August 2008 labeled as **'all'**) (a), for the Summer08 (S08) pulse (b), for the Winter07/08 (W07) pulse (c), and for the Summer07 (S07) pulse (d) on 18 August 2008. The thermal tropopause (**first-primary** in black dots and **second-secondary** in red dots) and **absolute** horizontal winds (black lines for 30, 40, 50, and 60 m/s) are shown. The **corresponding**-levels of pressure are marked by thin white lines. Note that the maximum value for the Winter07/08 (W07) pulse (c) is 2.4%.

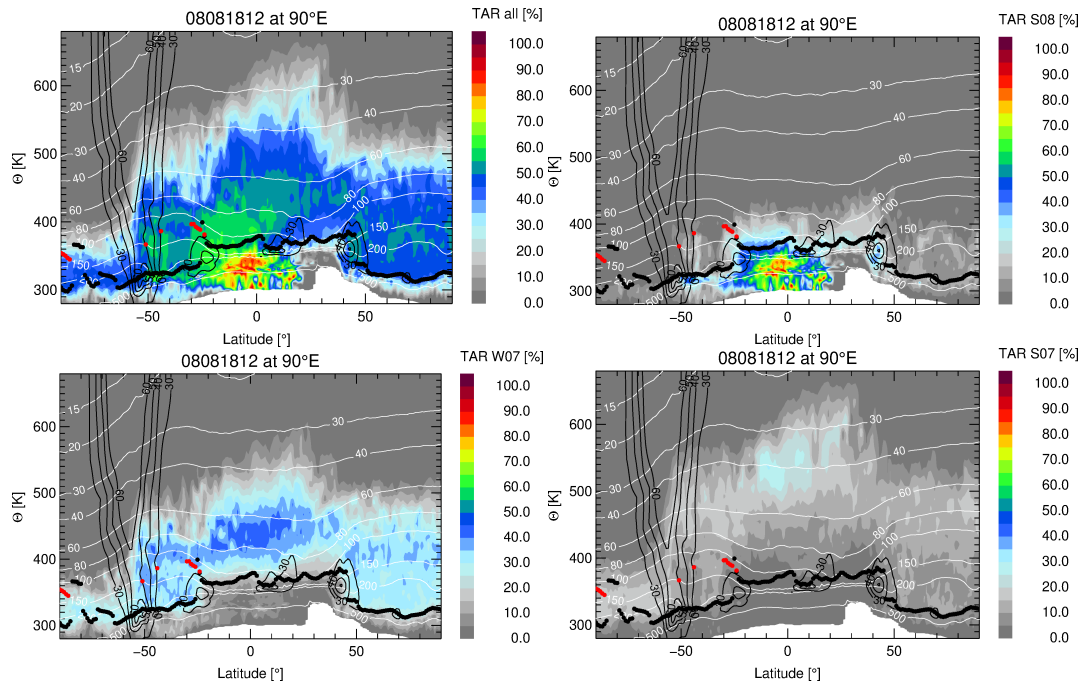


Figure 10. As Fig. 9 but for the fraction of the tracer for Southeast Asia (SEA)

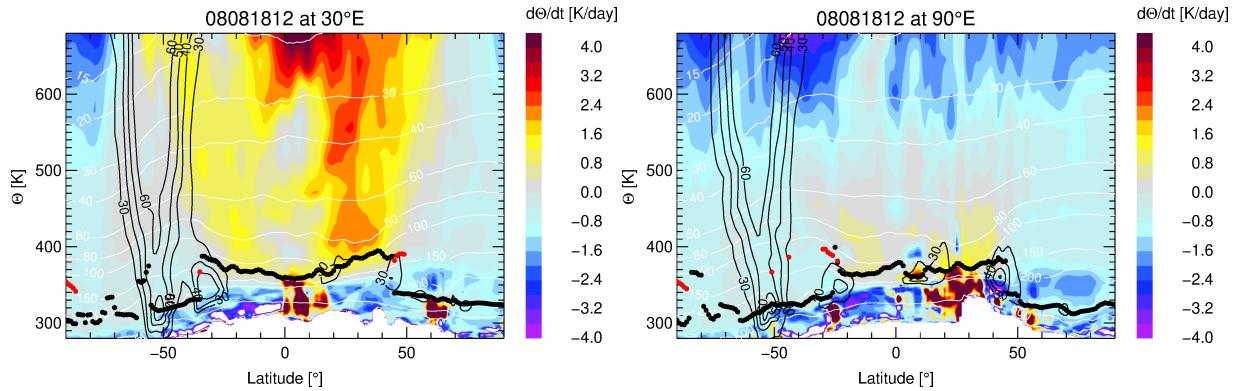


Figure 11. Latitude–theta cross section of $d\Theta/dt$ showing the radiative heating above the Asian monsoon anticyclone for the western (30°E) and eastern mode (90°E) of the anticyclone on 18 August 2008. The thermal tropopause (first primary in black dots and second secondary in red dots) and absolute horizontal winds (black lines for 30, 40, 50, and 60 m/s) are shown. The corresponding levels of pressure levels are marked by thin white lines.

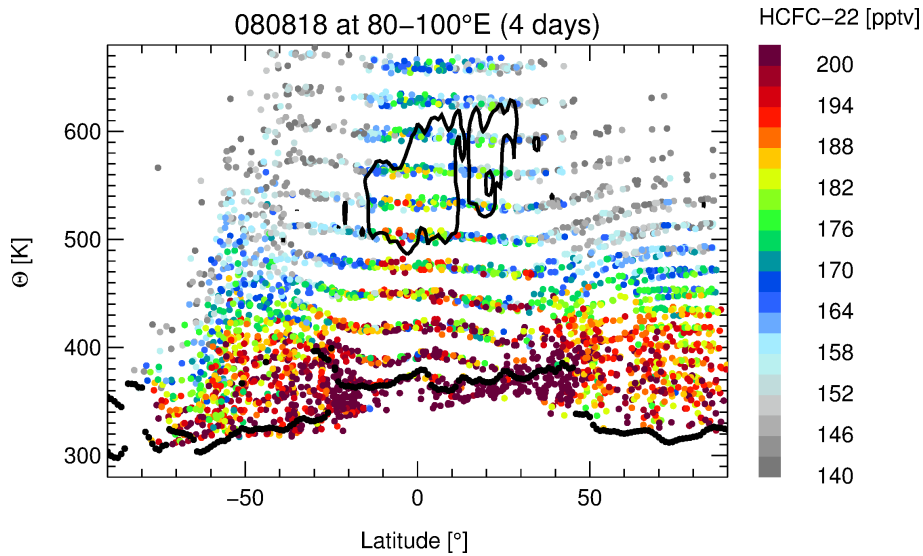


Figure 12. Latitude–theta cross sections of MIPAS HCFC-22 measurements crossing the ~~western (20°E–40°E) and eastern mode (80°E–100°E) mode~~ of the anticyclone up to 680 K potential temperature on 18 August 2008. The thermal tropopause is indicated by black dots. The contour line of 6% of the India/China tracer for the Summer07 pulse is shown by thick black lines as shown in Fig. 9. To highlight the MIPAS HCFC-22 signal within the tropical pipe the plot range of the data is up to 200 pptv. Note that the maximum values of MIPAS HCFC-22 in the troposphere are higher than 200 pptv.

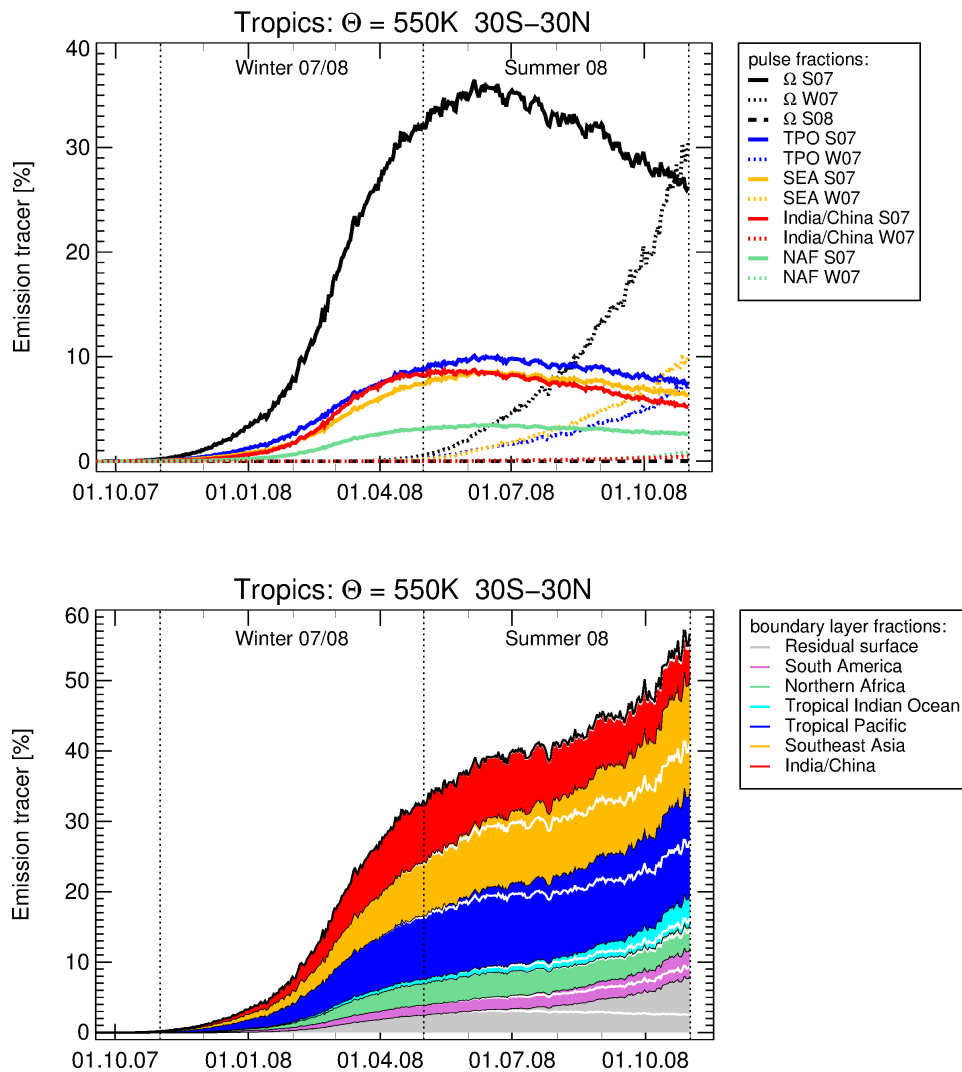


Figure 13. Top: The contribution of the three different time pulses S07, W07, and S08 (each set for a time period of 6 months marked the vertical dotted lines) for the entire Earth's surface (Ω_{S07} , Ω_{W07} , Ω_{S08}) to the tropical pipe between 30°S and 30°N at 550 K potential temperature from 1 October 2007 until the end of the simulation period (31 October 2008) (top, black lines). Emission tracers released during S08 have no contribution to the tropical pipe at 550 K -by October 2008. The contribution of several tracers of air mass origin to the individual pulses are shown in colours.

Bottom: Contribution of different emission tracers for the tropical Pacific Ocean, Southeast Asia, India/China, South America, Northern Africa, tropical Indian Ocean, and the residual surface (all other regions of the Earth's surface) to the tropical pipe between 30°S and 30°N at 550 K potential temperature from 1 October 2007 until the end of the simulation period (**bottom**). The contribution of the **three**-time pulses for the different emission tracers are marked by thin white lines for S07 and by thin black lines for W07.

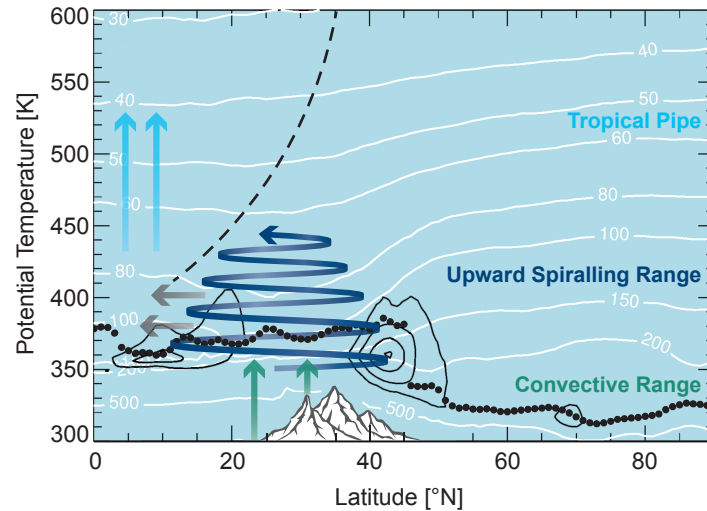


Figure 14. Latitude-theta cross section at about 90°E: The transport ~~pathway~~ of air masses from the region of the Asian monsoon into the tropical pipe occurs in three distinct steps: first, very fast uplift within the convective range up to ≈ 360 K within the Asian monsoon anticyclone and outside in the tropical adjacent regions (within a few days). ~~Second;~~ second, uplift above 360 K (up to ≈ 460 K) within the upward spiralling range (within a few months) and third, transport within the tropical pipe to altitudes higher than 460 K associated with the large-scale Brewer-Dobson circulation (within \sim one year). The thermal tropopause (black dots) and horizontal winds (black lines) are shown. The ~~corresponding~~ horizontal winds mark the edge of the anticyclone at its northern and southern flank. The levels of pressure are marked by thin white lines. Large grey arrows indicate isentropic transport from the Asian monsoon anticyclone into the tropics. The dashed line marks the tropical pipe which isolates tropical air masses largely from isentropic mixing with mid-latitude air (e.g., Plumb, 1996; Volk et al., 1996)

~

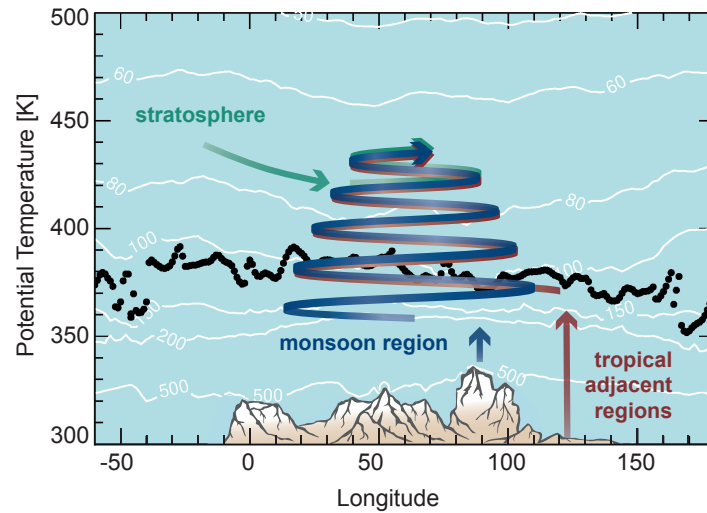


Figure 15. Longitude-theta cross section at about 30°N: At the top of the Asian monsoon anticyclone (above ≈ 360 K) air masses circulate around the anticyclone in a large-scale upward spiral extending from northern Africa to the western Pacific. In the upward spiralling range air masses from inside the Asian monsoon anticyclone (shown in blue) are mixed with air masses convectively uplifted outside the core of the Asian monsoon anticyclone in the tropical adjacent regions e.g. uplifted by tropical cyclones in the western Pacific ocean (shown in red). The higher above the thermal tropopause the larger is the contribution of air masses from outside the Asian monsoon anticyclone from the stratospheric background coming into the upward spiralling flow (shown in green). The levels of pressure are marked by thin white lines and the thermal tropopause is shown by black dots.

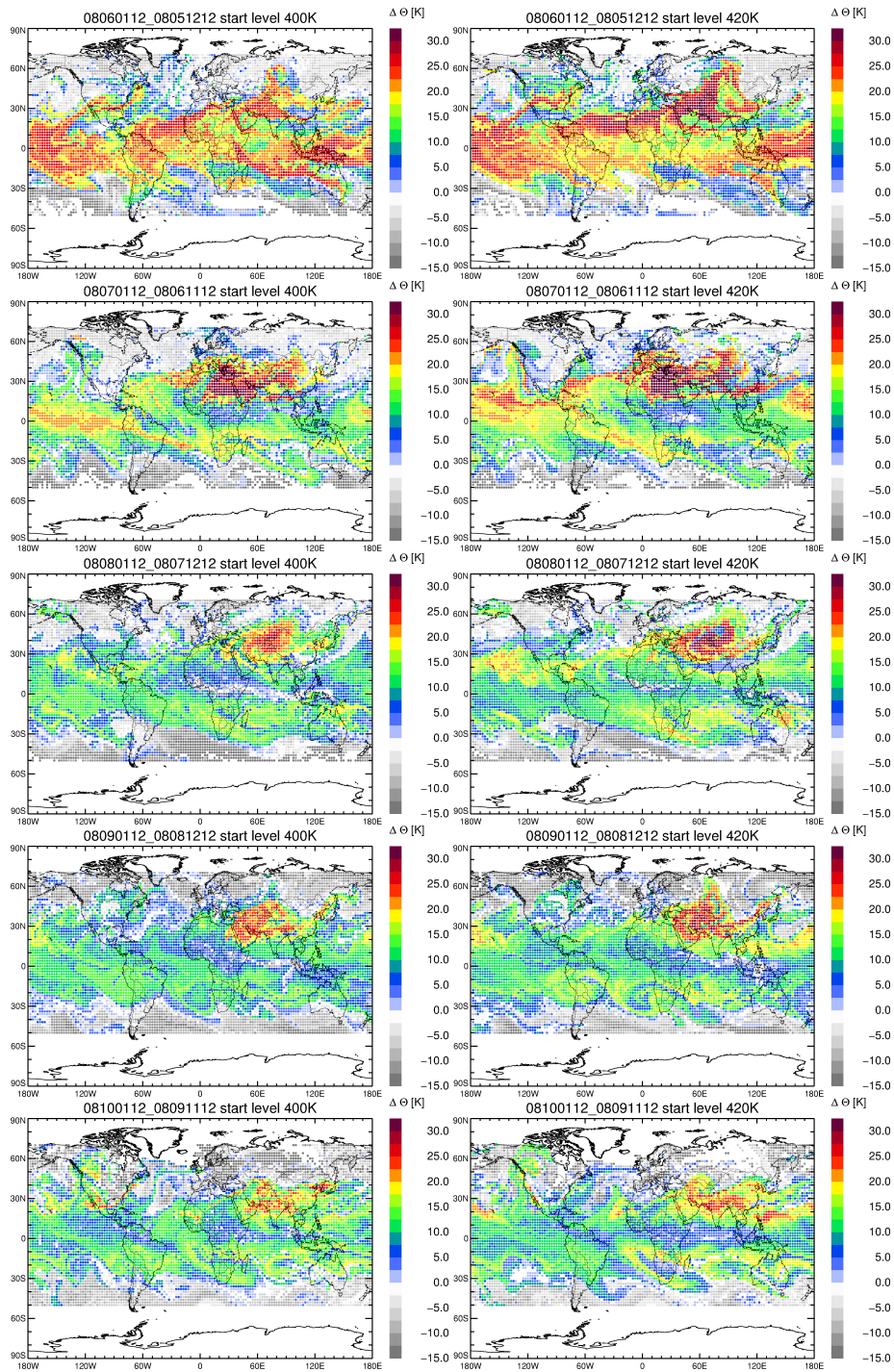


Figure A1. The change in potential temperature ($\Delta\Theta$) along 20-day backward trajectories initialised on 18 August 2008 are shown for different levels of potential temperature (400 K and 420 K) for different days from monsoon-onset until post-monsoon (1st June, 1st July, 1st August, 1st September, and 1st October 2008).

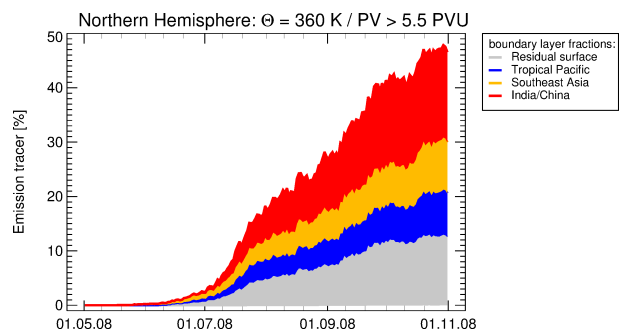


Figure A2. Contribution of different emission tracers from India/China, southeast Asia, the tropical Pacific Ocean, and residual surface to the northern lower stratosphere at 360 K from May to October 2008.